Graduate Theses, Dissertations, and Problem Reports

1983

Composite Operational Amplifiers And Their Applications In Active Networks

Sherif N. Michael-Nessim

INFORMATION TO USERS

This reproduction was made from a copy of a document sent to us for microfilming. While the most advanced technology has been used to photograph and reproduce this document, the quality of the reproduction is heavily dependent upon the quality of the material submitted.

The following explanation of techniques is provided to help clarify markings or notations which may appear on this reproduction.

1. The sign or "target" for pages apparently lacking from the document photographed is "Missing Page(s)". If it was possible to obtain the missing page(s) or section, they are spliced into the film along with adjacent pages. This may have necessitated cutting through an image and duplicating adjacent pages to assure complete continuity.

2. When an image on the film is obliterated with a round black mark, it is an indication of either blurred copy because of movement during exposure, duplicate copy, or copyrighted materials that should not have been filmed. For blurred pages, a good image of the page can be found in the adjacent frame. If copyrighted materials were deleted, a target note will appear listing the pages in the adjacent frame.

3. When a map, drawing or chart, etc., is part of the material being photographed, a definite method of "sectioning" the material has been followed. It is customary to begin filming at the upper left hand corner of a large sheet and to continue from left to right in equal sections with small overlaps. If necessary, sectioning is continued again—beginning below the first row and continuing on until complete.

4. For illustrations that cannot be satisfactorily reproduced by xerographic means, photographic prints can be purchased at additional cost and inserted into your xerographic copy. These prints are available upon request from the Dissertations Customer Services Department.

5. Some pages in any document may have indistinct print. In all cases the best available copy has been filmed.

8326652

Michael-Nessim, Sherif N.

COMPOSITE OPERATIONAL AMPLIFIERS AND THEIR APPLICATIONS IN ACTIVE NETWORKS

West Virginia University   PH.D.   1983

University
Microfilms
International   300 N. Zeeb Road, Ann Arbor, MI 48106

PLEASE NOTE:

In all cases this material has been filmed in the best possible way from the available copy. Problems encountered with this document have been identified here with a check mark ___√___ .

1.　Glossy photographs or pages _____

2.　Colored illustrations, paper or print _____

3.　Photographs with dark background _____

4.　Illustrations are poor copy _____

5.　Pages with black marks, not original copy __√__

6.　Print shows through as there is text on both sides of page _____

7.　Indistinct, broken or small print on several pages __√__

8.　Print exceeds margin requirements _____

9.　Tightly bound copy with print lost in spine _____

10.　Computer printout pages with indistinct print _____

11.　Page(s) _____ lacking when material received, and not available from school or author.

12.　Page(s) _____ seem to be missing in numbering only as text follows.

13.　Two pages numbered _____ . Text follows.

14.　Curling and wrinkled pages _____

15.　Other_____

University
Microfilms
International

COMPOSITE OPERATIONAL AMPLIFIERS

AND THEIR APPLICATIONS IN ACTIVE NETWORKS

DISSERTATION

Submitted to the Graduate School
of
West Virginia University
In Partial Fulfillment of the Requirements for
The Degree of Doctor of Philosophy

by
Sherif Michael-Nessim
B.S.E.E., M.S.I.E., P.E.
Morgantown
West Virginia
1983

ACKNOWLEDGEMENTS

The author wishes to express his sincere appreciation and gratitude to his research advisor, Dr. Wasfy B. Mikhael, who contributed counsel and assistance in every step of this research from conceptual stage to the final form. The helpful suggestions and constructive criticism of Dr. R. E. Swartwout, Dr. N. S. Smith, Dr. W. H. Iskander, and all the Committee members, were greatly appreciated.

For the financial support, the author feels highly obligated to Dr. R. L. Klein, the department chairman, Dr. W. B. Mikhael, and to Dr. Samy Elias for the teaching and research fellowships.

Special thanks are due to Mrs. Debbie Hamilton for all the time, patience, and effort spent on the word processor to prepare this dissertation.

Finally, the author is glad of this opportunity to acknowledge his indebtedness, to his parents for their unfailing encouragement, love and confidence in him during the writing of this dissertation. For without prayers and encouragements of them, his family and friends, he would not have finished in time.

TABLE OF CONTENTS

TABLE OF CONTENTS (Continued) Page

TABLE OF CONTENTS (Continued)   Page

LIST OF TABLES   Page

LIST OF FIGURES   Page

LIST OF FIGURES (Continued)   Page

LIST OF FIGURES (Continued)   Page

LIST OF FIGURES (Continued)   Page

LIST OF FIGURES (Continued)   Page

LIST OF FIGURES (Continued)   Page

LIST OF FIGURES (Continued)   Page

LIST OF FIGURES (Continued)   Page

LIST OF FIGURES (Continued)   Page

LIST OF IMPORTANT ABBREVIATIONS AND SYMBOLS

[a]	Chain Transmission Matrix
A	Operational Amplifier Open Loop Gain
A_o	Operational Amplifier DC Gain
A_{oc}	Composite Operational Amplifier DC Gain
$A_a(s)$	Operational Amplifier Non-inverting Open Loop Gain
$A_b(s)$	Operational Amplifier Inverting Open Loop Gain
AC	Alternating Current
AP	All-Pass
BP	Band-Pass
BW	Bandwidth
CMOS	Complementary Metal-Oxide-Semiconductor
CMRR	Common Mode Rejection Ratio
CNOA	Composite Operational Amplifier Using N Single OA's
C2OA	Composite Operational Amplifier Using 2 Single OA's
C3OA	Composite Operational Amplifier Using 3 Single OA's
C4OA	Composite Operational Amplifier Using 4 Single OA's
D	Denominator of the Transfer Function
DC	Direct Current
ECAP	Electronic Circuit Analysis Program
f_i	Unity-Gain Bandwidth
f_L	Operational Amplifier 3-dB Frequency
f_o	Band-Pass Filter Center Frequency
f_p	Pole Frequency
GBWP	Gain Bandwidth Product
G_i	Transfer Function of Individual Active Building Blocks
GIC	Generalized Immittance Converter
h(s)	Admittance Conversion Function
H	Transfer Function Multiplying Constant
HP	High-Pass
K	Amplifier Finite Gain
LP	Low-Pass
MFB	Multiple Feedback
N	Numerator of the Transfer Function
NF	Notch Filter
OA	Operational Amplifier
Q_p	Pole Quality Factor
Q_z	Zero Quality Factor
RHS	Right Hand Side of the S Plane
SFG	Signal Flow Graph
$T_a(s)$	Actually Realized Transfer Function
THD	Total Harmonic Distortion
$T_i(s)$	Ideal Transfer Function
T_i'	First Derivative of the Transfer Function

LIST OF IMPORTANT ABBREVIATIONS AND SYMBOLS (Continued)

T_i'' Second Derivative of the Transfer Function

V_{cc} Power Supply Voltage

VCVS   Voltage Controlled Voltage Source

Y_i Input Admittance

Y_L Load Admittance

Z_{in} Input Impedance

Z_{out} Output Impedance

ZSD   Zero Second Derivative

α Active Compensating Resistors Ratio

β Active Compensating Resistors Ratio

γ Active Compensating Resistors Ratio

τ_i Reciprocal of the Gain Bandwidth Product ω_i

τ_t Integrator Time Constant

ω_h Operational Amplifier Second Pole Corner Angular Frequency

ω_i Operational Amplifier Gain Bandwidth Product

ω_L Operational Amplifier 3-dB Angular Frequency

ω_n Notch Filter Central Angular Frequency

ω_o Band-Pass Filter Central Angular Frequency

ω_p Pole Angular Frequency

ω_t Reciprocal of the Integrator Time Constant τ_t

ω_z Zero Angular Frequency

ABSTRACT

A new general approach is presented for extending the useful operating frequencies of; linear active networks in general, inverting integrators, finite gain amplifiers, and active filters in particular, realized using Operational Amplifiers (OA). This is achieved by replacing each OA in the active network by a Composite Operational Amplifier (CNOA), constructed using N OA's. The technique of generating the CNOA's for any given N is proposed. The realizations, employing the CNOA's generated, are examined according to a stringent performance criterion satisfying the important properties such as extended bandwidth, stability with one and two pole OA model, low sensitivity to the active and passive components and OA mismatch, wide dynamic range...etc. Several families of CNOA's for $N = 2$, 3, and 4, satisfy the suggested performance criterion. The CNOA's thus obtained are found useful in most frequently used linear active networks, namely, functional building blocks (finite gain-positive, negative and differential-amplifiers) and inverting integrators. Several applications of CNOA's in active filters illustrate clearly the considerable improvements of the filters performance when composite amplifiers were used. This led to the introduction of two useful applications, a programmable filter and the use of CNOA's in inductance simulations. The results of the use of CNOA's in different active networks are given and shown theoretically and experimentally to compare favorably with the state of the art realizations using the same number of OA's.

CHAPTER I

INTRODUCTION

1.1 GENERAL

Linear active circuits, namely, positive, negative and differential finite gain amplifiers, integrators and active filters are mainly realized using Operational Amplifiers (OA's) as the active elements. These active elements have frequency dependent gains resulting in limited operating frequencies of the linear active circuits. The operating frequencies are defined as those over which the deviation in the response of an active realization from its ideal value due to the OA's frequency dependence, falls within a pre-determined acceptable range. For practical reasons, extending the useful Bandwidth (BW) of the most commonly used linear active circuits received the attention of many researchers in this field. This resulted in many valuable contributions, each deals with solving this frequency limitation in a specific area of application as will be discussed in the following section. In practice, the passive components limit the operating frequencies in a higher frequency range relative to the limitation due to the OA's nonideal behavior. Thus, if the ideal mathematically input-output relationship to be realized is $T_i(s)$ then the constructed active circuit yields $T_a(s)$ which is different from T_i, even if all the passive components in the circuit are ideal. The OA parameter variations with frequency, temperature and power supply

voltage result in corresponding variation in $T_a(s)$. The less $T_a(s)$'s dependence on the OA parameters, the smaller is the variations in $T_a(s)$.

Generally, three approaches were considered to minimize these variations. In the first approach, for a given fixed number of OA's, the passive configuration in which the OA's are embedded, and called the companion network, was carefully designed [1-3]. In the second approach, more OA's are used to realize a given $T_i(s)$. This results in extra degrees of freedom in choosing the companion network [1,4]. In the third approach each OA in a given configuration was simply replaced by an OA that has better characteristics such as wider Gain Bandwidth Product (GBWP) etc.

In this research, a new approach is considered to extend the useful BW. Each OA is replaced by a Composite Operational Amplifier (CNOA) [5,6], without changing the companion network. The CNOA is constructed using N regular OA's. The resulting CNOA's has 3 terminals, an inverting input, a non-inverting input, and an output. The CNOA's allow both amplitude and phase active compensation using resistor ratios as the controlling parameters. The CNOA has the same versatility as an OA. The use of the CNOA's in the popular active realizations examined, are found to greatly extend the useful operating frequencies relative to those obtainable using the state-of-the art designs employing a similar

number of OA's (N) as well as those using the single OA's employed in construcling the CNOA's [7,8].

1.2 RECENT DESIGN CONSIDERATIONS IN ACTIVE FILTERS

The concept of an ideal OA is a familiar one to signal-processing circuit designers and is widely adopted in the design of all active networks. Unfortunately, with the exception of some very low frequency applications [9], the assumption of ideality cannot always be sustained and, in particular, the complex nature of their open loop voltage gains must be accounted for. This is especially true in the area of highly selective RC-active filters where much of the literature [10-12] has been given over to just such a consideration.

A popular approach to the problem of finite and complex gain OA's has been to analyze the configuration under consideration using first-order lag amplifier model to predict the actual positions of the network poles and zeroes. The designer could then either suitably predistort the network components values or compute the degree of post-design trimming required. In practice, neither of these techniques was always suitable since predistortion requires that the amplifier gain characteristics be accurately specified while post-design trimming can be difficult or expensive, as, for example, where the RC elements are realized in thin-film [13] form.

Recently, several approaches were introduced in numerous contributions to deal with this problem of OA's finite GBWP limitations. These approaches can be generally categorized as mentioned before into these major approaches. The first is passive compensation. The passive compensation method produces an amount of phase lead that compensates for the phase lag of the imperfect amplifiers by using some additional passive components [14,15]. These passive components have to be adjusted at specific ambient temperature and power supply voltages to match the OA GBWP according to some design constraints. This requires that the OA GBWP be precisely measured. If the ambient temperature or the power supply voltage is changed the compensation will not longer be satisfactory. On the other hand, with the introduction of low-cost dual OA's having closely matched characteristics which track with changes in temperature and voltage, Bracket and Sedra have considered active compensation and have used this method with OA integrators [16]. This can be considered to belong to the second approach, where an extra OA is added to a particular structure in a specific application to improve the overall performance using active compensation. Example of this approach can be found in [17-25], but in most cases, no general formulation or justification can be followed to be used for other applications.

In the third approach, the single OA in any active network is

simply replaced by a wider GBWP OA to extend the BW of the application and reduce the effect of the OA pole. But this method requires the use of more expensive elements which might not be the ideal solution when large quantities of these applications are in demand.

In this research, a new approach is presented using two or more OA's to construct superior performance OA's (CNOA's) that can be used as regular OA in active circuit design. The availability of low-cost dual and quad amplifiers is one of the most important motivations for the development of such active compensation schemes.

1.3 SCOPE OF THE DISSERTATION

The aim of this dissertation is to describe the new approach for extending the BW of linear active network, and to illustrate the improvements contributed by this approach in different varieties of circuit applications.

In the following, the procedure for generating the CNOA's is presented in Chapter II. First, a general technique for the generation of C2OA's (N=2), using singular elements nullator-norator pairing is described [26-29]. Only four C2OA's are retained which are found acceptable according to a useful performance criterion described in Chapter II. Using the results obtained from this method, and to further illustrate the generality of the proposed technique, the generation of the CNOA's

for N > 2 is described. Sample results of C3OA's and C4OA's, that were found acceptable according to the above performance criterion, are presented.

Applications of the proposed CNOA's in active functional building blocks namely, finite gain positive, negative, differential amplifiers and inverting integrators are presented in Chapters III and IV respectively. Comparisons with the corresponding state of the art contributions illustrates the usefulness of these designs.

Appreciable performance improvements of the different types of existing active filters using the CNOA's are shown in Chapter V. In that chapter, the active filters are considered to belong to two categories. The first category contains filters realized using functional building blocks, while the second category contains filters in which the OA's are embedded in the passive network, and functional building blocks cannot be isolated from the filter structure. Experimental verification of the performance of the active filters in the first category was found to improve significantly at high operating frequencies when the proposed functional building blocks were used. This is illustrated in Section 5.3, by employing the C2OA's in the two integrator loop filter as an example. The BW extension was achieved while maintaining low sensitivity to passive and active elements, wide dynamic range and stable operation.

In Section 5.4, extending the active filters operating frequencies in the second category is illustrated by using both C2OA and C3OA structures in two different examples of the well known Multiple Feedback (MFB) networks, while also maintaining the practical useful features such as stability, low sensitivity to the compensating elements, and signal handling capacity.

A very important and useful application of C2OA is presented in Chapter VI. In this chapter, the excellent performance of C2OA when used in Generalized Immittance Converters (GIC's) to form new composite GIC's is illustrated. Two applications of the GIC's and the new composite GIC's are described. The first is the introduction of a new digitally programmable active filter [30]. This is a continuous time signal processing device that can be controlled by digital signals to select the filter topology and the transfer function parameters. Theoretical and experimental results of this filter shows the excellent performance when using composite GIC's.

The second applications of the composite GIC's is in inductance simulations. The improved results can be of great values in active filters design.

All applications of CNOA's throughout the dissertation are verified by computer simulations and experimental results. Also, comparison with the state of the art excellent designs are made, showing considerable improvements in bandwidth and stability.

CHAPTER II

GENERATION OF COMPOSITE OPERATIONAL AMPLIFIERS (CNOA'S) USING N

SINGLE OA'S

2.1 INTRODUCTION

The high frequency roll-off of the Operational Amplifier (OA) imposes a practical limitation to their usefulness in RC-active filter design. With the advent of low cost internally compensated dual and quad OA's, the design of active-compensated Voltage Controlled Voltage Sources (VCVS) is currently the most popular way to overcome such a limitation. In that sense, many ad-hoc circuit configurations have been reported for realizing compensated amplifiers but a clear statement of the connections among these structures is missing and it remains difficult to select anyone of them for a specific application. More over, most of the available structures are proposed for a particular application, e.g. finite gain blocks, integrators or active filters.

This chapter presents a unified new approach to the generation of active-compensated VCVS's. Starting from the basic active element, namely the OA itself, an exhaustive procedure is formulated for finding circuit implementations to realize an amplifier with amplitude and phase compensation. The results are composite active devices, each has three external terminals that resembles those of an OA. Each of the compensated composite OA was found to have the applications flexibility and versatility of

the regular single OA, while extending the useful BW considerably over that obtained using single OA.

2.2 GENERATION OF C2OA'S (N=2)

2.2.1 The Operational Amplifier (OA)

In the following section the aspects of an OA is briefly summarized. Fig. 2.1.a shows the circuit symbol for an OA, with the input terminals 1, 1' and the output terminal numbered 2. Terminal 1 is the positive or noninverting input terminal, while terminal 1' is the negative or inverting input terminal. The differential gain of the OA is denoted by A. Ideally A is infinite, the common-mode rejection ratio is infinite, the input impedances (both differential and common mode) are infinite and the output impedance is zero. With the exception of the finite frequency-dependent A, the other nonideal performance characteristics of the OA do not normally pose problems in active filters design.

A major concern in designing active networks employing OA's, is the finite OA frequency-dependent gain A. Fig. 2.1.b. shows a typical frequency response of an OA. One can note that A has a uniform 6 dB/octave or 20 dB/decade roll-off with a 3-dB frequency f_L and a unity-gain Bandwidth (BW) = f_i. Such a uniform 20 dB/decade roll-off is required to ensure stable operation of the amplifier, and is achieved by including frequency compensating networks either internally or externally. The first group of

amplifiers are referred to as "internally compensated" and are usually easier to work with. OA's that are not internally compensated offer the flexibility of tailoring the frequency response according to the application at hand, and thus increase the useful operating frequency range. Throughout all of our work here, we will assume that all OA's used are internally compensated and have the frequency response shown in Fig. 2.1.b. Thus, A is given by

$$A = \frac{A_o}{1+(s/\omega_L)} \qquad (2.1)$$

where A_o is the DC gain and ω_L is the 3 dB freqeuncy. For frequencies $\omega \gg \omega_L$, (2.1) can be approximated as,

$$A \simeq \frac{A_o \omega_L}{s} \qquad (2.2)$$

From Fig. 2.1.b, and (2.2), we have

$$\omega_i = A_o \omega_L \qquad (f_i = A_o f_L) \qquad (2.3)$$

where ω_i is the OA Gain Bandwidth Product (GBWP).

$$\text{Thus } A \simeq \frac{\omega_i}{s} , \qquad \omega \gg \omega_L \qquad (2.4)$$

$$\text{or } |A| \simeq \frac{\omega_i}{\omega} , \qquad \omega \gg \omega_L \qquad (2.5)$$

For a typical general purpose OA, that will be used throughout this work, such as the 741 type, $A_o \simeq 10^5$ and $f_i = 1$ MHz
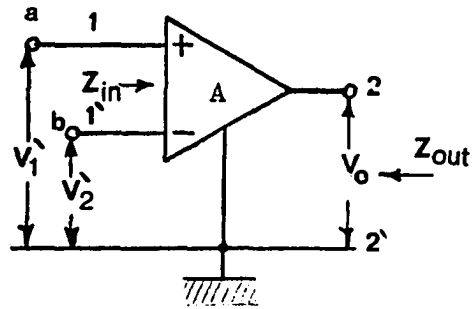
Fig. 2.1.a. Circuit Symbol for the Operational Amplifier (OA).
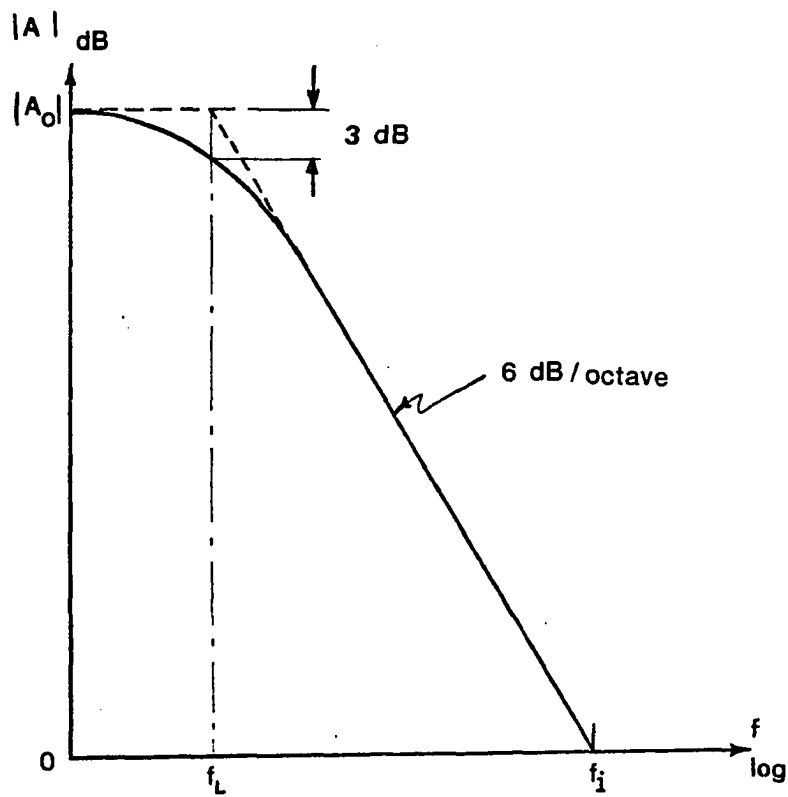
Fig. 2.1.b. Frequency Response of an OA having a Dominate-Pole Compensation ..

with tolerance usually around 10%. Furthermore, A_0 and f_i are usually temperature and power supply dependent. Hence, the characteristics of active networks whose response is highly dependent on A_0 and/or ω_i, will be subject to undue variations with changing temperature and power supply voltage. Thus, one of the critical factors in comparing or evaluating OA networks is the dependency of the response on A_0 and ω_i.

2.2.2 The OA Singular Elements Representation, the "Nullor"

In this section, an equivalence relating the singular elements to controlled sources is presented. This will be used in the derivation of the composite OA's in the following section.

The singular elements described here are the nullator and norator. The nullator shown in Fig. 2.2.a, is a 1-port which will neither sustain a voltage nor pass a current (i.e. $V = I = 0$). On the other hand, the norator in Fig. 2.2.b, is a 1-port which will sustain an arbitrary voltage and pass an arbitrary current which are independent of each other. A 2-port consisting of a nullator as port 1 and a norator as part 2, as shown in Fig. 2.2.c, has been defined as a nullor. It has been shown that an ideal transistor is equivalent to a nullor [27]. Also it has been proved that infinite-gain Voltage Controlled Voltage Source (VCVS), as well as the other three remaining types of infinite-gain controlled source, are equivalent to nullors [26-29].

An Operational Amplifier, as shown in Fig. 2.1.a, is a VCVS.

In the ideal case the input impedance $Z_{in} \to \infty$. This corresponds to the idealized model of Fig. 2.2.c, using nullator and norator singular elements [26-29]. The ideal OA is replaced by a nullor having:

$$\begin{bmatrix} V_1 \\ I_1 \end{bmatrix} = \begin{bmatrix} 0 & 0 \\ 0 & 0 \end{bmatrix} \cdot \begin{bmatrix} V_2 \\ -I_2 \end{bmatrix} \tag{2.6}$$

which is called the nullor chain transmission matrix of an ideal OA.

2.2.3 The C2OA's Generation Procedure

In any physical network that contains N OA's, if each OA is replaced by a nullor, we obtain a nullor equivalent network. The nullors then can be split into nullators and norators to yield a nullator-norator equivalent network.

In reverse, a nullator-norator equivalent network containing n nullators and n norators yields n! nullor equivalent networks, since nollators and norators can be paired into nullors in an arbitrary manner. For example, a nullator-norator equivalent network containing two nullators and two norators yields two nullor equivalent networks. Nullator X can be paired with norator X or Y, and nullator Y can be paired with norator Y or X, as shown in Fig. 2.3.

Although the nullator (or norator) is not admissible as an idealization of a physical network, the nullor, like an infinite-

$$V_1 = i_1 = 0$$

$$V_2, i_2 \text{ arbitrary}$$
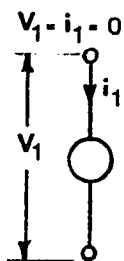
Fig. 2.2.a.   The Nullator .   **Fig. 2.2.b.**   The Norator .
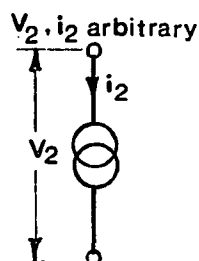
$Z_{in} \rightarrow \infty$

$Z_{out} \rightarrow 0$

$A \rightarrow \infty$
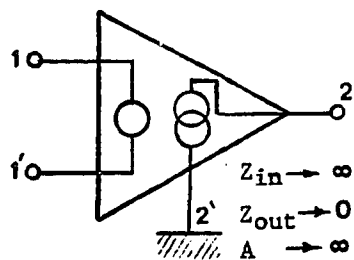
Fig. 2.2.c.   The OA (VCVS) Nullor Representation.

Fig. 2.2.   The Singular Elements Representation of the OA .
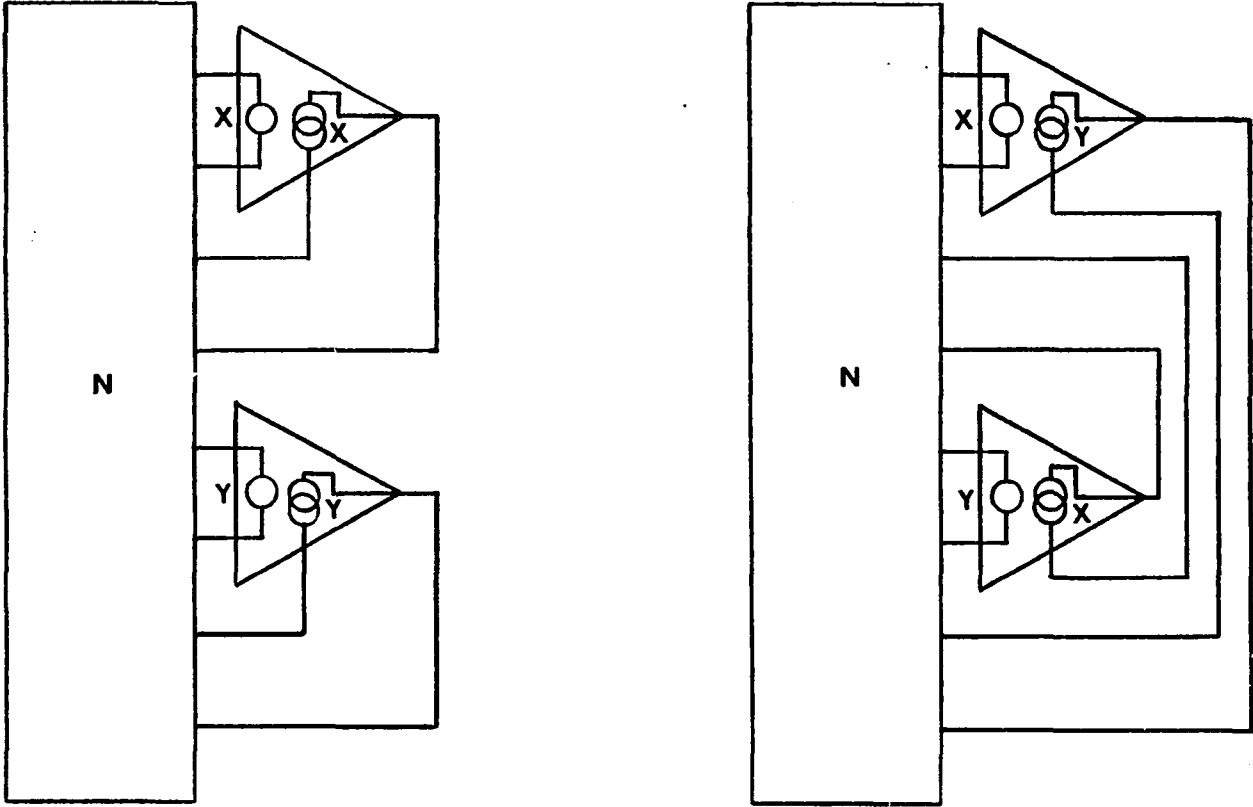
Fig. 2.3.   Two Alternative Nullor Equivalent Networks
             Obtained From a Single Nullator-Norator
             Equivalent Network .

gain controlled source, is admissible. The equivalence established is valid whether A $\rightarrow$ ∞ or A $\rightarrow$ $-\infty$ and so in practice, a nullor can be replaced by a high-gain differential controlled source in two ways as shown in Fig. 2.4. Thus the non-inverting-input terminal of the controlled source can be connected to a node K, and the inverting-input terminal to a node L (Fig. 2.4.b) or vice-versa (Fig. 2.4.c). Thus a nullor equivalent network containing two nullors corresponds to four physical networks, since either high-gain controlled source can be connected in two ways. In general, a nullor equivalent network containing n nullors, corresponds to 2^n physical networks. Each of these n! nullor networks yields a physical realization which has different dependence on the non-ideal active elements.

After this brief explanation, the procedure to generate the C2OA's is described as follows. In the first step, a redundant amplifier of finite gain $\pm$ H is combined with a single OA, such that the chain matrix of the resulting two amplifier network, assuming ideal amplifiers, corresponds to that of a nullor, as given by (2.6). In other words, although each network contains 2 VCVS's, the overall two-port network realizes one VCVS. Six topologies are obtainable from each of the four networks shown in Figs. 2.5.a to 2.5.d. Two topologies are obtained, one for + H and the other for - H, at each position of the three way switch, leading to six topologies per network. It is easy to show that 17
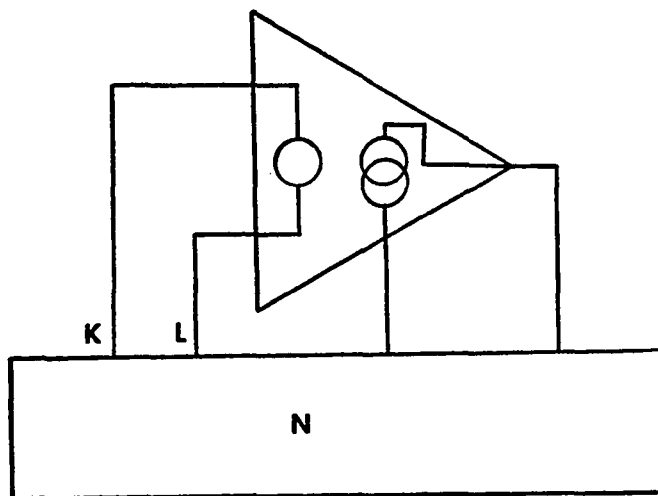
Fig. 2.4.a.   Circuit Containing One Nullor .
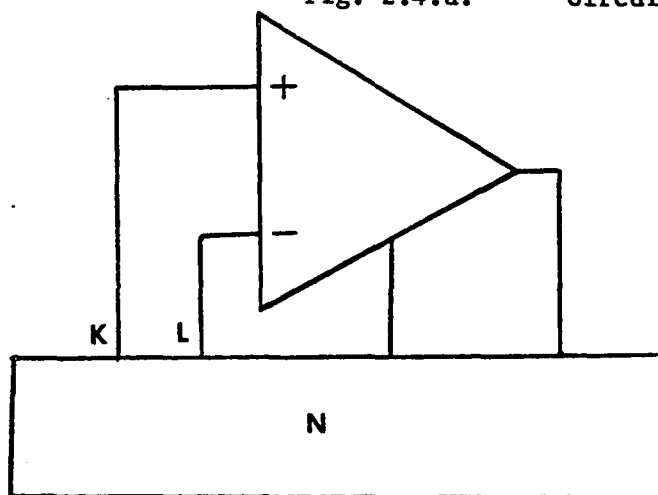
Fig. 2.4.b.
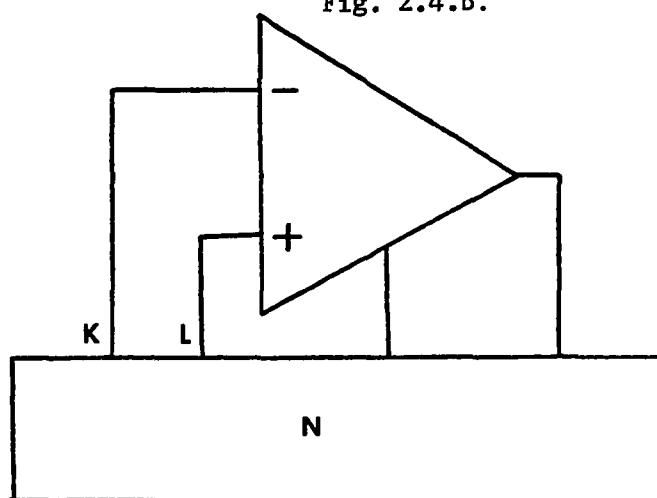
Fig. 2.4.c.

Fig. 2.4.b,c.   Two Alternative Physical Circuits .

Fig. 2.4.   Replacement of Nullors by Physical Networks .

out of the 24 topologies realize true nullors, i.e., none of the network elements or signals are required to assume certain values. Eight possible OA realizations can be obtained from each of these seventeen topologies (nullor) networks. This results in 136 Composite Operational Amplifiers (C2OA's), each constructed using two single OA's. The resulting C2OA's, Fig. 2.6, are examined according to the following performance criteria:

i). Let $A_a(s)$ and $A_b(s)$ be the non-inverting and inverting open loop gains of each of the 136 C2OA's examined. The denominator polynomial coefficients of $A_a(s)$ and $A_b(s)$ should have no change in sign. This satisfies the necessary (but not sufficient) conditions for stability. Also, none of the numerator or denominator coefficients of $A_a(s)$ and $A_b(s)$ should be realized through differences. This eliminates the need for single OA's of matched GBWP's and results in low sensitivity of the C2OA with respect to its components.

ii) The external three terminal performance of the C2OA-i should resemble, as close as possible, from the versatility point of view those of the single OA.

iii) No Right Half S plane (RHS) zeroes due to the single OA pole should be allowed in the closed loop gains of the C2OA's (for minimum phase shifts).

iv) The resulting input-output relationship $T_a(s)$ in the
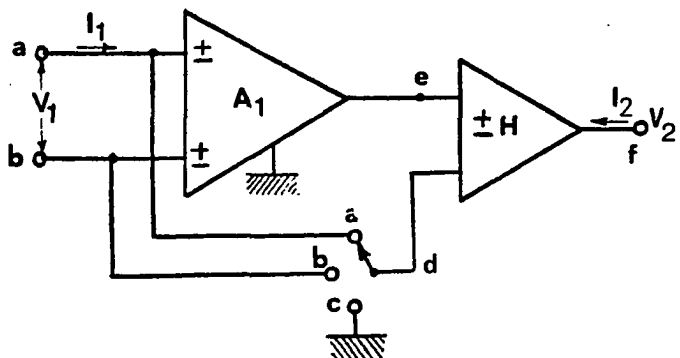
Fig. 2.5.a.
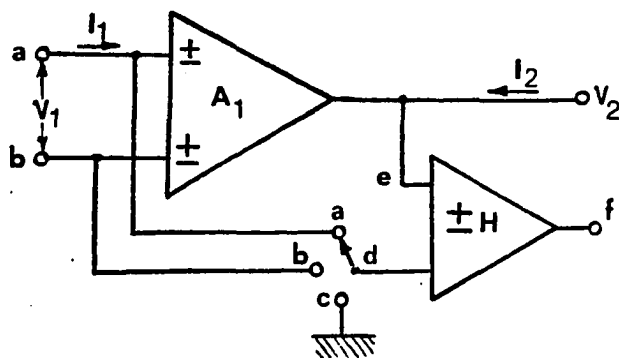
Fig. 2.5.b.
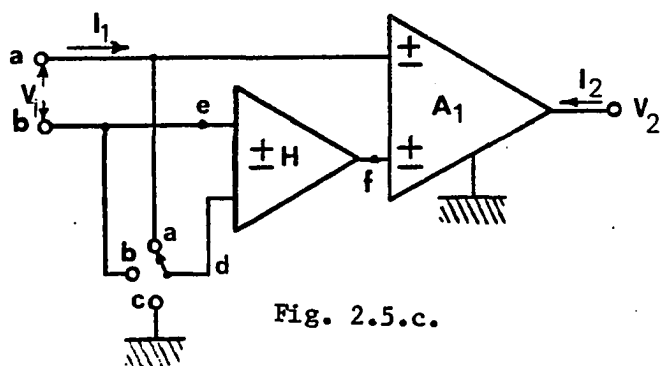
Fig. 2.5.c.
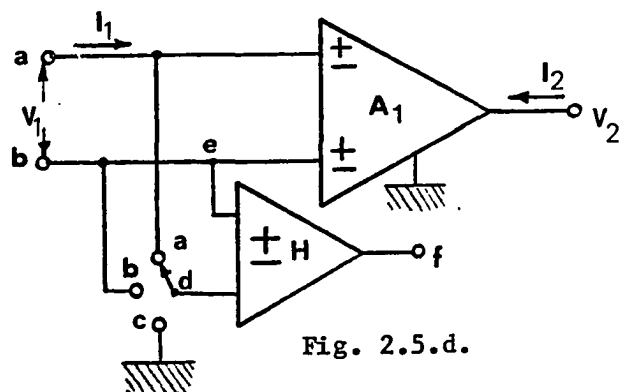
Fig. 2.5.d.
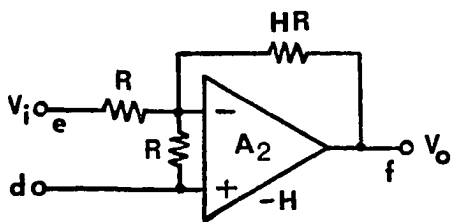
Fig. 2.5.e.
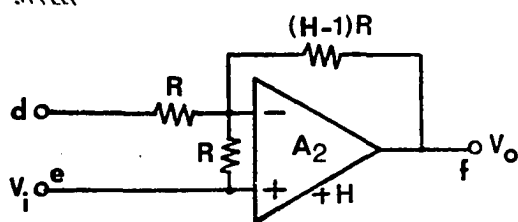
Fig. 2.5.f.

Fig. 2.5.a-d.   The Four Different Networks for Generating
                the Composite Operational Amplifiers Using
                Two Single OA's (C2OA's) . . . .

Fig. 2.5.e,f.   The $\pm$ H Finite Gain Amplifier Realizations
                Used in Figs. 2.5.a to 2.5.d .

$$V_o = V_a A_a - V_b A_b$$
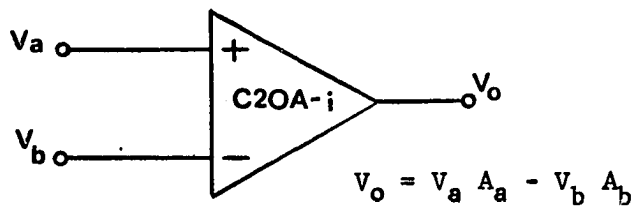
Fig. 2.6.   The Composite Operational Amplifier
                (C2OA-i) Symbol .

applications considered should have extended frequency operation with minimum gain and phase deviation from the ideal transfer function $T_i(s)$. The improvement should be enough to justify the increased number of OA's.

Twenty-seven composite OA structures out of 136 examined, are found to have acceptable performance according to the criteria mentioned above. These are to be found in Appendix A.

Four C2OA's referred to as C2OA-1, C2OA-2, C2OA-3 and C2OA-4 were found to out perform the remaining C2OA's structures, and were carefully selected to be used in different applications as one to one replacement of the single OA's. These are given in Fig. 2.7 as general purpose operational amplifiers.

It is interesting to note that by applying the nullator-norator concept to the transistors in a Darlington pair, C2OA-3 can be obtained [2.5]. Thus, C2OA-3 ($\alpha=0$), can be considered as a special case of the Darlington network, since the norators are both C grounded in the Darlington pair nullator network to be able to convert it into an OA realization.

The open loop gain of the single OA's, used in constructing the C2OA's, assuming a single pole model (2.1), can be expressed as

$$A_i = \frac{A_{oi}\,\omega_{Li}}{\omega_{Li} + s} = \frac{\omega_i}{s + \omega_{Li}} \tag{2.7}$$
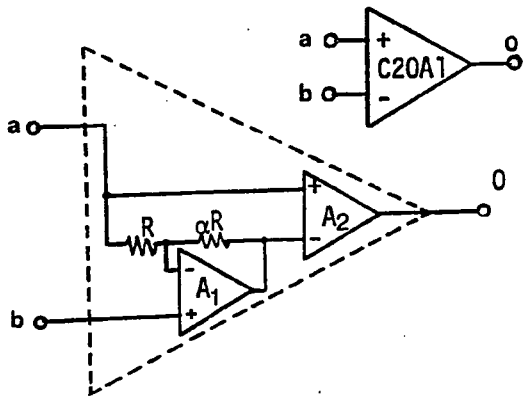
Fig. 2.7.a. C20A-1 .
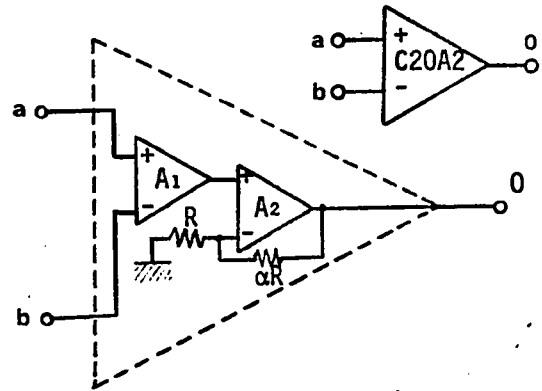
Fig. 2.7.b. C20A-2 .
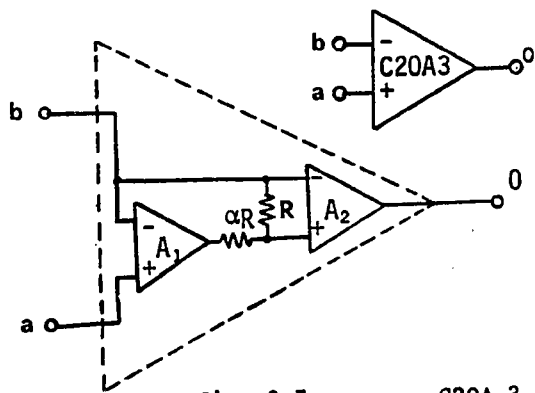
Fig. 2.7.c. C20A-3 .
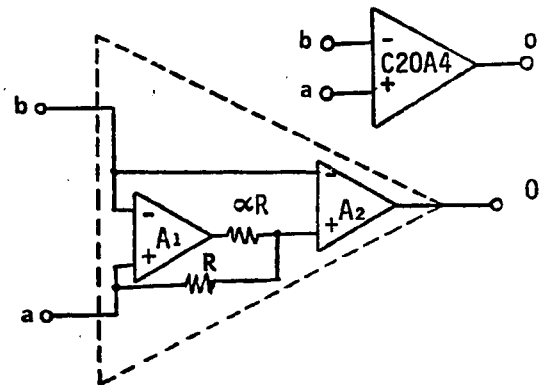
Fig. 2.7.d. C20A-4 .

Fig. 2.7. The Extended Bandwidth Composite Operational Amplifiers (C20A's) .

where A_{oi}, ω_{Li} and ω_i are the DC open loop gain, the 3-dB

Bandwidth, and the GBWP of the ith single OA, respectively.

It can be easily shown that the open loop input-output

relationships of C2OA-1 to C2OA-4 are given by

$$V_{oi} = V_a A_{ai}(s) - V_b A_{bi}(s) \qquad (i=1 \text{ to } 4) \qquad (2.8)$$

where for C2OA-1

$$V_{01} = V_a \frac{A_2 (1+A_1) (1+\alpha)}{A_1 + (1+\alpha)} - V_b \frac{A_1 A_2 (1+\alpha)}{A_1 + (1+\alpha)} \qquad (2.9)$$

for C2OA-2:

$$V_{02} = V_a \frac{A_1 A_2 (1+\alpha)}{A_2 + (1+\alpha)} - V_b \frac{A_1 A_2 (1+\alpha)}{A_2 + (1+\alpha)} \qquad (2.10)$$

for C2OA-3:

$$V_{03} = V_a \frac{A_1 A_2}{(1+\alpha)} - V_b \frac{A_2 (1+A_1)}{(1+\alpha)} \qquad (2.11)$$

and for C2OA-4:

$$V_{04} = V_a \frac{A_2 (A_1+\alpha)}{(1+\alpha)} - V_b \frac{A_2 [A_1+(1+\alpha)]}{(1+\alpha)} \qquad (2.12)$$

where α is a resistor ratio as illustrated in Fig. 2.7.

Assuming identical OA's, i.e.

$A_{o1} = A_{o2} = A_o$ and $\omega_1 = \omega_2 = \omega_i$,

it is interesting to examine the open loop gains given by (2.9) to

(2.12) in the single ended inverting application, i.e., $V_a = 0$.

For C20A-1 and C20A-2 the DC gain A_{oc1} is given by

$$A_{oc1} = \frac{A_o(1+\alpha)}{1 + (1+\alpha)/A_o} \qquad (2.13.a)$$

$$\simeq A_o(1+\alpha) \quad \text{for } (1+\alpha) \ll A_o$$

From (2.13.a), the composite amplifier has a single pole roll-off from $[\omega_i/A_o]$ to $[\omega_i/(1+\alpha)]$ where the second pole occurs. As α increases, the DC gain increases while the second pole frequency decreases.

Also, from (2.11) and (2.12), each of C20A-3 and C20A-4 has a DC gain given by

$$A_{oc2} = \frac{A_o^2}{(1+\alpha)} \qquad (2.13.b)$$

A_{oc2} has double poles (12 dB/octave) at $[\omega_i/A_o]$, and as α increases the DC gain decreases without affecting the second pole location.

Only C20A-2 has identical expressions for the positive and negative open loop gains A_a and A_b. Thus Common Mode Rejection Ratio (CMRR) problems should not be encountered using C20A-2 even for relatively large common mode signal applications. From (2.9), (2.11) and (2.12), the CMRR of C20A-1 and C20A-3 is $(A_{o1} + \frac{1}{2})$, while that of C20A-4 is $(A_{o1} + \alpha + \frac{1}{2})$. For single ended applications (small common mode signal), no problem should be encountered using C20A-1, C20A-3 and C20A-4 as verified

experimentally later.

It is important and easy to show that the voltage swing at the first OA (A_1) output, which is an internal node, in each of C2OA-1 to C2OA-4, is always less than the output voltage V_o. Hence, the dynamic range is determined by the voltage swing of the output voltage V_o. Thus, no dynamic range reduction of V_o or harmonic distortion problems should arise as verified experimentally later in Chapter V.

2.3 GENERATION OF CNOA'S (N>2)

Following the same approach proposed here, Composite Multiple Operational Amplifiers (CNOA's) for N>2, can be generated for extending further the operating frequencies at the expense of extra amplifiers. The CNOA's can be obtained in two different ways. The first approach starts from the basic single OA with additional redundant amplifiers. Then, nullator-norator pairing is used as described in Section 2.2.3.

In the second approach, the C2OA's are used as single OA replacements in the C2OA structure. Although this second approach is not exhaustive, it will be shown to yield excellent results. Thus C3OA's can be obtained by starting with one of the proposed C2OA's and replacing one of its single OA's by any of the C2OA's in Fig. 2.7. Thirty-two possible combinations of C3OA's can be obtained using the four proposed C2OA's. Some of these amplifiers are shown in Appendix B. Six designs of C3OA's that proved

theoretically and experimentally to have superior performance were selected. These C30A structures are shown in Fig. 2.8, while their corresponding open loop expressions are presented in Table 2.1.

Similarly, C40A's can be obtained by replacing each of the single OA's in a C20A by any of the C20A's or C30A's or replacing one of the single OA's in C30A's by a C20A. This results in many possible combinations of C40A's. The process can be continued (by using C20A's, C30A's and C40A's) to obtain CNOA's for any number N. Although this is theoretically interesting, the number of OA's N should be limited in practice. The increased complexity is expected to give rise to practical problems in spite of the extended bandwidth advantage.

Samples of C40A novel designs that showed better character-istics over those tested theoretically and experimentally of Appendix C are illustrated in Fig. 2.9. The open loop expressions of these selected C40A designs are shown in Table 2.2 It is assumed that $A_1 = A_2 = A_3 = A_4 = A$ for simplicity, where $A \simeq \omega_i/s$ as shown in (2.4). It is also worthwhile to mention that all the selected C30A's and C40A's novel designs were chosen according to the performance criteria described in Section 2.2.3.

2.4 CONCLUSIONS

A new general approach is presented in this Chapter for

Fig. 2.8.a.   C30A-1 .

Fig. 2.8.b.   C30A-2 .

Fig. 2.8.d.   C30A-4 .

Fig. 2.8.c.   C30A-3 .

Fig. 2.8.e.   C30A-5 .

Fig. 2.8.f.   C30A-6 .
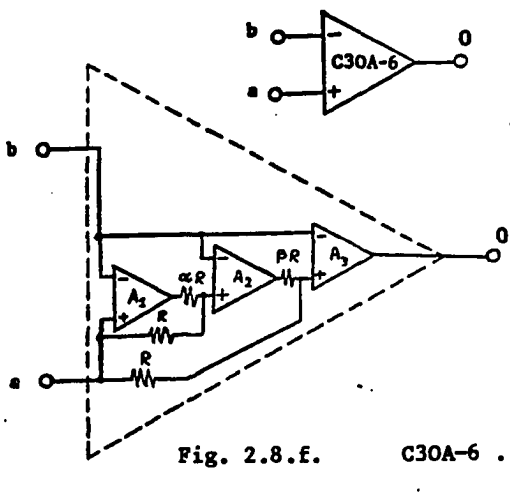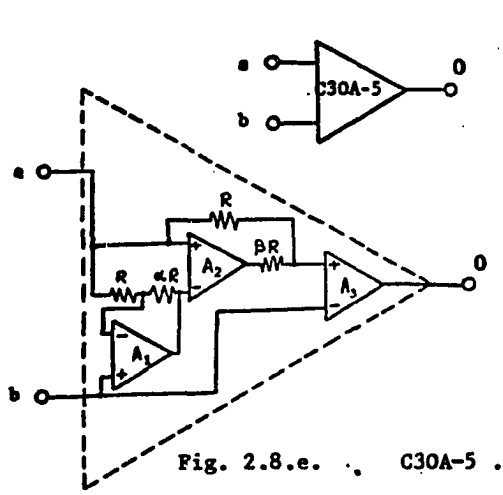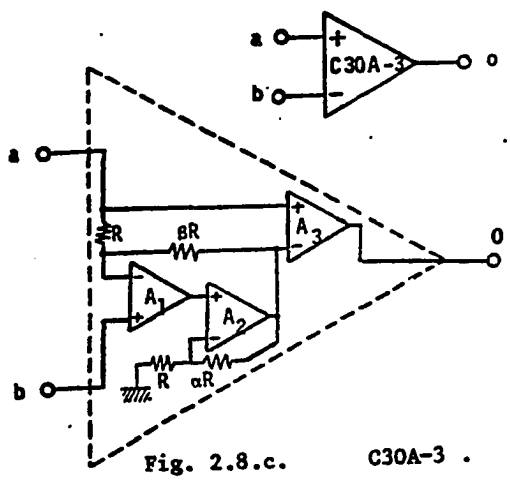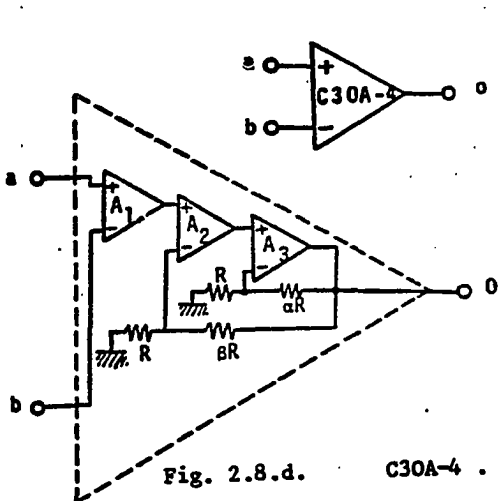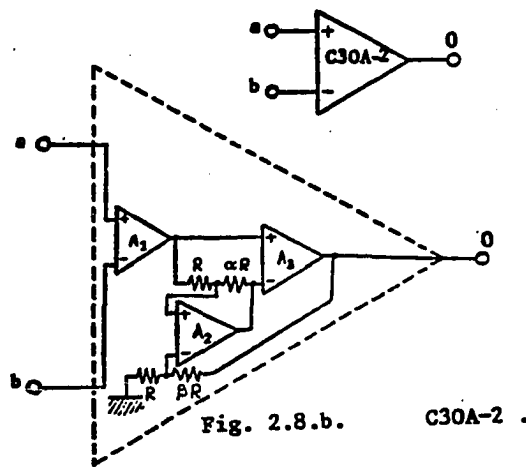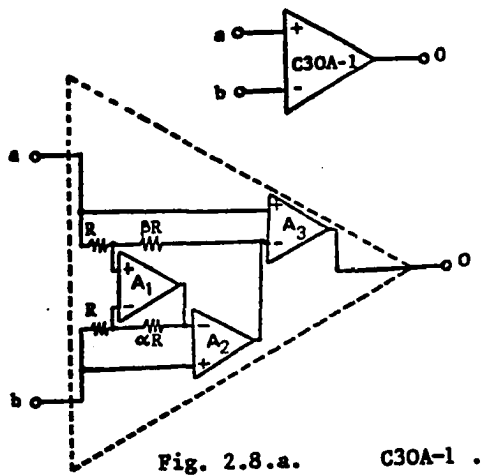
Fig. 2.8.   The Extended Bandwidth Composite Operation-
al Amplifiers (C30A's) .

$C30A_i$	Open Loop Gain Input-Output Relationship
C30A-1	$$V_o = \frac{V_a[A_1A_2A_3(1+\beta) + A_1A_2\frac{(1+\beta)}{(1+\alpha)} + A_3(1+\beta)] - V_b[A_1A_2A_3(1+\beta) + A_2A_3(1+\beta)]}{A_1A_2 + \frac{(1+\beta)}{(1+\alpha)}A_1 + (1+\beta)}$$
C30A-2	$$V_o = \frac{(V_a-V_b)[A_1A_2A_3(1+\beta) + A_3(1+\beta)]}{A_2A_3 + A_3\frac{(1+\beta)}{(1+\alpha)} + (1+\beta)} \quad \cdots$$
C30A-3	$$V_o = \frac{V_a[A_1A_2A_3(1+\alpha)(1+\beta) + A_2A_3(1+\beta) + A_3(1+\alpha)(1+\beta)] - V_b[A_1A_2A_3(1+\alpha)(1+\beta)]}{A_1A_2(1+\alpha) + A_2(1+\beta) + (1+\alpha)(1+\beta)}$$
C30A-4	$$V_o = \frac{(V_a-V_b)[A_1A_2A_3(1+\alpha)(1+\beta)]}{A_2A_3(1+\alpha) + A_3(1+\beta) + (1+\alpha)(1+\beta)}$$
C30A-5	$$V_o = \frac{V_a[A_1A_2A_3(1+\alpha) + A_2A_3(1+\alpha) + \beta A_3] - V_b[A_1A_2A_3(1+\alpha) + A_1A_3(1+\beta) + A_3(1+\alpha)(1+\beta)]}{A_1(1+\beta) + (1+\alpha)(1+\beta)}$$
C30A-6	$$V_o = \frac{V_a[A_1A_2A_3 + A_2A_3\alpha + A_3\beta(1+\alpha)] - V_b[A_1A_2A_3 + A_2A_3(1+\alpha) + A_3(1+\alpha)(1+\beta)]}{(1+\alpha)(1+\beta)}$$

TABLE 2.1.　The C30A's Open Loop Gain Input-Output Relationships .

27
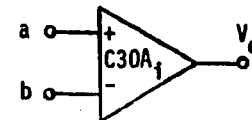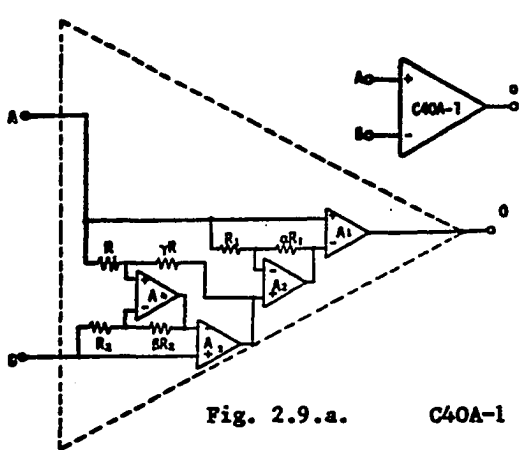
Fig. 2.9.a.   C40A-1 .
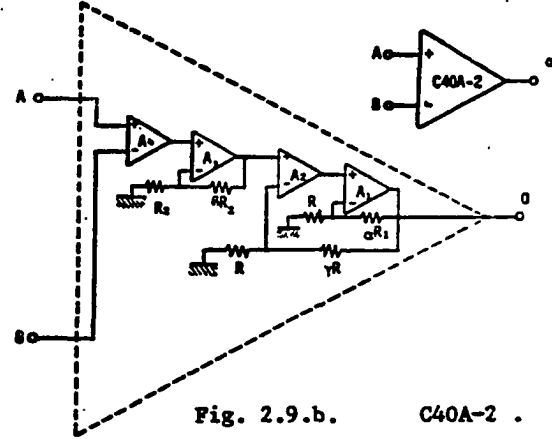
Fig. 2.9.b.   C40A-2 .
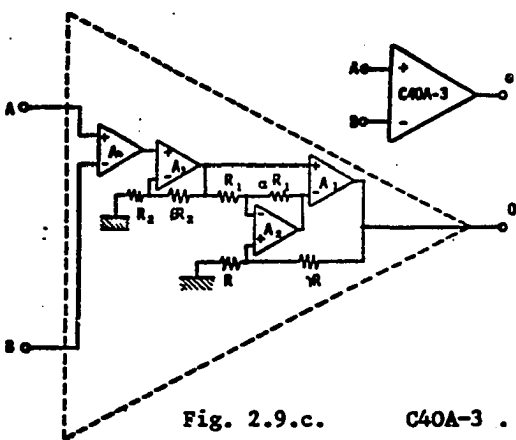
Fig. 2.9.c.   C40A-3 .
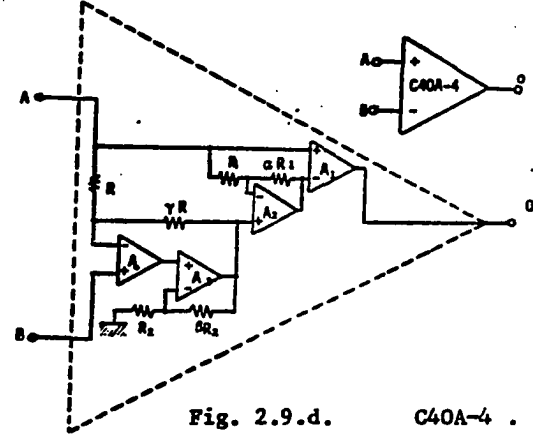
Fig. 2.9.d.   C40A-4 .
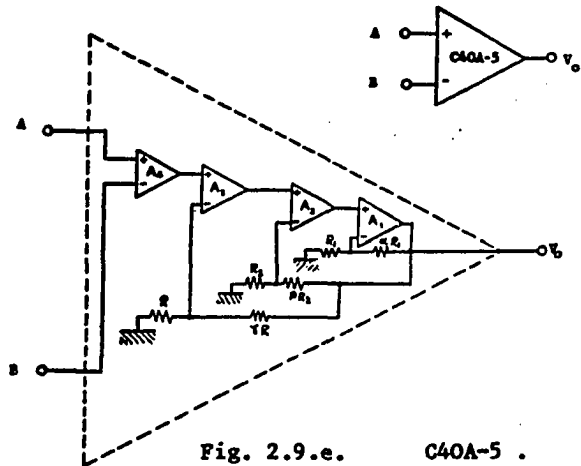
Fig. 2.9.e.   C40A-5 .

Fig. 29.   The Extended Bandwidth Composite Operational Amplifiers (C40A's) .

C40A	Open Loop Gain Input-Output Relationships
C40A-1	$$V_o = \frac{V_a\{A^4[(1+\alpha)(1+\beta)(1+\gamma)]+A^3(1+\alpha)[(1+\beta)+(1+\gamma)]+A^2(1+\alpha)(1+\gamma)(2+\beta)+A(1+\alpha)(1+\beta)(1+\gamma)\} -V_b\{A^3(1+A)(1+\alpha)(1+\beta)(1+\gamma)\}}{A^3(1+\beta) + A^2[(1+\alpha)(1+\beta)(1+\gamma)] + A(1+\gamma)[(1+\alpha)+(1+\beta)] + (1+\alpha)(1+\beta)(1+\gamma)}$$
C40A-2	$$V_o = \frac{V_a\{A^4(1+\beta)(1+\gamma)\} - V_b\{A^4(1+\beta)(1+\gamma)\}}{A^3 +[(\frac{1+\gamma}{1+\alpha})+(1+\beta)]\,A^2+ [(1+\gamma)+\frac{(1+\beta)(1+\gamma)}{1+\alpha}]\,A + (1+\beta)(1+\gamma)}$$
C40A-3	$$V_o = \frac{V_a\{A^3(1+A)(1+\alpha)(1+\beta)(1+\gamma)\} - V_b\{A^3(1+A)(1+\alpha)(1+\beta)(1+\gamma)\}}{A^3(1+\alpha) + A^2[(1+\gamma)+(1+\alpha)(1+\beta)] + A(1+\gamma)[(1+\alpha)+(1+\beta)] + (1+\alpha)(1+\beta)(1+\gamma)}$$
C40A-4	$$V_o = \frac{V_a\{A^4(1+\alpha)(1+\gamma)+A^3(1+\alpha)[1+\frac{1+\gamma}{1+\beta}]+A^2(1+\alpha)(1+\gamma)[1+\frac{1}{1+\beta}]+A(1+\alpha)(1+\gamma)\} - V_b\{A^4(1+\alpha)(1+\gamma)\}}{A^3 + [(1+\alpha)+\frac{1+\gamma}{1+\beta}]\,A^2 + (1+\gamma)[1+\frac{1+\alpha}{1+\beta}]\,A + (1+\gamma)(1+\alpha)}$$
C40A-5	$$V_o = \frac{V_a\{A^4(1+\beta)(1+\gamma)\} - V_b\{A^4(1+\beta)(1+\gamma)\}}{A^3(1+\beta) + A^2(1+\gamma) + A\frac{(1+\beta)(1+\gamma)}{(1+\alpha)} + (1+\beta)(1+\gamma)}$$
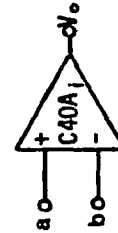
TABLE 2.2. The C30A's Open Loop Gain Input-Output Relationships. (Assuming $A_1 = A_2 = A_3 = A_4 = A$ for Simplicity).

extending the useful operating frequencies of linear active networks realized using Operational Amplifiers. This is achieved by replacing each OA in the active network by a Composite Operational Amplifier, constructed using N OA's. The technique of generating the CNOA's for N equals two using nullator-norator pairing is proposed. The C2OA's generated are examined theoretically and experimentally according to a stringent performance criteria satisfying the important properties such as extended bandwidth, stability with one and two pole models, wide dynamic range...etc. Four such C2OA's that were shown to satisfy the suggested performance criteria are selected out of all the possible combinations. The C2OA's thus obtained are found to possess superior performance as will be shown later in different applications in the following chapters.

To further extend the useful operating frequency beyond the range offered by the C2OA's, composite OA's were generated that employs more than two OA's. The techniques for the generation of these amplifiers are also presented. Example of these CNOA's, that passed the stringent performance criteria are described along with their open loop expressions. Applications of most of the selected CNOA's in different active networks shows the considerable theoretical and experimental improvements contributed by these structure as will be shown in the coming chapters.

CHAPTER III

REALIZATION OF POSITIVE, NEGATIVE, AND DIFFERENTIAL FINITE GAIN AMPLIFIERS USING CNOA'S

3.1 INTRODUCTION

Finite gain amplifiers find numerous applications in various areas such as instrumentation, oscillators and RC active filters [3,31,32]. Ideally, the gains of these amplifiers should be real, i.e. independent of frequency. However these amplifiers are invariably realized using high gain compensated OA's along with resistive feedback. The finite bandwidth of the OA's used, makes the finite gains realized frequency dependent. This frequency dependence of magnitude and phase characteristics of the amplifiers may cause the actual circuit response to deviate drastically from the desired one. The circuit may even become unstable due to these effects. For example, in the realizations of RC active filters, if the frequency of operation is beyond a few kilohertz (even with OA's of GBWP in excess of 1 MHz), the pole Q and pole frequency actually realized may be widely different from the desired values. High Q filters may even start oscillating, if the changes in the filter characteristics are such as to cause severe Q enhancement. The effect of the finite GBWP of the OA's has been examined by several researchers [10,33,34, 35]. It has also been pointed out that the frequency of oscillation may also be affected by the finite GBWP's of the OA's

used [36]. One of the ways to overcome this problem is to incorporate the finite value of the GBWP in the design equations [37-39]. This method, of course, requires OA's of very stable GBWP. Such OA's are not yet inexpensive commercial items. Another method is to provide (passive compensation) in the overall network, which will reduce the effect of finite bandwidth of the OA's [40-42]. Yet another solution to this problem will be to improve the performance of the active elements themselves through the use of actively compensated OA's that possesses superior characteristics such as the previously proposed CNOA's.

In this chapter, the applications of the Composite Operational Amplifiers CNOA's (for N = 2,3,4), in positive negative, and differential finite gain amplification, are presented. The transfer functions of the four C2OA designs previously presented in Chapter II are given as well as theoretical and experimental results in finite gain applications. Effect of single OA's second pole on the design stability is discussed.

For the different C3OA and C4OA designs presented in the previous chapter, the finite gain expressions, as well as the theoretical, computer simulations and experimental results are also presented.

Comparison of all CNOA's in finite gain applications with the state of the art designs illustrates the excellent performance of

these general designs.

3.2 FINITE GAIN APPLICATIONS USING THE PROPOSED C2OA'S

Several C2OA's were examined in finite gain applications. A total of twenty-seven different finite gain transfer functions were derived for all the twenty-seven promising designs, Appendix B. After applying the performance criteria described in Chapter II, the four previously selected C2OA's were found to be superior to all other designs.

The application of these four proposed C2OA's in positive and negative finite gain amplification is given in Table 3.1. Also, for the sake of illustration, the use of C2OA-2 as a differential finite gain amplifier, Fig. 3.1, can be shown to have the input-output relationship given by:

$$V_o = T_{i1} \left[\frac{1}{1+s/\omega_p Q_p+s^2/\omega_p^2}\right] V_1 + T_{i2} \left[\frac{1}{1+s/\omega_p Q_p+s^2/\omega_p^2}\right] V_2 \qquad (3.1)$$

where

$$T_{i1} = X (1+K)/(1+X)$$

$$T_{i2} = -K$$

$$\omega_p = \sqrt{\omega_1\omega_2}/(1+K)$$

$$Q_p = \sqrt{\omega_1/\omega_2} \cdot (1+\alpha)/\sqrt{1+K}$$

x and K are resistor ratios as shown in Fig. 3.1.

In all the applications given in this chapter, each of the actual input-output relationships T_a is in the form

$$T_a = T_i \cdot N/D \qquad (3.2)$$

C20A	Negative Finite Gain Trans. Function (Ta)	Positive Finite Gain Trans. Function (Ta)	ω_p	Q_p
C20A-1	$T_1 \dfrac{1}{1 + (S/\omega_p Q_p) + (S^2/\omega_p^2)}$	$T_1 \dfrac{(1+S/\omega_1)}{1 + (S/\omega_p Q_p) + (S^2/\omega_p^2)}$	$\sqrt{\dfrac{\omega_1\omega_2}{1+k}}$	$\dfrac{(1+\alpha)}{\sqrt{1+k}}\sqrt{\dfrac{\omega_2}{\omega_1}}$
C20A-2	$T_1 \dfrac{1}{1 + (S/\omega_p Q_p) + (S^2/\omega_p^2)}$	$T_1 \dfrac{1}{1 + (S/\omega_p Q_p) + (S^2/\omega_p^2)}$	$\sqrt{\dfrac{\omega_1\omega_2}{1+k}}$	$\dfrac{(1+\alpha)}{\sqrt{1+k}}\sqrt{\dfrac{\omega_1}{\omega_2}}$
* C20A-3	$T_1 \dfrac{(1+S/\omega_1)}{1 + (S/\omega_p Q_p) + (S^2/\omega_p^2)}$	$T_1 \dfrac{1}{1 + (S/\omega_p Q_p) + (S^2/\omega_p^2)}$	$\sqrt{\dfrac{\omega_1\omega_2}{(1+k)(1+\alpha)}}$	$\sqrt{\dfrac{(1+k)(1+\alpha)\cdot\omega_1}{\omega_z}}$
C20A-4	$T_1 \dfrac{[1+(1+\alpha)S/\omega_1]}{1 + (S/\omega_p Q_p) + (S^2/\omega_p^2)}$	$T_1 \dfrac{(1+\alpha S/\omega_1)}{1 + (S/\omega_p Q_p) + (S^2/\omega_p^2)}$	$\sqrt{\dfrac{\omega_1\omega_2}{(1+k)(1+\alpha)}}$	$\sqrt{\dfrac{(1+k)}{(1+\alpha)}}\cdot\dfrac{\omega_1}{\omega_2}$
	$\dfrac{V_0}{V_1} = -k = T_1$	$\dfrac{V_0}{V_1} = (1+k) = T_1$	T_1(Ideal Transfer Function)	

* $\alpha R_1 \ll kR$ (for maximum ω_p)

TABLE 3.1. Negative and Positive Finite Gain Transfer
Functions Using the C20A's .
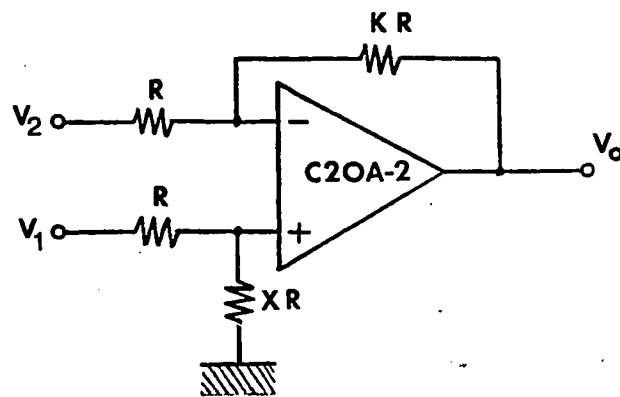
Fig. 3.1.   Application of the C2OA-2 as a Differential
Finite Gain Amplifier .

where T_i = The transfer function realized assuming ideal OA's.

$N = 1 + as = 1 + (s/\omega_z)$. [a is zero $(\omega_z \to \infty)$ in some cases].

$D = a + b_1 s + b_2 s^2 = 1 + (s/\omega_p Q_p) + (s^2/\omega_p^2)$.

Thus, (N/D) determines the amplitude and phase deviation of T_a from T_i. Also b_1 and b_2 determine the stability of T_a. a, b_1, and b_2 and consequently ω_z, ω_p and Q_p, are functions of the circuit parameters which are ω_1, ω_2 and α (as well as τ_t, the integrator time constant in the inverting integrator case, as will be shown later in Chapter IV). None of the a and b coefficients is realized through differences. This guarantees the low sensitivity of T_a, ω_z, ω_p, and Q_p to the circuit parameters. On the other hand, the b coefficients are always positive (assuming single pole OA model), which guarantees the stability of the transfer function. From Table 3.1, a ±5% mismatch in ω_1 and ω_2 results in ±5% change in ω_p and ±2.5% change in Q_p. Hence single OA's with mismatch gain bandwidth products within practical ranges can be used without appreciably affecting the stability or the sensitivity of the finite gain.

3.2.1 Effect of the Single OA's Second Pole on the Stability of the C2OA's

In the following, the stability properties of the positive and negative finite gain amplifier realizations using a two pole open loop model of the single OA's is studied. A_1 is assumed equal to A_2. The analysis is simplified without affecting the

reliability of the conclusions. This is due to the absence of gain differences in all the gain expressions obtained as seen from (2.3) to (2.6) and (3.1) and Table 3.1.

Let $A = A_1 = A_2$

where $1/A$ is given by

$$(1/A) = \left[1+(s/\omega_h)\right] \cdot \left[(s/A_o\omega_L)+(1/A_o)\right] \tag{3.3}$$

$\omega_h \gg \omega_L$ as shown in Fig. 3.2.

By applying the Routh-Hurwitz stability criterion, the necessary and sufficient condition for stability using C20A-1 or C20A-2 realizations is found to be

$$(1+\alpha) < (1+K)/2 \tag{3.4}$$

For C20A-3 the condition is found to be

$$(1+\alpha) > \sqrt{(1+K)} \tag{3.5}$$

Also, for C20A-4, the condition is given by

$$(1+\alpha) > 4 (1+K) \tag{3.6}$$

From (3.2), it is desirable to choose α such that Q_p and ω_p result in acceptable amplitude and phase deviation in T_a from T_i, while satisfying the necessary and sufficient conditions for stability. Table 3.2 gives the values of α for $Q_p = 1/\sqrt{2}$ (maximally flat) and $Q_p = 1$ for the realizations in Table 3.1. The relative useful BW of the different finite gain amplifiers can be obtained by comparing the ω_p's in Table 3.2. As ω_p increased for a fixed Q_p, both amplitude and phase deviations of T_a from T_i at a given frequency ω ($\omega < \omega_p$)

C20A$_i$	1+α	Q_p	ω_p	Stability Condition for α used
C20A-1 &	$\sqrt{1+k}$	1	$\dfrac{\omega_i}{\sqrt{1+k}}$	Satisfied
C20A-2	$\sqrt{\dfrac{1+k}{2}}$	$\dfrac{1}{\sqrt{2}}$	(independent of α)	Satisfied
C20A-3	0	$Q_{p_{min}} = \sqrt{1+k}$	$\dfrac{\omega_i}{\sqrt{1+k}}$	Unsatisfied
C20A-4	(1+k)	1	$\dfrac{\omega_i}{1+k}$	Unsatisfied
	2(1+k)	$\dfrac{1}{\sqrt{2}}$	$\dfrac{\omega_i}{\sqrt{2}(1+k)}$	Unsatisfied

TABLE 3.2. Values of α for Maximally Flat & for Q_p = 1, their Corresponding Bandwidth and Stability Conditions of C20A's in the Finite Gain Applications .

decreases. It is clear that C2OA-1 and C2OA-2 are the two most attractive configurations from the BW and stability considerations. It is to be noted that some special cases of finite gain amplifiers using C2OA-1, C2OA-2, C2OA-3, and C2OA-4 in positive finite gain applications were reported in the literature [4,7,31,32,43,54,62] and cited for their improved performance.

3.2.2 The Bandwidth Improvements Using C2OA's in Finite Gain

Applications

The BW of a finite gain amplifier, realized using a single OA, shrinks approximately by a multiplying factor $(1/K)$ relative to its unity gain 3 dB BW (ω_i). Also the optimum (maximally flat), 3 dB BW using a cascade of two (single OA realization) finite gain amplifiers, is obtained when each amplifier has a gain of $\sqrt{K}$, to realize an overall gain K. The resulting BW shrinks by $\sqrt{0.44}/\sqrt{K} = 0.66/\sqrt{K}$ relative to ω_i [31]. The BW of C2OA-1 and C2OA-2 circuits can be designed to shrink only by a factor of $\approx 1/\sqrt{K}$ for $Q_p = 0.707$ (maximally flat), and greater than $1/\sqrt{K}$ for $Q_p=1$ $(K\gg1)$. In addition, the C2OA's require only two accurate gain determining components compared with four in the cascade realization. Fig. 3.3 shows the improvement by comparing the BW's obtainable in these different cases.

3.2.3 Experimental Results Using C2OA's in Finite Gain

Applications

Experimental results of negative finite gain amplifier realizations are given in Figs. 3.4.a - 3.4.d using the C2OA-1 of
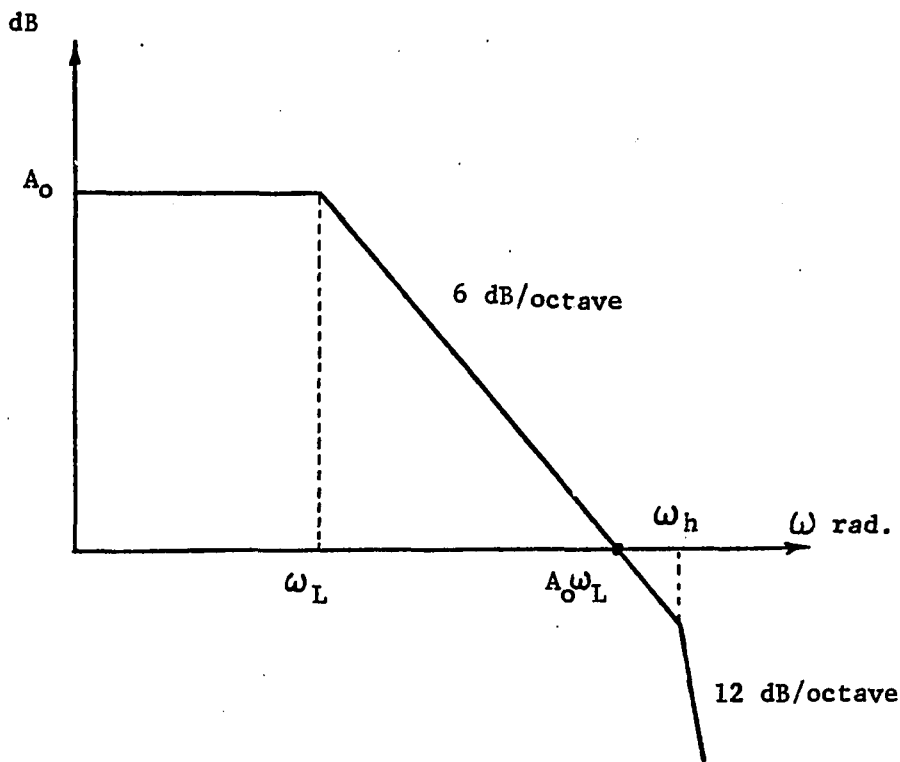
Fig. 3.2.   Open Loop Frequency Response of a Two-Pole
OA .

(1) Single OA.

(2) Two cascaded single OA's.

(3) C2OA-1.
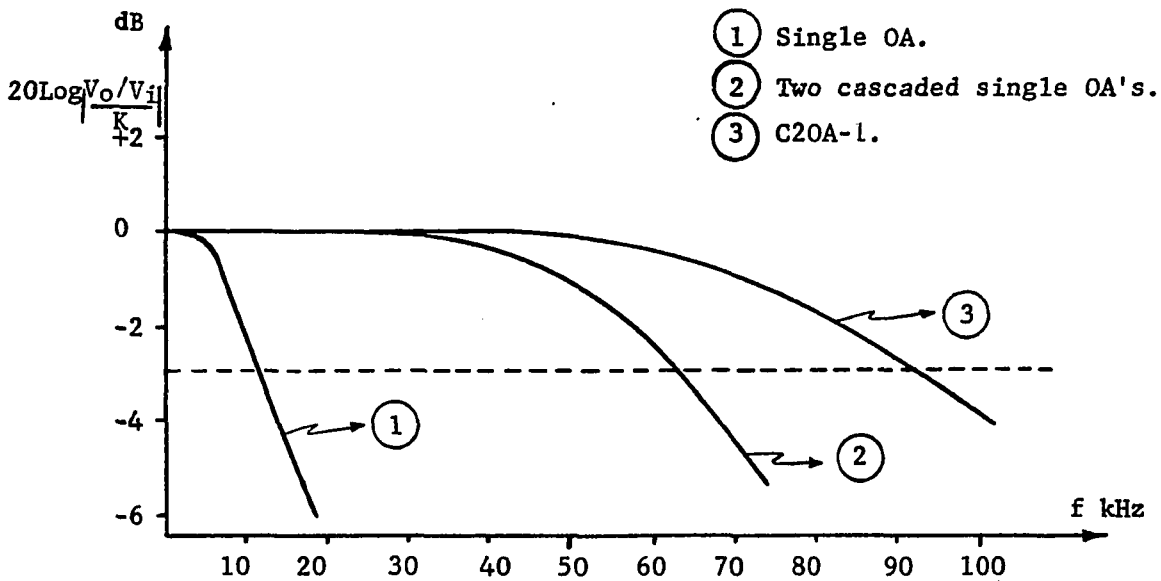
Fig. 3.3.   Theoretical Frequency Response of Negative
Finite Gain Amplifiers Realized Using Single
OA, Two Cascaded Single OA's, and C2OA-1 for
Negative Gain of 100. (Assuming OA GBWP =
1 MHz) .

Fig. 2.6.a. LM747 Dual OA's with GBWP $\simeq 1$ to 1.5 MHz are used to implement the C2OA's in this chapter as well as in the entire experimental work throughout this dissertation. Fig. 3.4.a shows the maximally flat response ($Q_p = 0.707$) for closed loop gain of -25, -50, and -100. The BW extension shown here complies with the expected results according to table 3.1, e.g. for a gain K of -100 the 3 dB BW $\simeq \sqrt{\omega_1 \omega_2/(1+K)} \simeq 1000/\sqrt{101} \simeq 100$ K Hz. In Fig. 3.4.b, the effect of active compensation on extending the BW for a gain of +100 is illustrated for $Q_p = 0.5$, 0.707 and 1. This is achieved by only controlling the compensating resistor ratio α. The stability and low sensitivity to the power supply and to the active compensation resistor variations are examined as shown in Figs. 3.4.c and 3.4.d, for maximally flat response of gain +50 and +100. Comparing the results in Fig. 3.4 with those of the single amplifier realizations in Fig. 3.5.a and 3.5.b, for the same GBWP and gain K, illustrates the considerable improvement in the useful BW, without sacrificing any of the single OA attractive features, namely, the low sensitivity to circuit elements and power supply variations, stability and versatility.

The sensitivity and stability properties of the differential finite gain amplifier using C2OA-2, Fig. 3.1, can be shown to be similar to those derived for C2OA-2 in positive and negative finite gain amplification above.

To illustrate the usefulness of the derived C2OA's, a common application is chosen; namely, negative finite gain amplification.
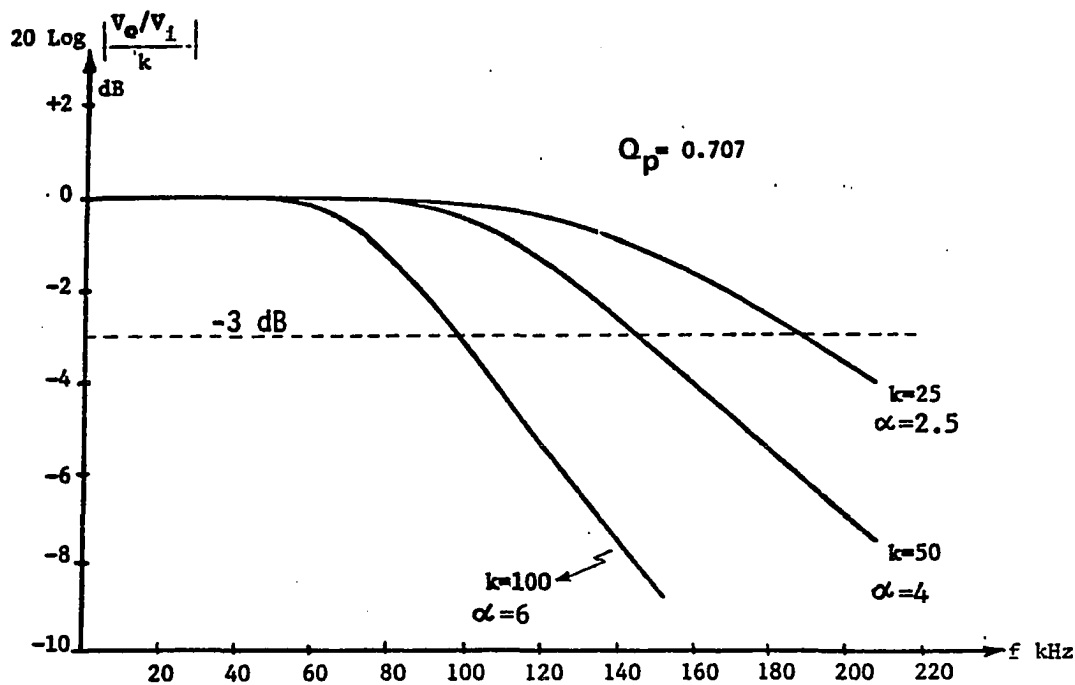
Fig. 3.4.a.   Maximally Flat ($Q_p = 0.707$) Responses,
Closed Loop Gains = -25, -50, -100 .
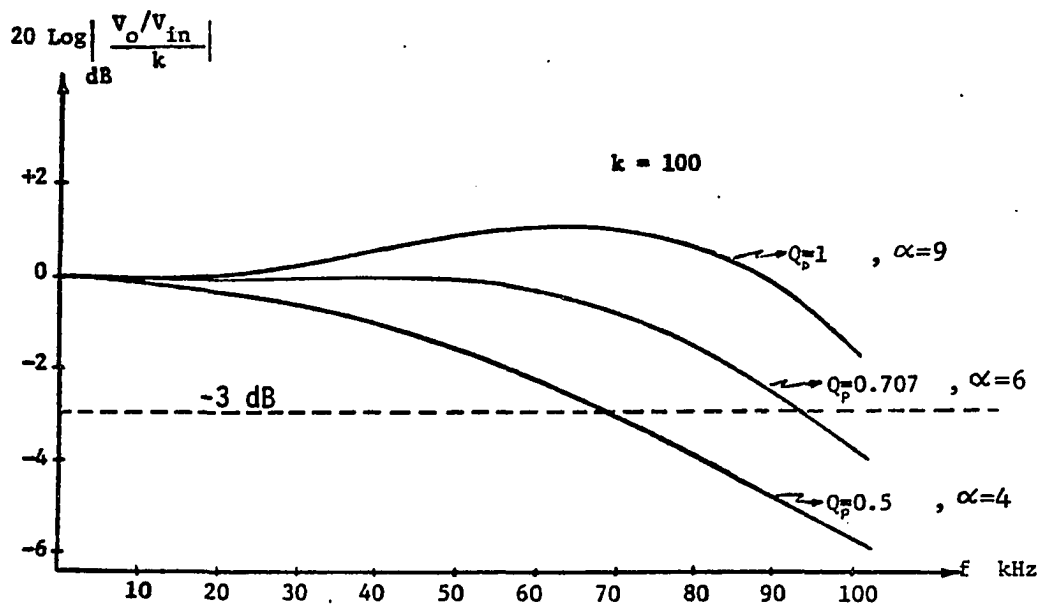
Fig. 3.4.b.   Effect of Active Compensation on Extending
the Bandwidth .

$20 \log \left|\dfrac{V_o/V_i}{k}\right|$
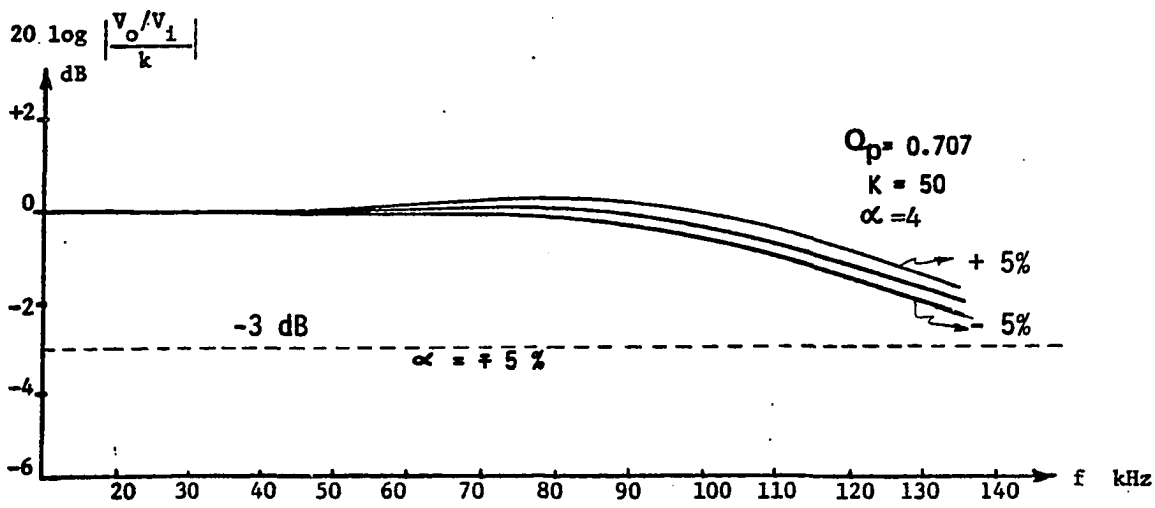
Fig. 3.4.c.   Effect of Compensation Resistor-Ratio Variations by ±5% .

$20 \log \left|\dfrac{V_o/V_{in}}{k}\right|$
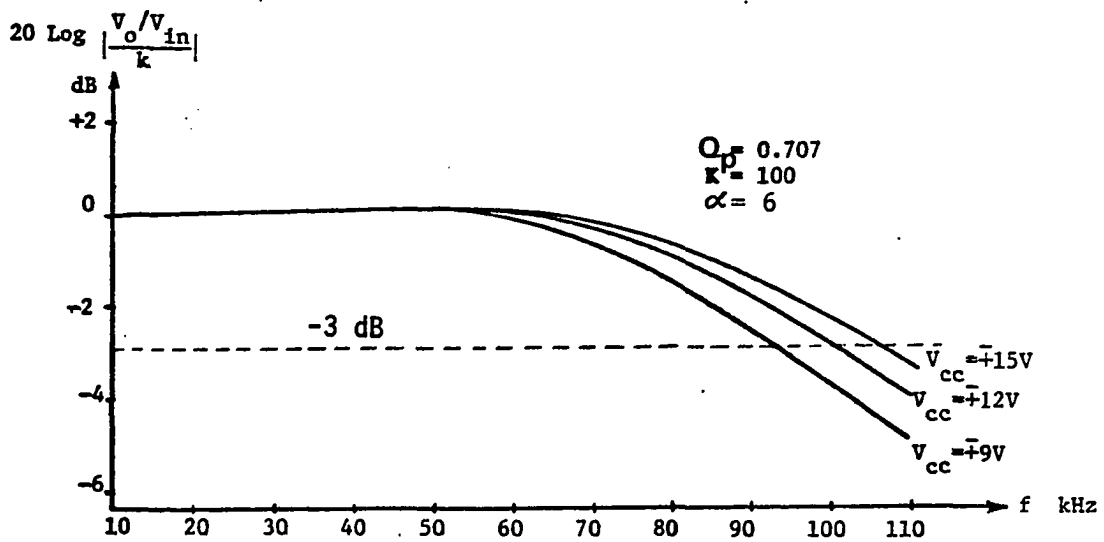
Fig. 3.4.d.   Effect of Power Supply Variations From ±9V to ±15V .

Fig. 3.4.   Experimental Results Using C20A-1 in Negative Finite Gain Applications .
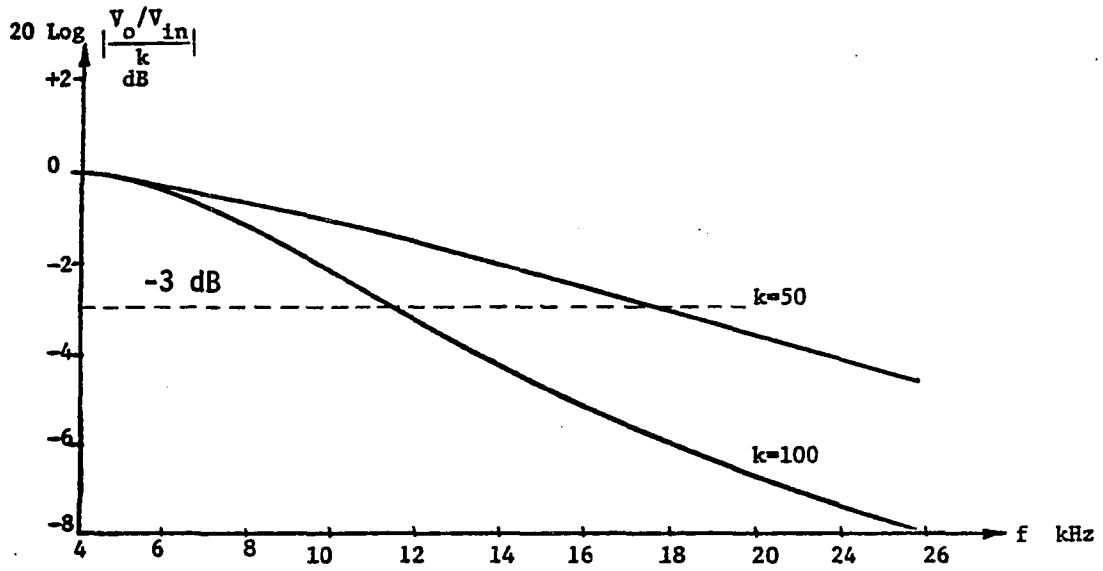
Fig. 3.5.a.   Single OA Frequency Response For Closed
                Loop Gain of -50 and -100 .
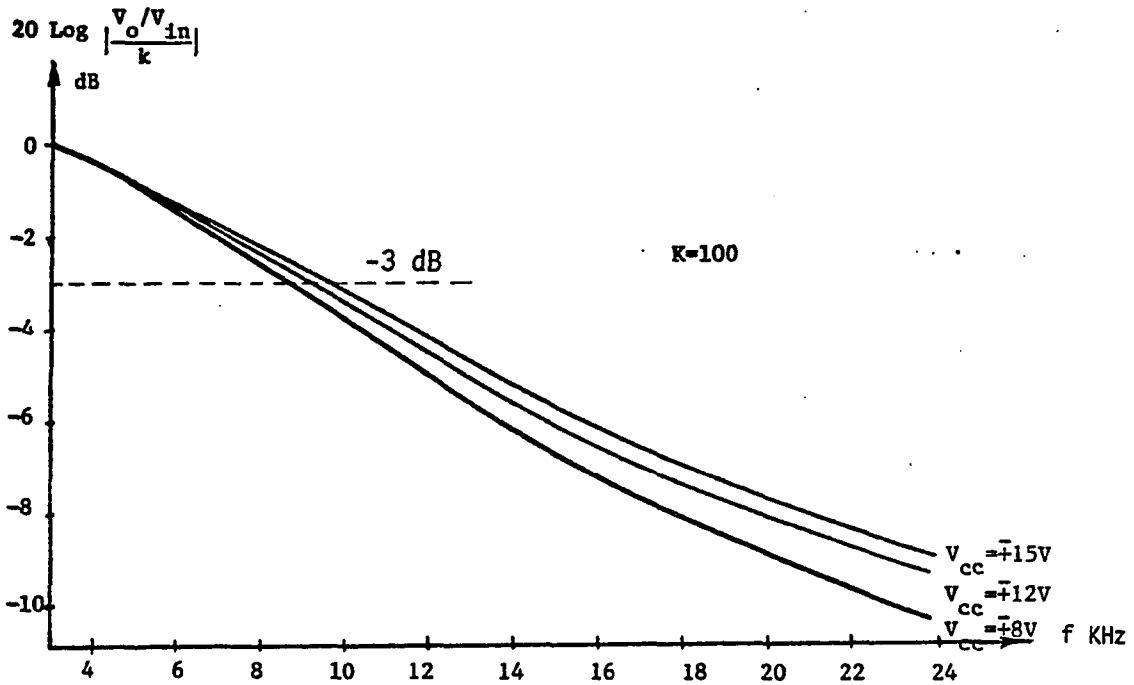
Fig. 3.5.b.   Effect of Power Supply Variations.From ±8V
                to ±15V .

Fig. 3.5.   Experimental Results Using Single OA's
                (LM 747 OA) .

The performance of the C2OA-1 and C2OA-2 in this application is compared with some of the best recently reported negative finite gain realiztions using a similar number of OA's [19-25,43]. It is to be noted that the realizations reported in [19] and [21] are special case of C2OA-4, where $\alpha = 0$, i.e., the controlling parameter α disappears, and the designs will lack only control on magnitude and phase compensation.

The results are shown in Fig. 3.6 for nominal gains $\gg$ 1 for practical reasons since as K increases the useful BW shrinks and extending the operating frequencies becomes more important. The results in Fig. 3.6.a and 3.6.b show clearly the excellent gain and phase performance of the proposed realizations relative to the state-of-the-art designs.

3.3 FINITE GAIN APPLICATIONS USING C3OA'S AND C4OA'S

Wideband positive, negative and differential composite amplifiers can be designed using the CNOA's structures proposed in Chapter II, and shown in Figs. 2.8 and 2.9.

Positive finite gain and negative finite gain expressions for several C3OA's and C4OA's are shown in Appendices C and D. Four of those expressions of each of the C3OA's and C4OA's realizations that showed superior performance are given in Table 3.3 and 3.4 respectively. As can be seen from these expressions in Table 3.3 and 3.4, as well as the open loop expressions of the corresponding CNOA's of Table 2.1 and 2.2, no differences in the transfer function coefficients are encountered, thus low coefficient

dB

37

36

35

34

33

32

30

[43]

[24]

51.14 dB
at 140 kHz.

[19,21]
C20A-4
$\alpha = 0$

C20A-1 Proposed design
for $Q_p = 1$
$\alpha = 6.15$

C20A-1 Proposed design
for $Q_p = -.707$
$\alpha = 4$

f kHz.

10 20 30 40 50 60 70 80 90 100 110 120 130 140 150
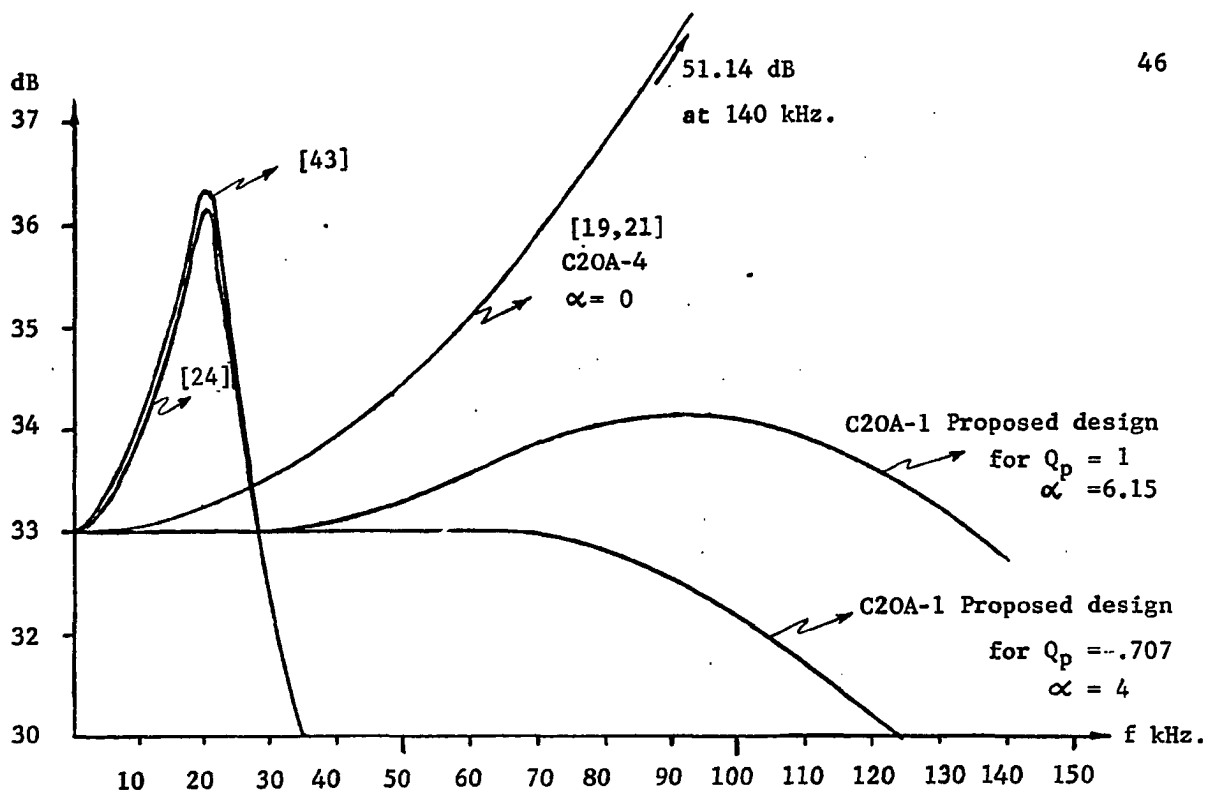
Fig. 3.6.a.   Amplitude Frequency Responses of Negative
Finite Gain Amplifiers .

$\phi°$

0

-10

-20

-30

-40

-50

-60

-70

-80

[19,21]
C20A-4
$\alpha = 0$

C20A-1
$\alpha = 6.15$

[24]

C20A-1
$\alpha = 4$

[43]

f kHz.

10 20 30 40 50 60 70 80 90 100 110 120 130 140 150
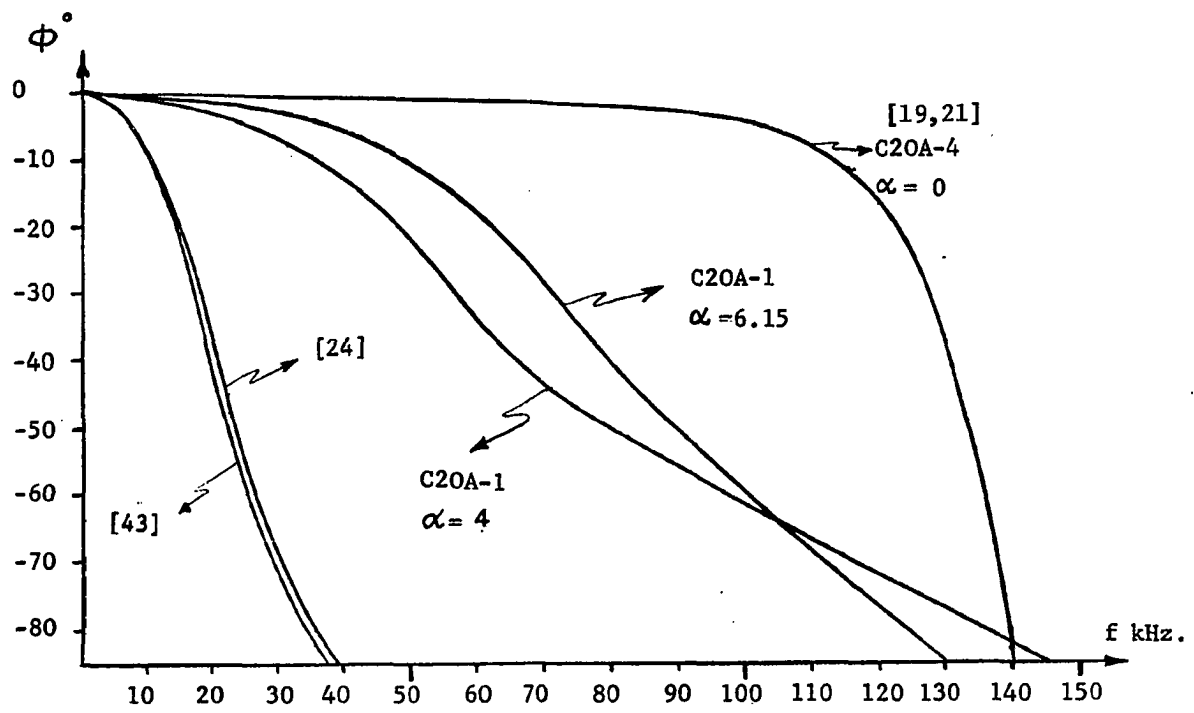
Fig. 3.6.b.   Phase Responses of Negative Finite Gain
Amplifiers .

Fig. 3.6.   Comparison of the Negative Finite Gain
Amplifiers Using C20A's with the State of
the Art Two-OA's Realizations (OA GBWP =
1 MHz) .

C30A	Finite Gain Transfer Function		Stability Condition
C30A-1	$$\frac{V_o}{V_i} = \frac{-k(1+\frac{S}{\omega_1})}{1 + (1+\frac{1+k}{1+\beta})\frac{S}{\omega_1} + (\frac{1+k}{1+\alpha})\frac{S^2}{\omega_2\omega_3} + (1+k)\frac{S^3}{\omega_1\omega_2\omega_3}}$$	Negative Finite Gain Trans. Func.	$(1+k) > \alpha(1+\beta)$
	$$\frac{V_o}{V_i} = \frac{(1+k)(1+\frac{1}{1+\alpha}\frac{S}{\omega_3} + \frac{S^2}{\omega_1\omega_2})}{1+(1+\frac{1+k}{1+\beta})\frac{S}{\omega_1} + (\frac{1+k}{1+\alpha})\frac{S^2}{\omega_2\omega_3} + (1+k)\frac{S^3}{\omega_1\omega_2\omega_3}}$$	Positive Finite Gain Trans. Func.	
C30A-2	$$\frac{V_o}{V_i} = \frac{-K(1+S/\omega_2)}{1+ [\frac{1}{\omega_2} + \frac{1+k}{\omega_1(1+\beta)}]S + \frac{(1+k)}{(1+\alpha)}\frac{S^2}{\omega_1\omega_2} + (1+k)\frac{S^3}{\omega_1\omega_2\omega_3}}$$	Negative Finite Gain Trans. Func.	$(1+k) > \alpha(1+\beta)$
	$$\frac{V_o}{V_i} = \frac{(1+K)(1+S/\omega_2)}{1+ [\frac{1}{\omega_2} + \frac{1+k}{\omega_1(1+\beta)}]S + \frac{(1+k)}{(1+\alpha)}\frac{S^2}{\omega_1\omega_2} + (1+k)\frac{S^3}{\omega_1\omega_2\omega_3}}$$	Positive Finite Gain Trans. Func.	
C30A-3	$$\frac{V_o}{V_i} = \frac{-K}{1 + (\frac{1+k}{1+\beta})\frac{S}{\omega_3} + (\frac{1+k}{1+\alpha})\frac{S^2}{\omega_1\omega_3} + (1+k)\frac{S^3}{\omega_1\omega_2\omega_3}}$$	Negative Finite Gain Trans. Func.	$(1+k) > (1+\alpha)(1+\beta)$
	$$\frac{V_o}{V_i} = \frac{(1+K)(1+\frac{1}{1+\alpha}\frac{S}{\omega_1} + \frac{S^2}{\omega_1\omega_2})}{1 + (\frac{1+k}{1+\beta})\frac{S}{\omega_3} + (\frac{1+k}{1+\alpha})\frac{S^2}{\omega_1\omega_2} + (1+k)\frac{S^3}{\omega_1\omega_2\omega_3}}$$	Positive Finite Gain Trans. Func.	
C30A-4	$$\frac{V_o}{V_i} = \frac{-K}{1 + (\frac{1+k}{1+\beta})\frac{S}{\omega_1} + (\frac{1+k}{1+\alpha})\frac{S^2}{\omega_1\omega_2} + (1+k)\frac{S^3}{\omega_1\omega_2\omega_3}}$$	Negative Finite Gain Trans. Func.	$(1+k) > (1+\alpha)(1+\beta)$
	$$\frac{V_o}{V_i} = \frac{(1+K)}{1 + (\frac{1+k}{1+\beta})\frac{S}{\omega_1} + (\frac{1+k}{1+\alpha})\frac{S^2}{\omega_1\omega_2} + (1+k)\frac{S^3}{\omega_1\omega_2\omega_3}}$$	Positive Finite Gain Trans. Func.	

Negative Finite Gain Configuration
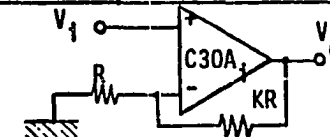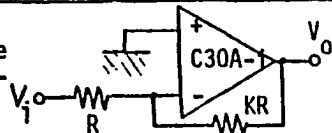
Positive Finite Gain Configuration

TABLE 3.3.   Negative and Positive Finite Gain Transfer Functions Using the C30A's .

47

C40A	Finite Gain Transfer Function	
C40A-1	$$\frac{V_o}{V_i} = \frac{-k(1+S/\omega)}{1+\frac{S}{\omega}[1+\frac{(1+k)}{(1+\alpha)(1+\gamma)}]+\frac{S^2}{\omega^2}(1+k)[\frac{1}{1+\gamma}+\frac{1}{(1+\alpha)(1+\beta)}]+\frac{S^3}{\omega^3}(1+k)[\frac{1}{1+\beta}+\frac{1}{1+\alpha}]+\frac{S^4}{\omega^4}(1+k)}$$	Negative Finite Gain Trans. Func.
	$$\frac{V_o}{V_i} = \frac{\{1+k\}\{1+\frac{S}{\omega}[\frac{1}{1+\beta}+\frac{1}{1+\gamma}]+\frac{S^2}{\omega^2}[\frac{2+\beta}{1+\beta}]+\frac{S^3}{\omega^3}\}}{1+\frac{S}{\omega}[1+\frac{(1+k)}{(1+\alpha)(1+\gamma)}]+\frac{S^2}{\omega^2}(1+k)[\frac{1}{1+\gamma}+\frac{1}{(1+\alpha)(1+\beta)}]+\frac{S^3}{\omega^3}(1+k)[\frac{1}{1+\beta}+\frac{1}{1+\alpha}]+\frac{S^4}{\omega^4}(1+k)}$$	Positive Finite Gain Trans. Func.
C40A-2	$$\frac{V_o}{V_i} = \frac{-k}{1+\frac{S}{\omega}[\frac{(1+k)}{(1+\gamma)(1+\beta)}]+\frac{S^2}{\omega^2}[\frac{1+k}{1+\gamma}+\frac{(1+k)}{(1+\alpha)(1+\beta)}]+\frac{S^3}{\omega^3}[\frac{1+k}{1+\alpha}+\frac{1+k}{1+\beta}]+\frac{S^4}{\omega^4}[1+k]}$$	Negative Finite Gain Trans. Func.
	$$\frac{V_o}{V_i} = \frac{(1+k)}{1+\frac{S}{\omega}[\frac{(1+k)}{(1+\gamma)(1+\beta)}]+\frac{S^2}{\omega^2}[\frac{1+k}{1+\gamma}+\frac{(1+k)}{(1+\alpha)(1+\beta)}]+\frac{S^3}{\omega^3}[\frac{1+k}{1+\alpha}+\frac{1+k}{1+\beta}]+\frac{S^4}{\omega^4}[1+k]}$$	Positive Finite Gain Trans. Func.
C40A-3	$$\frac{V_o}{V_i} = \frac{-k(1+S/\omega)}{1+\frac{S}{\omega}[1+\frac{(1+k)}{(1+\beta)(1+\gamma)}]+\frac{S^2}{\omega^2}[1+k][\frac{1}{(1+\alpha)(1+\beta)}+\frac{1}{1+\gamma}]+\frac{S^3}{\omega^3}[1+k][\frac{1}{1+\alpha}+\frac{1}{1+\beta}]+\frac{S^4}{\omega^4}[1+k]}$$	Negative Finite Gain Trans. Func.
	$$\frac{V_o}{V_i} = \frac{(1+k)(1+S/\omega)}{1+\frac{S}{\omega}[1+\frac{(1+k)}{(1+\beta)(1+\gamma)}]+\frac{S^2}{\omega^2}[1+k][\frac{1}{(1+\alpha)(1+\beta)}+\frac{1}{1+\gamma}]+\frac{S^3}{\omega^3}[1+k][\frac{1}{1+\alpha}+\frac{1}{1+\beta}]+\frac{S^4}{\omega^4}[1+k]}$$	Positive Finite Gain Trans. Func.
C40A-4	$$\frac{V_o}{V_i} = \frac{-k}{1+\frac{S}{\omega}[\frac{(1+k)}{(1+\alpha)(1+\gamma)}]+\frac{S^2}{\omega^2}[1+k][\frac{1}{1+\gamma}+\frac{1}{(1+\alpha)(1+\beta)}]+\frac{S^3}{\omega^3}[1+k][\frac{1}{1+\alpha}+\frac{1}{1+\beta}]+\frac{S^4}{\omega^4}[1+k]}$$	Negative Finite Gain Trans. Func.
	$$\frac{V_o}{V_i} = \frac{\{1+k\}\{1+\frac{S}{\omega}[\frac{1}{1+\beta}+\frac{1}{1+\gamma}]+\frac{S^2}{\omega^2}[1+\frac{1}{1+\beta}]+\frac{S^3}{\omega^3}\}}{1+\frac{S}{\omega}[\frac{(1+k)}{(1+\alpha)(1+\gamma)}]+\frac{S^2}{\omega^2}[1+k][\frac{1}{1+\gamma}+\frac{1}{(1+\alpha)(1+\beta)}]+\frac{S^3}{\omega^3}[1+k][\frac{1}{1+\alpha}+\frac{1}{1+\beta}]+\frac{S^4}{\omega^4}[1+k]}$$	Positive Finite Gain Trans. Func.

Negative Finite Gain Configurat.
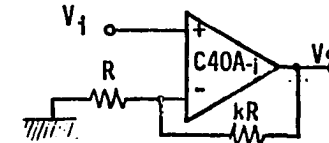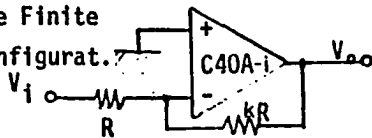
Positive Finite Gain Configuration

TABLE 3.4. Negative and Positive Finite Gain Transfer Functions Using the C40A's .

48

sensitivities are obtained and reasonable OA mismatch is tolerated. It is clear from these expressions, that all the denominator coefficients are positive which is necessary for stability. Using the same technique used in Chapter II and in Section 3.2 of this Chapter, it can be shown that the resistor ratios α, β and γ can be chosen for extended BW and to satisfy the necessary and sufficient stability conditions, assuming single pole models.

3.3.1 The BW Improvements Using CNOA's in Finite Gain

Applications

The optimum maximally flat 3 dB BW using three, (four), single OA finite gain building blocks is obtained by cascading three, (four), identical blocks, each of gain $K^{1/3}$, ($K^{1/4}$), to realize an overall gain K. The overall BW shrinks by a multiplying factor $0.51/K^{1/3}$, ($0.435/K^{1/4}$), relative to ω_i [31]. The new proposed C30A, (C40A), circuits BW are formed to shrink only by a factor $1/K^{1/3}$, ($1/K^{1/4}$), ($K \gg 1$).

Using the results found in this Section and in Section 3.2.2, a general expression for the BW of CNOA's in finite gain applications can be shown to be

$$BW = \omega_i/(K^{1/N}) \text{ for } (K \gg 1) \tag{3.4}$$

where N is the number of single OA used in the CNOA structure.

Maximally flat response (Butterworth) as well as Chebychev characteristics can be achieved by controlling the resistor ratios

α, β, and γ, while satisfying the stability conditions. Computer plots of the simulated C3OA-1 and C4OA-1 transfer functions (magnitude and phase), in positive and negative finite gain configurations are given in Fig. 3.7 and 3.8. In both figures, different compensating values were used to achieve BW extension as well as different Butterworth and Chebychev characteristics for positive and negative finite gain of 100. The 3 dB BW realized in the figure agrees with the BW expression (3.4) e.g. the 3 dB BW of Fig. 3.8.a $\cong$ 350 KHz assuming the GBWP of the single OA used of 1 MHz. All of these finite gain designs have the same attractive dynamic range, stability and low sensitivity properties as the C2OA's designs in Section 3.2. Also, it is worthwhile mentioning that some of the finite gain designs presented here (C3OA-2, C3OA-4, C4OA-2, C4OA-3, and C4OA-5) have identical N/D multiplying factors in the positive and negative gain applications which makes them suitable in differential gain applications with no common mode rejection problem.

3.3.2 <u>Experimental Results Using C3OA's and C4OA's in Finite Gain</u>

<u>Applications</u>

Only sample experimental results are given to illustrate the improvement using C3OA-1 and C4OA-1. Fig. 3.9 gives the experimental results using C3OA-1 in positive finite gain application (K=+38.7). The figure shows the effect of variation of the compensating resistor ratios α and β. The gain of 38.7 is chosen to be the same as the gain used in [44] to be able to
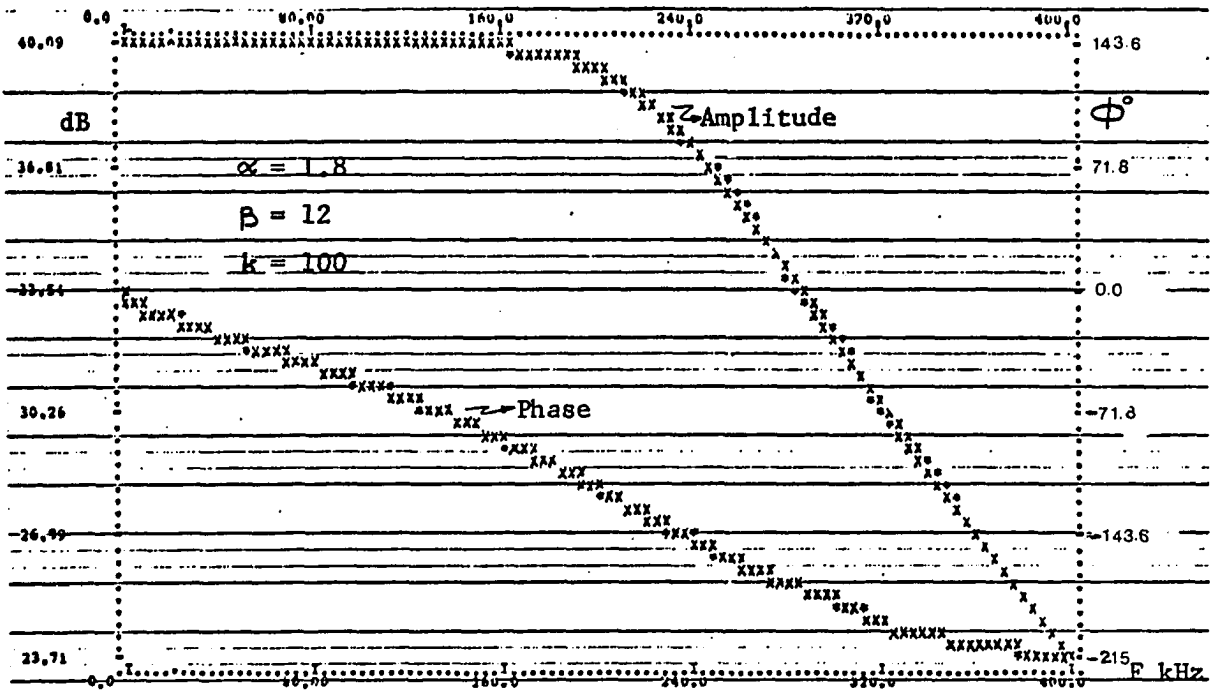
Fig. 3.7.a. Maximally Flat Computed Frequency Response (Amplitude & Phase) of the Positive Finite Gain Amplifier (K=100) Using C30A-1 .
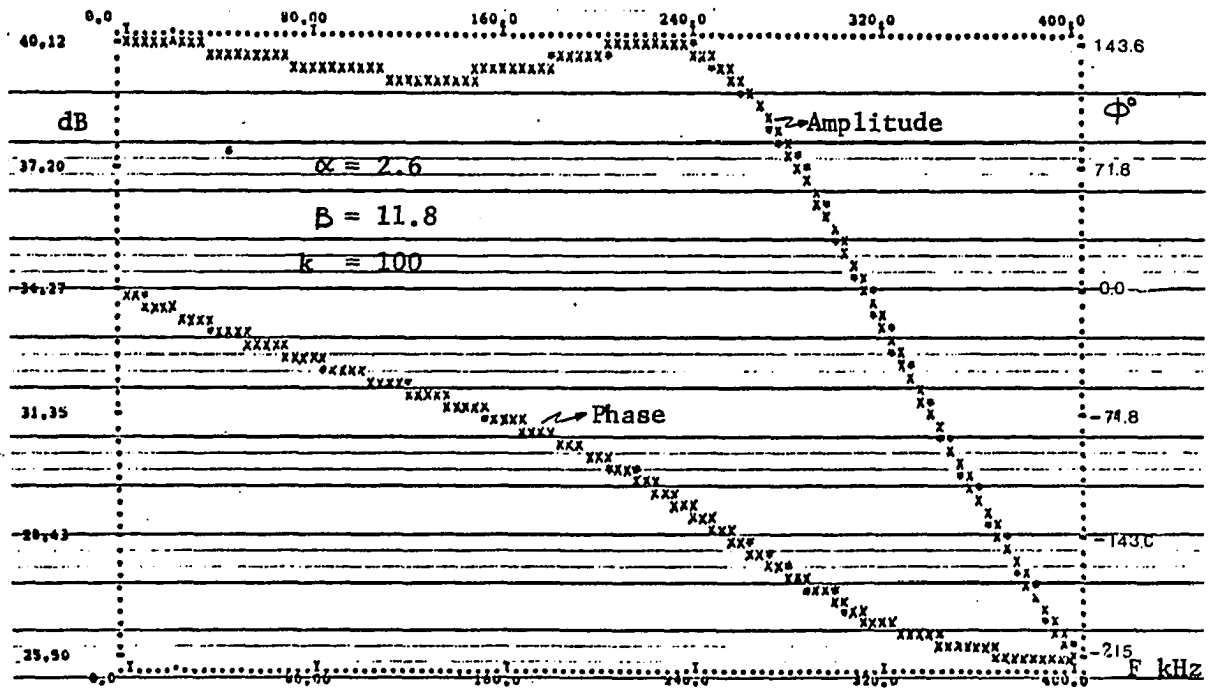
Fig. 3.7.b. Chebychev Computed Frequency Response (Amplitude & Phase) of the Positive Finite Gain Amplifier (K=100) Using C30A-1 .

Fig. 3.7. Computer Plots (Amplitude & Phase) of the C30A-1 Finite Gain Transfer Function for a Gain of 100 (OA GBWP = 1 MHz) .
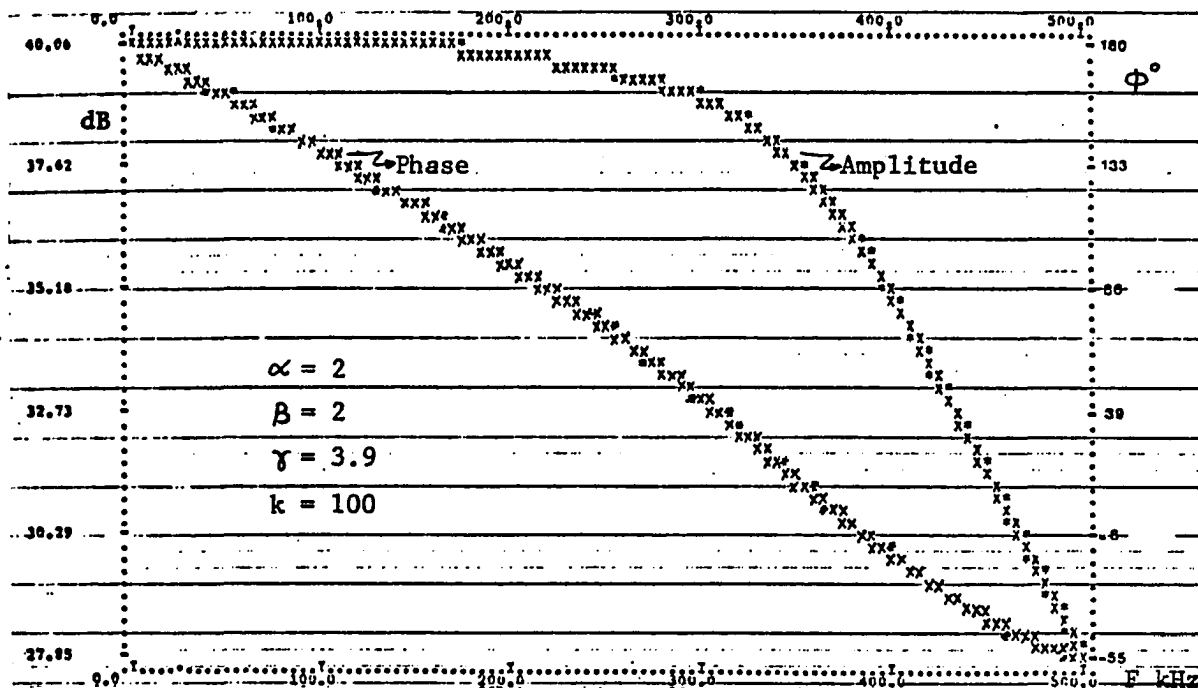
Fig. 3.8.a.   Maximally Flat Computed Frequency Response
(Amplitude & Phase) of the Positive Finite
Gain Amplifier (K=100) Using C40A-1.
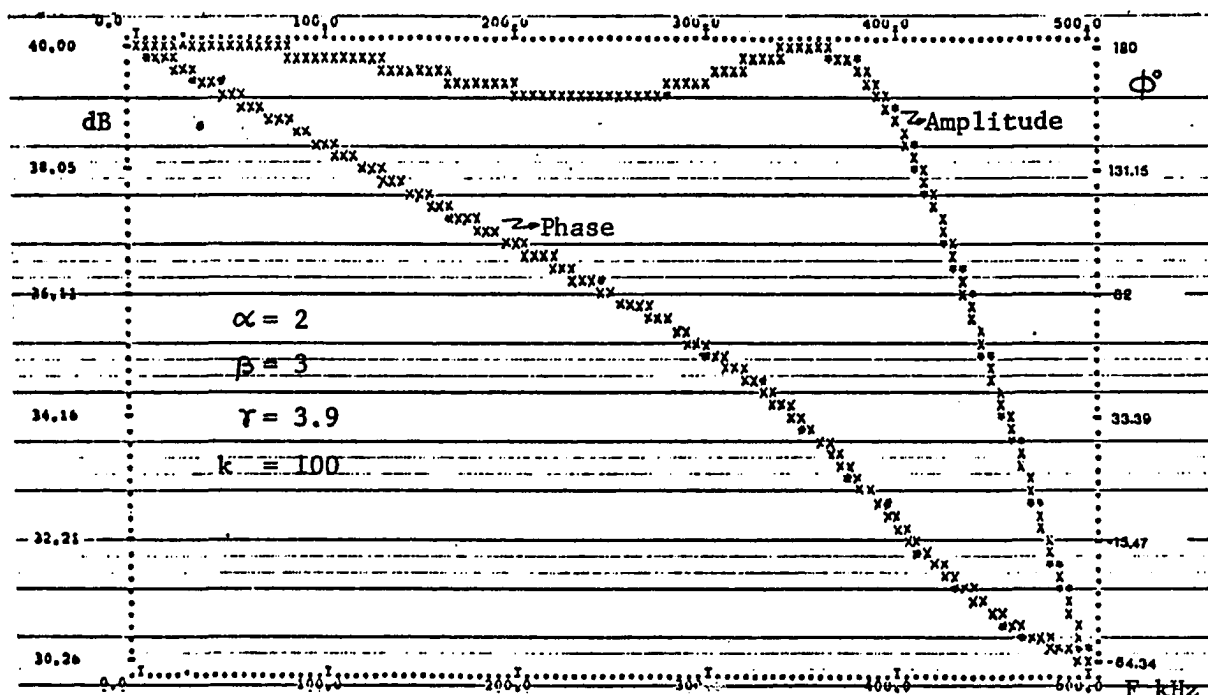
Fig. 3.8.b.   Chebychev Computed Frequency Response (Am-
plitude & Phase) of the Positive Finite
Gain Amplifier (K=100) Using C40A-1.

Fig. 3.8.   Computer Plots (Amplitude & Phase) of the
C40A-1 Finite Gain Transfer Function for a
Gain of 100 (OA GBWP = 1 MHz) .
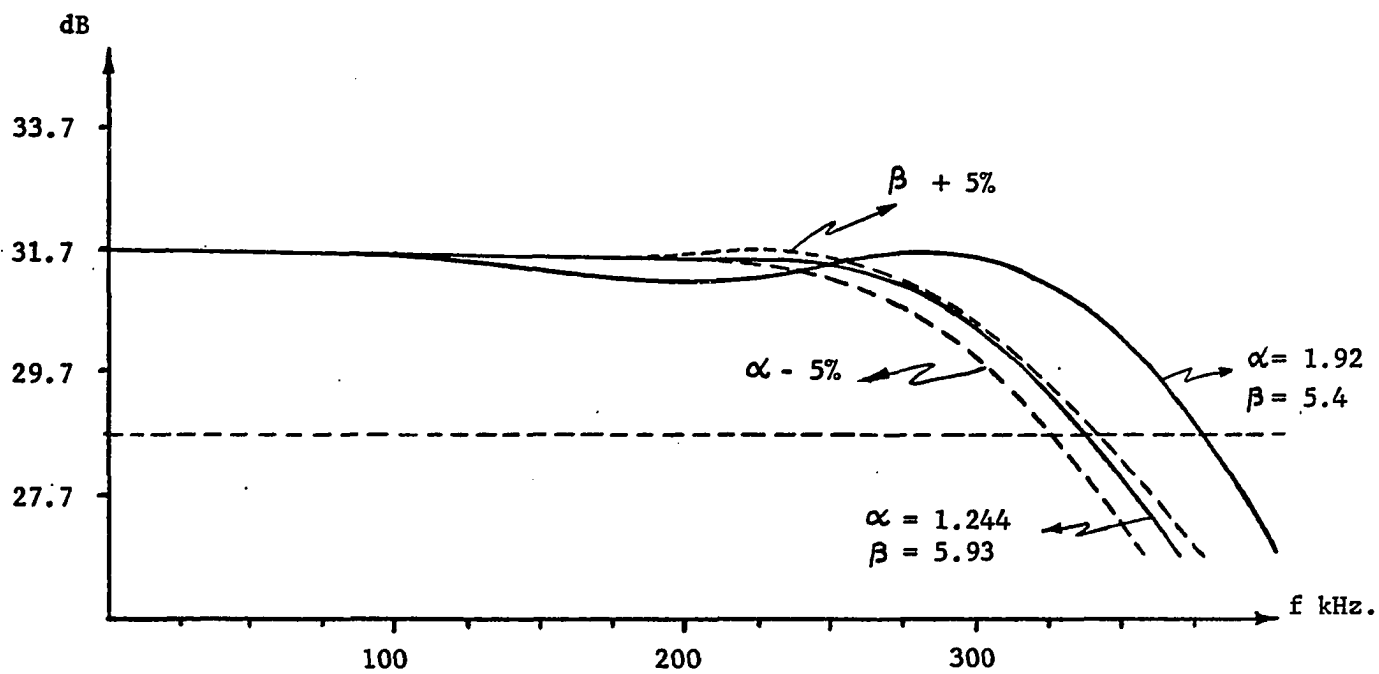
Fig. 3.9.   Experimental Results of C30A-1 in Positive
Finite Gain Application, For a Gain of 38.7,
and the Effect of Variation of the Compen-
sating resistor ratios α and β (LM 747
0A) .

compare with theoretical results using the Zero Second Derivative finite gain amplifier (ZSD), Fig. 3.10, proposed in [44]. For practical reasons, both amplifiers are designed such that the stability condition, using Routh's test on the third order denominator coefficients, is exceeded by a margin of 10%. The best theoretical results using ZSD are obtainable with the minimum stability margin, i.e. $(r_1-1) = 1.1$ βK in Fig. 3.10. This theoretical response as well as the best possible unstable theoretical responses are illustrated in Figs. 3.11.a and 3.11.b for comparison. The figures show the magnitude and phase characteristics of C30A-1 and C40A-1 amplifiers, while satisfying the stability constraints, in positive finite gain of 38.7, for different compensation values. The figure illustrates the extended frequency range of these designs (in both Butterworth and Chebychev responses), over that of the state of the art design [44], or by using 3, (4), stages of cascaded single OA's in the same applications. It is also interesting to note that the condition for stability of the amplifier shown in Table 3.3 using C30A-1 is

$$\alpha < 39.7/(1+\beta) \tag{3.5}$$

This is satisfied by a wide margin in the C30A-1 responses of Figs. 3.11.a and 3.11.b, since $\alpha = 1.25$ and $\beta = 5.93$ in the maximally flat response, and $\beta = 5.4$ in the Chebychev response. The reason for using theoretical responses in the comparison, was
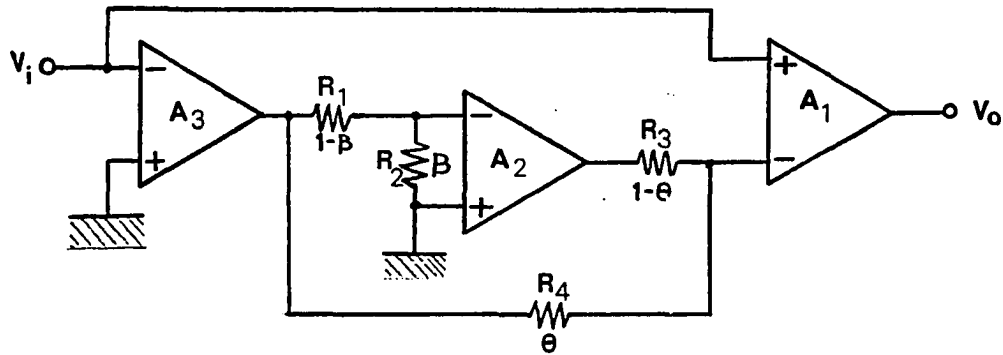
$$\frac{V_o}{V_i} \simeq \frac{\theta\beta + \frac{S}{\omega_2}(1-\theta) + \frac{S^2}{\omega_2\omega_3}}{S^3/\omega_1\omega_2\omega_3}$$

Fig. 3.10.a.   The Zero Second Derivative (ZSD) Infinite
Gain Amplifier .
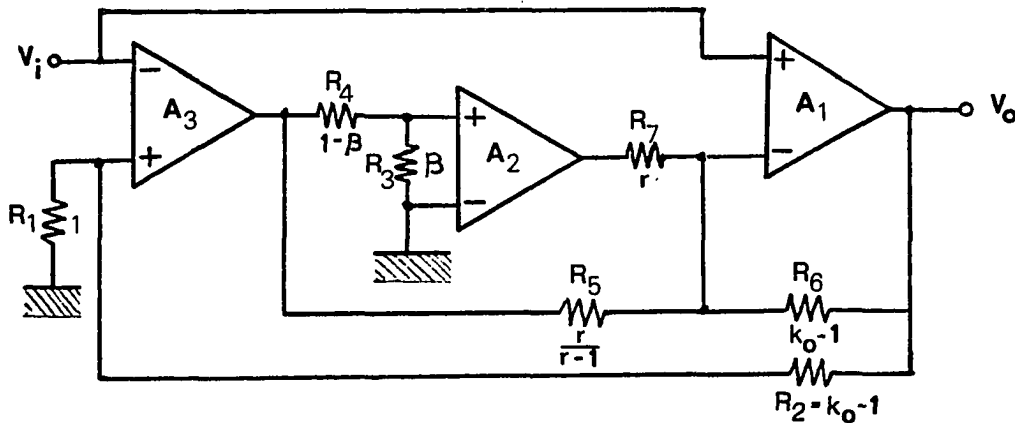
$$\frac{V_o}{V_i} = k_o \frac{1 + \frac{S}{\omega_2}\frac{(r-1)}{\beta} + \frac{S^2}{\omega_2\omega_3}\frac{r}{\beta}\frac{k_o}{(k_o-1)}}{1 + \frac{S}{\omega_2}\frac{(r-1)}{\beta} + \frac{S^2}{\omega_2\omega_3}\frac{r}{\beta}\frac{k_o}{(k_o-1)} + \frac{S^3}{\omega_1\omega_2\omega_3}\frac{r}{\beta}\frac{k_o^2}{(k_o-1)}}$$

Fig. 3.10.b.   The Zero Second Derivative (ZSD) Finite
Gain Amplifier .

Fig. 3.10.   The Zero Second Derivative Amplifier (ZSD)
Proposed in [44] .

20 Log $\left|\dfrac{V_o}{V_i}\right|$

dB

(1) [44] r=1.1 , β=10^{-8} (stable with min. margin)

(2) [44] r= 2 , β=0.2 (unstable).

(3) C30A-5 α= 1.9 , β = 5.4.

(4) C30A-5 α= 1 , β = 6.4.

(5) C40A-5 α= .6 , β = 2.4 , γ = 12.5.

(6) Cascade of 3 stages of OA's each of gain $(38.7)^{\frac{1}{3}}$

(7) Cascade of 4 stages of OA's each of gain $(38.7)^{\frac{1}{4}}$

38
37
36
35
34
33
32
31
30

100   200   300   400   f KHz.
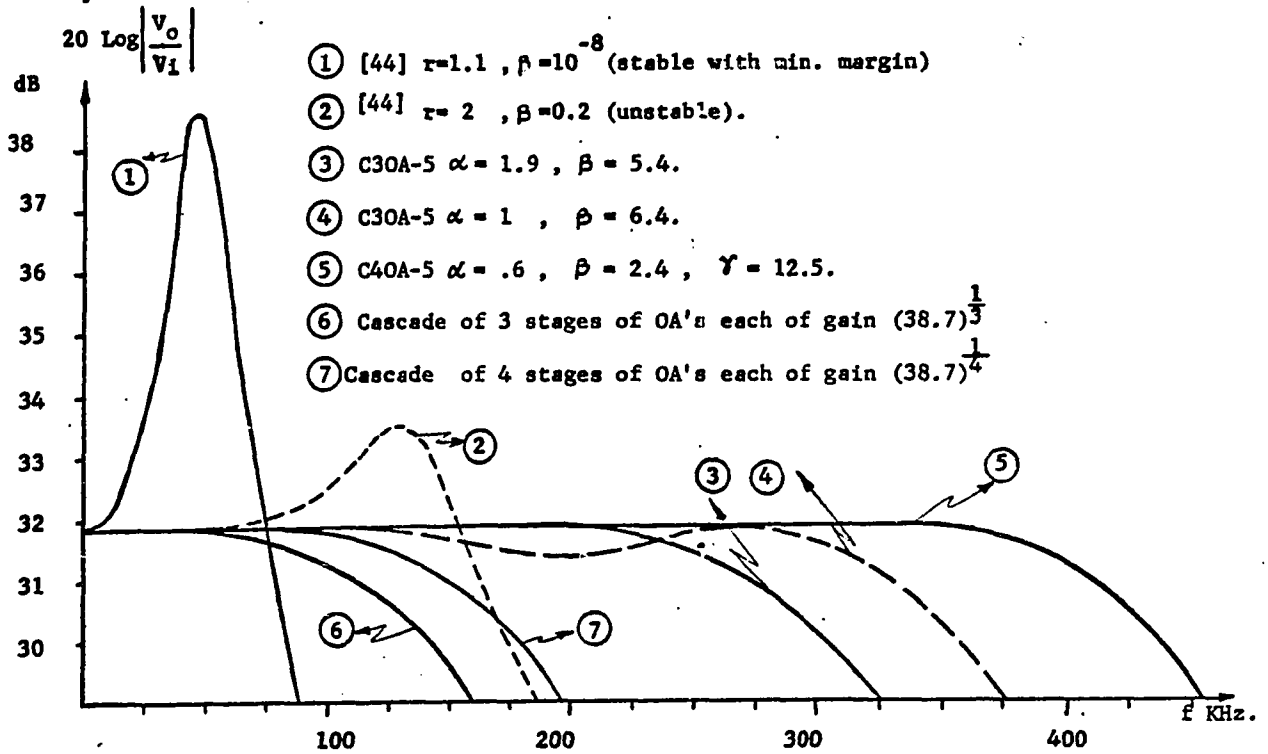
Fig. 3.11.a.   Theoretical Amplitude Responses of C30A-5, C40A-5, and [44]   for Positive Finite Gain Applications .

$|\phi_0|$

0
10
20
30
40
50
60
70
80
90

100   200   300   400   f KHz.
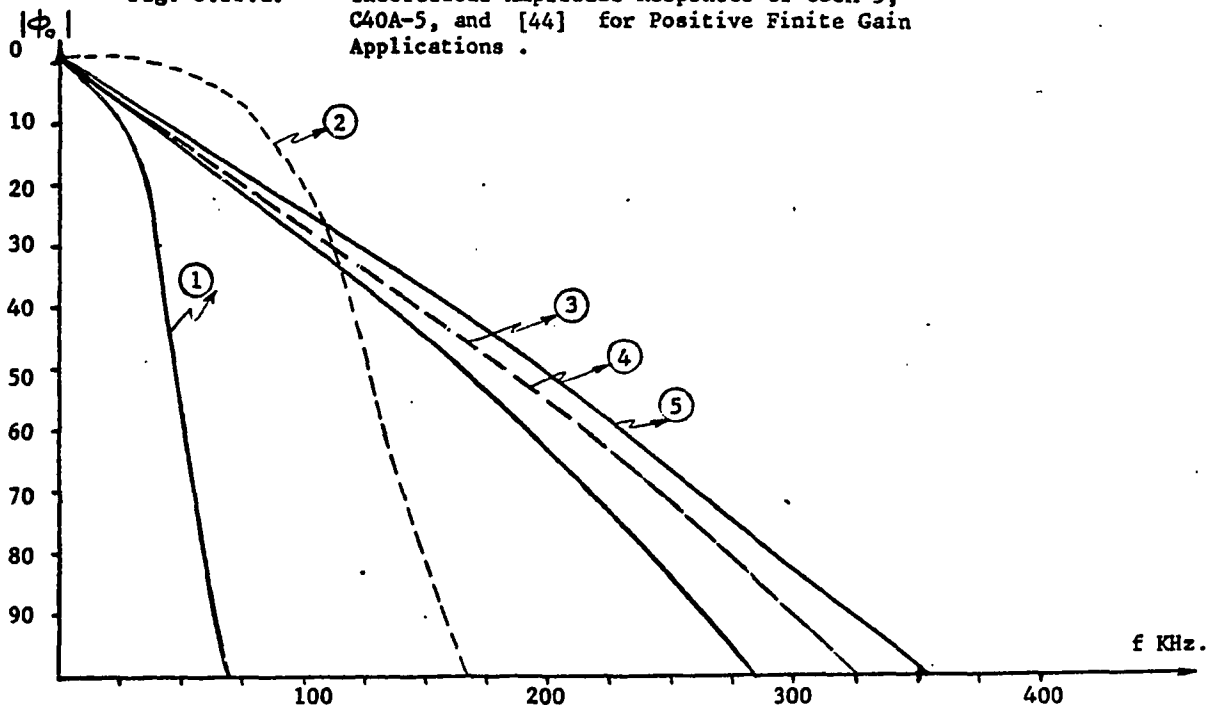
Fig. 3.11.b.   Theoretical Phase Responses of C30A-5, C40A-5, and [44]   for Positive Finite Gain Applications .

Fig. 3.11.   Theoretical Frequency Responses of C30A-5, C40A-5, and [44]   for Positive Finite Gain Applications (Gain K = 38.7) .

due to the fact that the ZSD amplifier is unstable in practice, and limiting diodes had to be added in the amplifier structure to prevent the Trapozoidal oscillations [44].

Experimental results of maximally flat (Q_p=0.707) negative finite gain amplifier realizations using C4OA-1 for different gains are shown in Fig. 3.12. The figure shows the improvement in the BW of the negative finite gain amplifiers using the C4OA's over those using C2OA's and C3OA's, particularly as the gain K increases. The computer frequency response plots of C4OA-1 negative finite gain realization, are in close agreement with the experimental results of Fig. 3.13.

The stability and low sensitivity to power supply as well as to the active compensation resistor variations are verified as shown in Figs. 3.14a and 3.14b, for the C4OA-1 negative finite gain amplifiers.

3.4 CONCLUSIONS

In this chapter the application of the proposed CNOA's in positive, negative and differential finite gain amplifications are presented. Theoretical and experimental results of the CNOA's (N=2,3,4) in finite gain applications show the excellent performance properties of the realizations. The performance examined included wide dynamic range, stability with one and two pole models, low active and passive sensitivity to the OA GBWP and to the compensating resistors, and the BW extension. Comparisons with the state of the art contributions using similar number of

$$20 \text{ Log } \left| \frac{V_o/V_i}{k} \right|$$
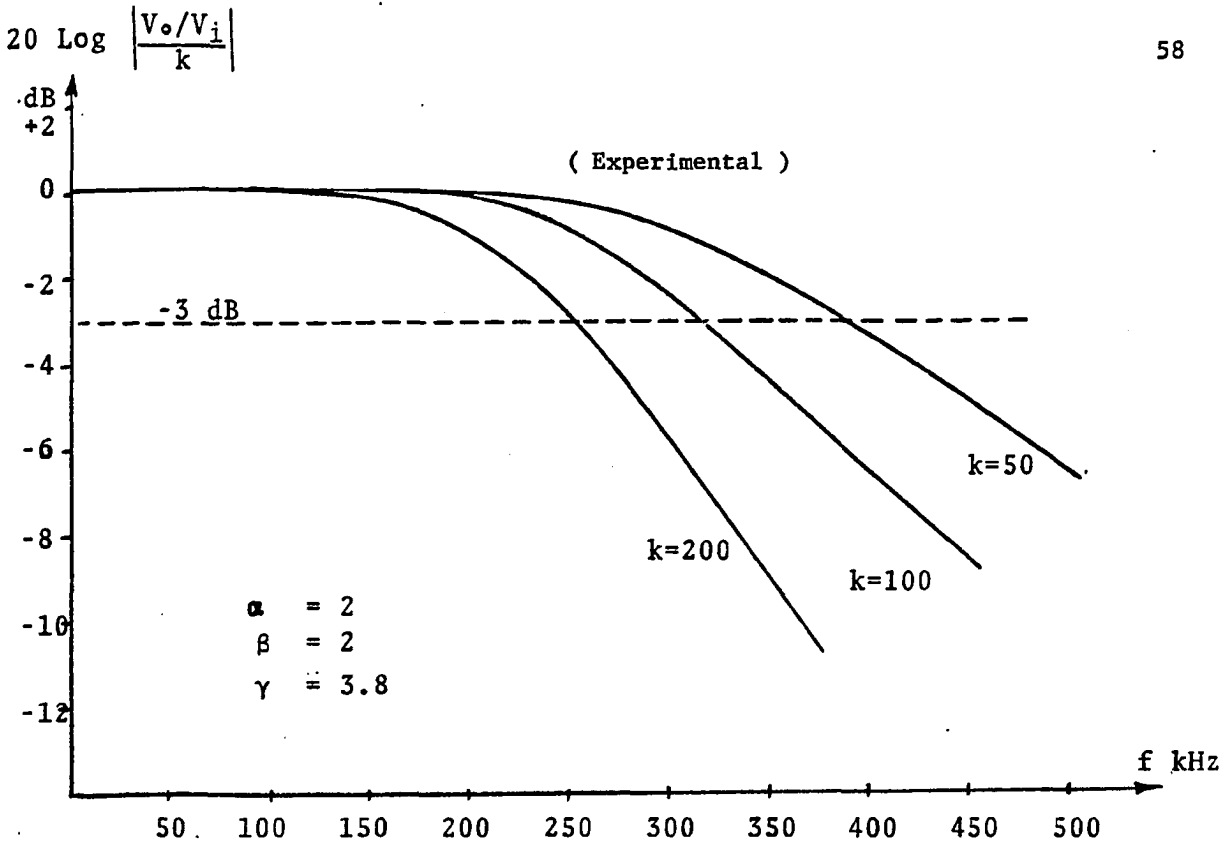
Fig. 3.12. Maximally Flat Experimental Frequency Responses of C40A-1 for a Gain of 50, 100 & 200 (Using LM 747 OA) .

$$20 \text{ Log } \left| \frac{V_o/V_i}{k} \right|$$
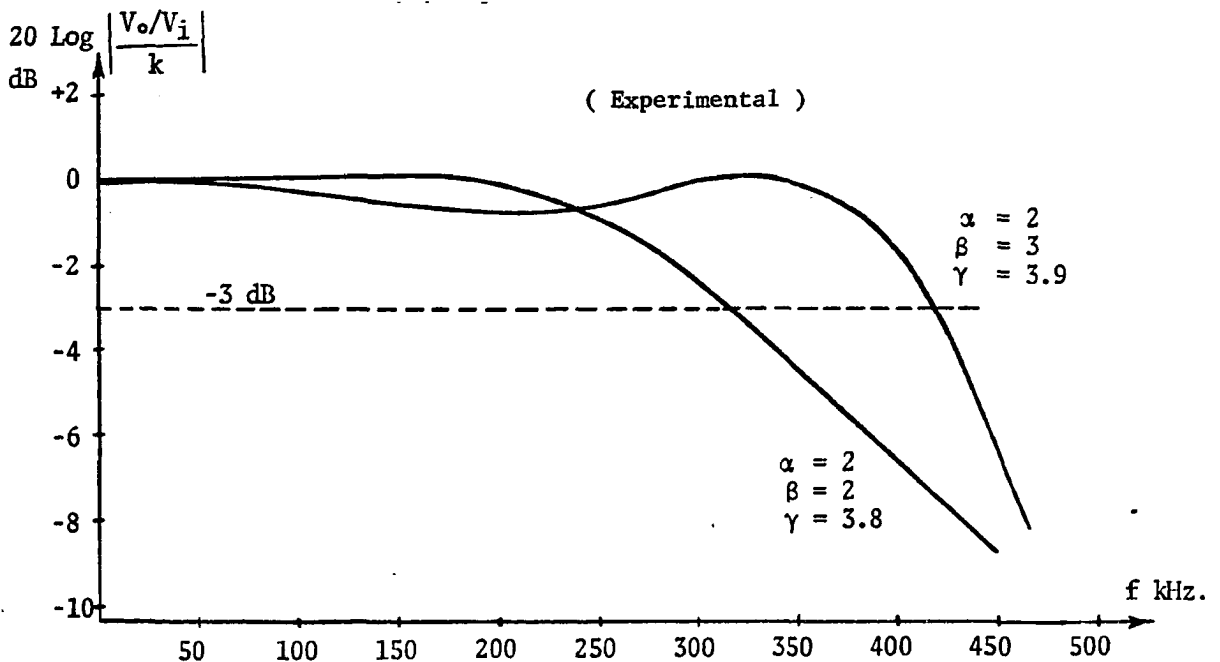
Fig. 3.13. The Effect of Active Compensation on Extending the Bandwidth of the C40A-1 in Finite Gain Application (Using LM 747 OA) .

$20 \text{ Log} \left| \dfrac{V_o/V_i}{k} \right|$

dB

+2

0

-2

-3 dB

-4

-6

-8

(Experimental)

$\alpha = 2$
$\beta = 2$
$\gamma = 3.8$

$V_{cc} = \mp 15V$

$V_{cc} = \mp 12V$

$V_{cc} = \mp 8V$

f   kHz.

50   100   150   200   250   300   350   400   450   500
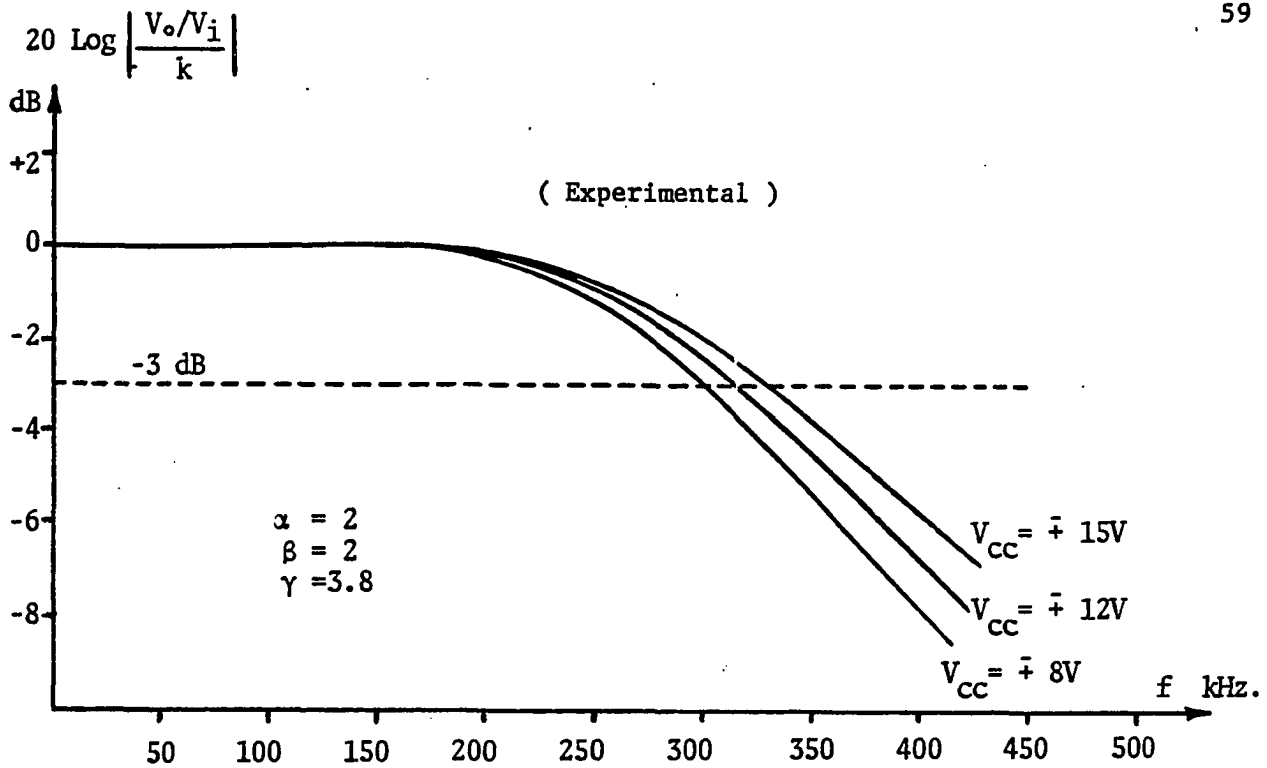
Fig. 3.14.a.   Effect of Power Supply Variations on C40A-1
                 for a Gain of 100.

$20 \text{ Log} \left| \dfrac{V_o/V_i}{k} \right|$

dB

+2

0

-2

-3 dB

-4

-6

-8

(Experimental)

k = 100

$\gamma = \mp 5 \%$

$\alpha = 2$
$\beta = 2$
$\gamma = 3.8$

+ 5%

-5%

f   kHz.

50   100   150   200   250   300   350   400   450   500
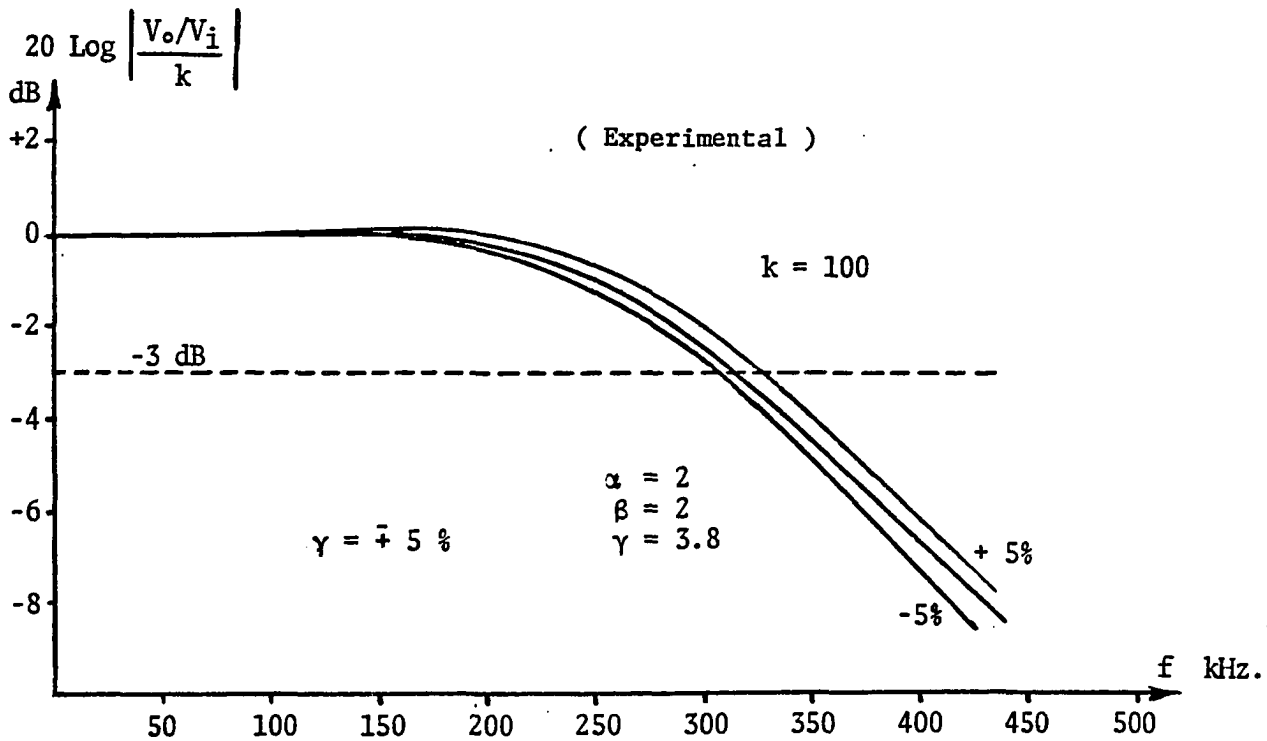
Fig. 3.14.b.   Effect of Active Compensation Elements
                 Variations by 5% on C40A-1 for a Gain of 100 .

Fig. 3.14.   Effect of Power Supply and Active Compen-
                sation Resistor Variations on C40A-1 for
                Maximally Flat Finite Gain Applications
                (Using LM 747 OA) .

OA's, in finite gain applications have shown the appreciable improvements of the realization obtained using the CNOA's proposed with respect to stability and useful BW.

Although the examples given, using the CNOA's, are for high gain applications, it is easy to show that the deviation in amplitude and phase from ideal is much lower than other existing realizations, even for closed loop gains as low as unity.

In addition, it is worthwhile to mention that although these proposed composite operational amplifiers are general OA design and can be used in place of regular OA's in any application, the results show their superior performance in comparison with the state of the art structures that were designed specifically for particular applications.

CHAPTER IV

REALIZATION OF INVERTING INTEGRATORS USING THE PROPOSED CNOA'S

4.1 INTRODUCTION

Integrator circuits, especially those realized using OA's, play an important role in the design of active-RC filter networks. Specifically, there is a number of biquadratic filter circuits that employ two integrators in a feedback loop. Notable among these (two-integrator loop) realizations are the Two-Thomas biquad [45-47] and the Akerberg-Mossberg biquad [40]. In any two-integrator loop, one of the integrators has to be an inverting one while the other is noninverting. Traditionally, the Miller circuit has been employed to realize the inverting integrator. In the Tow-Thomas biquad, the noninverting integrator is realized using cascade connection of a Miller circuit and an inverting amplifier. Akerberg and Mossberg implement the noninverting integrator using an inverting amplifier in the feedback loop of the inverting integrator. This latter circuit has been called a (phase-lead) integrator [16].

Another application of integrators is in the design of high-order active filters based on the (operational simulation) of LC ladder networks. Example of this approach are the leap-frog technique [48] and the more general Signal-Flow Graph (SFG) method [49]. In both methods, inverting integrators are used to simulate

the operation of ladder capacitors while noninverting inte-grators simulate the operation of ladder inductors. It has been shown [16] that using the Miller circuit for the inverting inte-grator together with the phase-lead circuit for the noninverting integrator results in a considerable reduction in the deviations that usually occur in the filter attenuation function due to the OA frequency response.

In this chapter, a new method is presented for the compensa-tion of inverting integrators. These improved inverting inte-grators are achieved through the use of the Composite Operational Amplifiers CNOA's in place of the single OA. Transfer functions of the CNOA's integrators, as well as the effect of the OA parasitic poles on the integrator stability are presented. A comparison study with the best reported negative integrator realizations shows clearly the improvement achieved using this technique.

4.2 INVERTING INTEGRATORS USING C2OA'S

The actually realized transfer functions T_a's using C2OA-1 to C2OA-4 as inverting integrators, assuming OA single pole model, are given in Table 4.1. The T_a's have the same general form expressed by (3.2). This leads to the same desirable features regarding the stability (assuming single pole OA model) and the low sensitivity of T_a to the different elements of the realiza-tion as well as the mismatch of single OA GBWP's. Again let us assume a two pole OA open loop gain (3.3). It is easy to show that, for identical single OA's the necessary and sufficient

C20A	Negative Integrator Transfer Function (T_a)	ω_p	Q_p
C20A-1 & C20A-2	$T_i \cdot \left[\dfrac{1}{1+S/\omega_p Q_p + S^2/\omega_p^2}\right] \cdot \dfrac{\tau\omega_1(1+\alpha)}{1+\tau\omega_1(1+\alpha)}$	$\sqrt{\omega_1\omega_2\left[1 + \dfrac{1}{\tau\omega_1(1+\alpha)}\right]}$	$\dfrac{\sqrt{\dfrac{\omega_1}{\omega_2}\left[1 + \dfrac{1}{\tau\omega_1(1+\alpha)}\right]}}{\left[\dfrac{1}{1+\alpha} + \dfrac{1}{\tau\omega_2}\right]}$
C20A-3	$T_i \cdot \left[\dfrac{1 + S/\omega_1}{1 + S/\omega_p Q_p + S^2/\omega_p^2}\right]$	$\sqrt{\dfrac{\omega_1\omega_2\left[1 + \dfrac{G_1}{\tau\omega_2 G}\right]}{(1+\alpha)}}$	$\dfrac{\sqrt{\dfrac{(1+\alpha)}{\omega_1\omega_2}\left[1 + \dfrac{G_1}{\tau\omega_2 G}\right]}}{\dfrac{1}{\omega_1} + \dfrac{G_1}{\tau\omega_1\omega_2 G} + \dfrac{(1+\alpha)}{\tau\omega_1\omega_2}}$
C20A-4	$T_i \cdot \left[\dfrac{1 + (1+\alpha) S/\omega_1}{1 + S/\omega_p Q_p + S^2/\omega_p^2}\right]$	$\sqrt{\dfrac{\omega_1\omega_2}{1+\alpha}}$	$\dfrac{\sqrt{(1+\alpha)/(\omega_1\omega_2)}}{\dfrac{1+\alpha}{\omega_1} + \dfrac{1+\alpha}{\tau\omega_1\omega_2}}$

Ideal Transfer Function $T_i = \dfrac{V_o}{V_i} = \dfrac{-\omega_i}{S} = \dfrac{-1}{\tau_i S}$

(Where τ_t is the integrator time constant = $RC = 1/\omega_t$.)

TABLE 4.1. Inverting Integrators Transfer Functions Using C20A's .

63
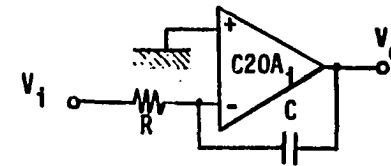
stability conditions (the parasitic poles are in the left half of the s plane) for the C2OA-1 and C2OA-2 integrator realizations are given by

$$\omega_h > \omega_i \left[4(1+\alpha)^2/(3+2\alpha)\right] \qquad\qquad (4.1)$$

For C2OA-3, the condition is given by

$$\omega_h > \omega_i \left[(3+4\alpha)/(2+2\alpha)\right] \qquad\qquad (4.2)$$

Also, for C2OA-4 the stability condition is given by

$$\omega_h > \omega_i \left[(3-\alpha)/(2+2)\right] \qquad\qquad (4.3)$$

It is clear from (4.1), (4.2) and (4.3) that for a given α, there is a minimum value of (ω_h/ω_i) to satisfy the stability condition. α equals zero, in C2OA-1 and C2OA-2 integrators, results in the minimum value for ω_h since ω_h increases as α increases. ⁻ The C2OA-2 integrator requires (ω_h/ω_i) to be greater than 3/2 for stable operation when α equals zero, and (ω_h/ω_i) to be greater than 2 when α tends to infinity. The C2OA-4 integrator has an advantage that for $\omega_h=\omega_i$ (the worst case value of ω_h for internally compensated OA's) a value of α exists $(\alpha=1/3)$ for which the integrator is stable. In general, as ω_h increases, the stability is improved. From physical consideration if $\omega_h\to\infty$, all the integrators become stable as can be seen from Table 4.1, since the OA two pole model reduces to a single pole one (2.2). The stability conditions for some special values of α are summarized in Table 4.2. From the data sheets for

C20A	α	Q_p	ω_p	Stability for α used
C20A-1	0	1	$\approx \omega_i$	$\omega_h > \dfrac{4\omega_i}{3}$
	Unrealizable	$\dfrac{1}{\sqrt{2}}$	-	-
C20A-2	0	1	$\approx \omega_i$	$\omega_h > \dfrac{4\omega_i}{3}$
	Unrealizable	$\dfrac{1}{\sqrt{2}}$	-	-
C20A-3	0	1	$\approx \omega_i$	$\omega_h > \dfrac{3\omega_i}{2}$
	Unrealizable	$\dfrac{1}{\sqrt{2}}$	-	-
C20A-4	0	1	$\approx \omega_i$	$\omega_h > \dfrac{3\omega_i}{2}$
	1	$\approx \dfrac{1}{\sqrt{2}}$	$\approx \omega_i/\sqrt{2}$	$\omega_h > \dfrac{1}{2}\omega_i$
	$\dfrac{1}{3}$	≈ 0.866	$\approx \omega_i/1.15$	$\omega_h = \omega_i$

TABLE 4.2. Values of α for Maximally Flat and for $Q_p = 1$ and their Corresponding Stability Conditions for the Inverting Integrators Using the C2OA's .

internally compensated OA's such as 741's and 747's, ω_h is shown to be higher than ω_i on the graphs [50]. This achieves stable realization down to 0 dB closed loop gain. For externally compensated OA's such as the 702's and 709's, the compensation can be chosen to guarantee the stability conditions.

A comparison of C2OA-4 negative integrator with the state of the art negative integrator realizations [51-53], is given in Fig. 4.1 for $\omega_t/\omega_i = 0.05$ ($\omega_t = 1/\tau_t$ where τ_t is the integrator time constant). This shows that the percentage deviation in magnitude and phase from ideal of the negative integrator for $\alpha = 1/3$ is very close to the excellent performance of the Geiger's integrator [51]. (The C2OA-4 integrator for $\alpha = 0$, becomes identical to that of Geiger's). On the other hand, stability problem will arise in the latter when internally compensated OA's used with a phase margin less than $60°$ at 0 dB closed loop gain ($\omega_h/\omega_i < 3/2$). Thus, the value of the controlling parameter α is apparent since it results in guaranteed stable operation using commercial internally compensated OA's.

4.3 INVERTING INTEGRATORS USING C3OA'S

In this section three high frequency integrators using actively compensated multiple OA's (CNOA's) for N=3 are introduced. Fig. 2.7 (b,e,f) shows the different structures of these C3OA's. The actually realized open loop transfer function for each of these CNOA designs are given in Table 2.1.

Using the C3OA-2, C3OA-5 and C3OA-6 in the inverting

|% deviation from ideal|

|H|

8 %

7 %

6 %   [52]   C20A-4
                         [53] Q_p=.707
5 % α=.95   C20A-4
                                                           Q_p=.835
4 % α=.334

3 %   [51]

2 %

1 %
                                                  Log$\frac{\omega}{\omega_i}$

     -1.6   -1.4   -1.2   -1.0   -0.8   -0.6

|% deviation from ideal| |ϕ| Fig. 4.1.a.   Inverting Intergators Transfer Function
                                                    Amplitude Response for ($1/\tau\omega_i$ = 0.05).

6 %

5 %

4 %   C20A-4
                                                  Q_p=.835
                        C20A-4 α=.334
                        Q_p=.707
3 % α=.95

                        [53]
2 %
                                                              [51]

1 %
                                                              [52]
                                               Log$\frac{\omega}{\omega_i}$

     -1.6   -1.4   -1.2   -1.0   -0.8   -0.6

Fig. 4.1.b.   Inverting Integrators Transfer Function
                 Phase Response for ($1/\tau\omega_i$ = 0.05) .
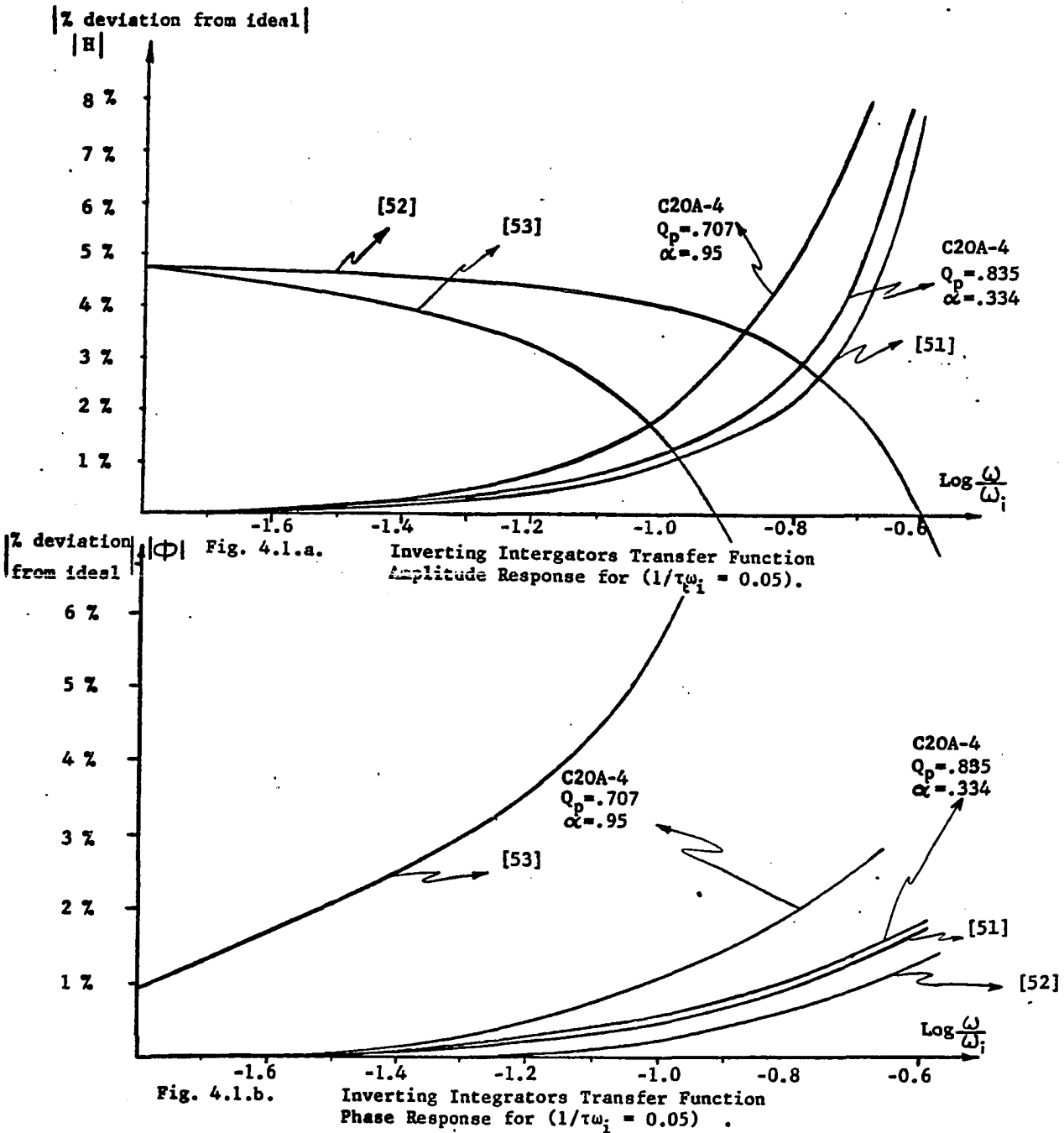
Fig. 4.1.   Comparison of the C20A-4 Negative Integrator
                for (Q_p = 0.707, Q_p = 0.835) with the State
                of the Art Integrators Proposed in [51,52,53]

integrators yields the following integrator transfer functions

$(T_a\text{'s} = T_i \cdot N/D)$

Using C30A-2:

$$T_a = T_i \cdot \frac{1 + \dfrac{s}{\omega_i}}{[1 + \dfrac{\omega_t}{\omega_i(1+\beta)}] + [1 + \dfrac{1}{(1+\beta)} + \dfrac{\omega_t}{\omega_i(1+\alpha)}]\dfrac{s}{\omega_i} + [\dfrac{1}{1+\alpha} + \dfrac{\omega_t}{\omega_i}]\dfrac{s^2}{\omega_i^2} + \dfrac{s^3}{\omega_i^3}}$$

$$(4.4)$$

using C30A-5:

$$T_a = T_i \cdot \frac{[1 + \dfrac{1+\beta}{1+\alpha}\dfrac{s}{\omega_i} + (1+\beta)\dfrac{s^2}{\omega_i^2}]}{1 + [\dfrac{1+\beta}{1+\alpha}(1+\dfrac{\omega_t}{\omega_i})]\dfrac{s}{\omega_i} + [(1+\beta) + \dfrac{(1+\beta)}{(1+\alpha)} + \dfrac{\omega_t}{\omega_i}(1+\beta)]\dfrac{s^2}{\omega_i^2} + (1+\beta)\dfrac{s^3}{\omega_i^3}}$$

$$(4.5)$$

and using C30A-6:

$$T_a = T_i \cdot \frac{[1 + (1+\alpha)\dfrac{s}{\omega_i} + (1+\alpha)(1+\beta)\dfrac{s^2}{\omega_i^2}]}{1 + (1+\alpha)\dfrac{s}{\omega} + [(1+\alpha)(1+\beta) + \dfrac{\omega_t}{\omega_i}(1+\alpha)(1+\beta)]\dfrac{s^2}{\omega_i^2} + [(1+\alpha)(1+\beta)]\dfrac{s^3}{\omega_i^3}}$$

$$(4.6)$$

where ω_i is the GBWP of the OA used

T_i = the ideal integrator transfer function = $-\omega_t/s$ and

$N/D \to 1$ as the OA gain A_i's $\to \infty$

From (4.4) to (4.6), it can be easily shown that no differences

appear in any of the numerator and denominator coefficents. Thus, the low coefficient sensitivities are achieved, amplifiers do not need to be matched, and the necessary conditions for stability are satisfied. Assuming single pole OA model, the necessary and sufficient conditions for stability, i.e. for the roots of D to be in the left half of the s plane, are given by:

$$[\frac{1}{1+\alpha}][1+ \frac{1}{1+\beta} + \frac{\omega_t}{\omega_i(1+\alpha)}]+[\frac{\omega_t}{\omega_i}][1+ \frac{\omega_t}{\omega_i(1+\alpha)}] >1 \qquad (4.7.a)$$

(for C30A-2 integrator)

$$[\frac{1+(\omega_t/\omega_i)}{1+\alpha}][(1+\beta) + \frac{1+\beta}{1+\alpha} + \frac{\omega_t}{\omega_i} (1+\beta)] >1 \qquad (4.7.b)$$

(for C30A-5 integrator)

$$(1+\alpha)(1+ \frac{\omega_t}{\omega_i}) >1 \qquad (4.7.c)$$

(for C30A-6 integrator)

The new integrators are designed to satisfy the above stability conditions with a practical margin consequently allowing a wide range of α and β variations. For illustration, sample results are shown in Figs. (4.2.a) and (4.2.b) using C30A-6 and comparison is made with an excellent recently proposed integrator [51] that uses two OA's. The trade off between magnitude and phase, which will be in the next chapter, can be easily achieved by controlling α and β.

|% deviation in magnitude from ideal|
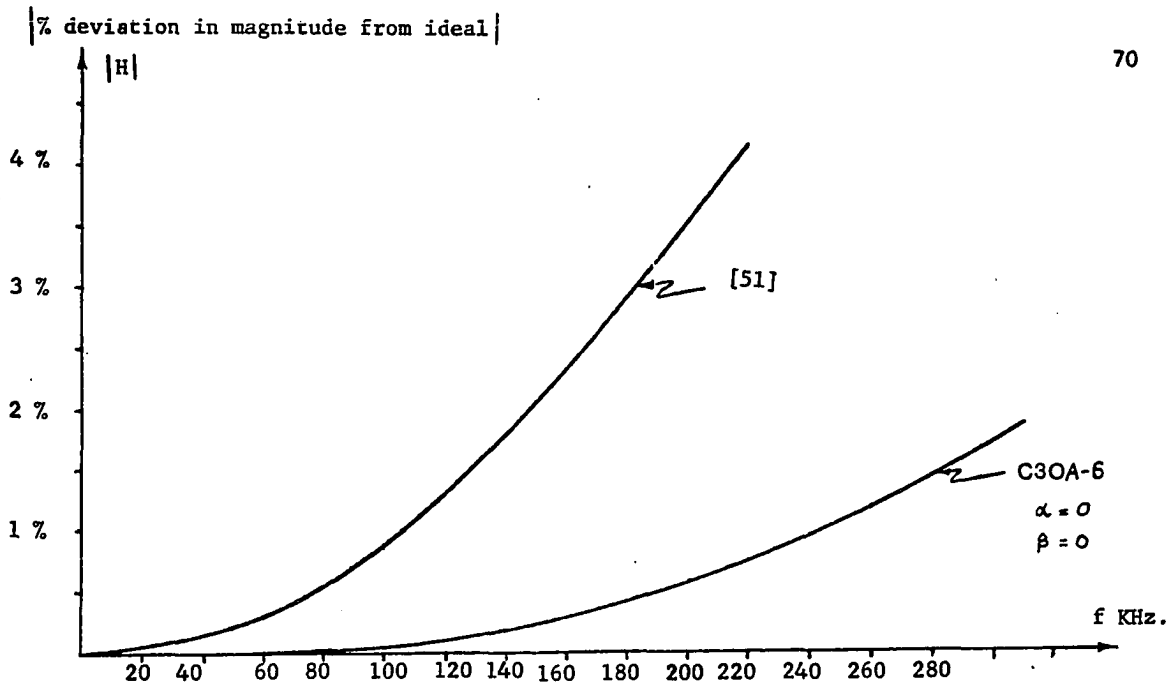
Fig. 4.2.a.   Transfer Function Percentage Magnitude
                      Deviation from Ideal .

|% deviation in phase from ideal|
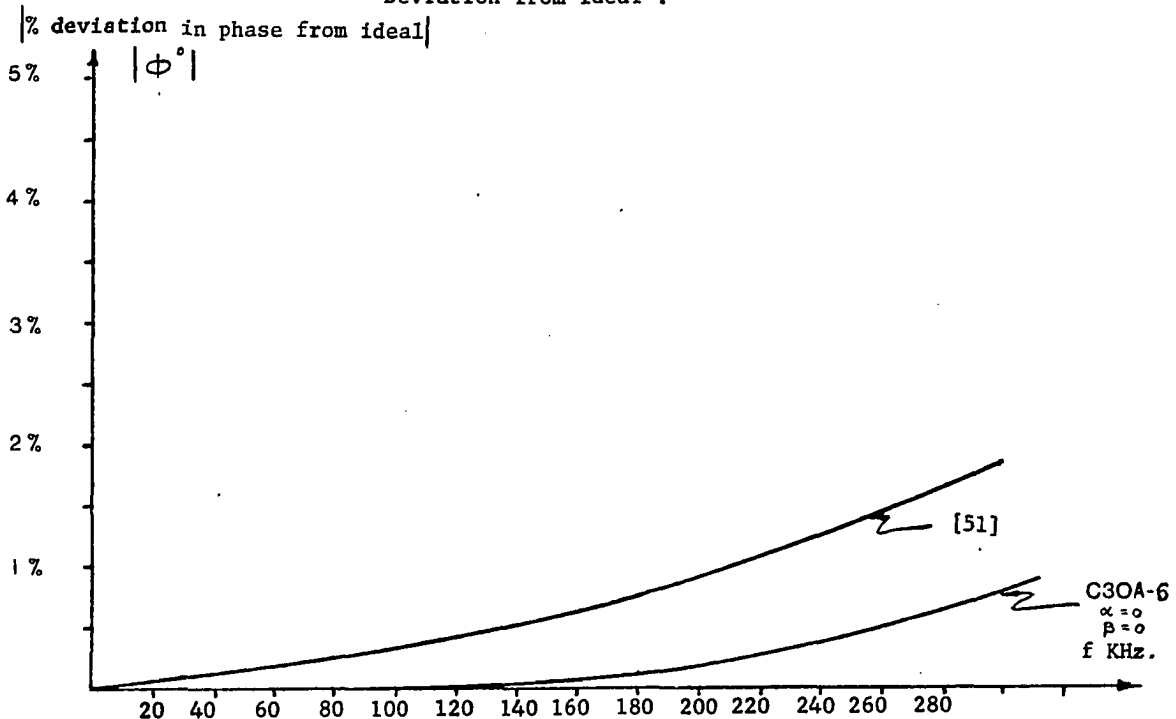
Fig. 4.2.b.   Transfer Function Percentage Phase Deviation
                      from Ideal .

Fig. 4.2.   Comparison of C30A-6 Inverting Integrator
                      and the One Proposed in [51]   for $(1/\tau\omega_i = 0.1)$.

4.4 CONCLUSIONS

In this chapter, the application of the proposed CNOA's (N=2,3) in inverting integrators is presented. This is a new technique for magnitude and phase compensation of inverting integrators. The transfer functions of the realized integrators are given. The effect of the second parasitic pole of the OA on the stability of the proposed realiztions are studied. Comparing the CNOA's integrators with the state of the art designs show clearly the significant improvements in the integrator performance, namely, stability and magnitude and phase compensation.

In addition, it is worthwhile to mention that the same conclusion at the end of Chapter III is also valid here. That is although the integrator active compensation is achieved here through the use of a general composite OA's (that can be used in any active realizations), the results in integrator applications outperform the results of the best available realizations that was specifically designed as integrators.

CHAPTER V

EXTENDING ACTIVE FILTERS OPERATING FREQUENCIES USING CNOA'S

5.1 INTRODUCTION

In recent years, a great deal of attention has been directed to designing active-RC second-order filters that have low sensitivities with respect to the active element. It is well known that the poles are displaced from their nominal positions because of the finite value of the GBWP of the OA. In some circuits the GBWP also affects the zeroes. Although the dependence of the transfer function on the GBWP has been extensively studied for a large number of filter circuits, no comprehensive discussion has been presented to discuss the effect of GBWP on filter performance in a general way. Indeed, even for specific circuits, no consistent method for evaluating active filters performance has been used.

In this chapter, a new general characterization of active-RC filters employing one, two, and three OA's is presented. Active compensation of each type of these filters is accomplished through the use of the Composite OA's CNOA's. Extensive theoretical and experimental results are given. The active filters characteristics using CNOA's compare favorably with the state of the art designs.

5.2 GENERAL CLASSIFICATIONS OF ACTIVE FILTERS AND A NEW APPROACH FOR ACTIVE COMPENSATIONS

Active filters have been designed using a wide range of approaches [2,3,54]. In this chapter, active filters are considered to belong to one of two categories. The first category is realized using functional building blocks, namely, inverting integrators and/or finite gain amplifiers. Examples are the positive gain Sallen and Key, two integrator loop and SFG filters [2]. The second category contains the complement of the first category, i.e., those filters where the OA's are embedded in the passive network and functional building blocks cannot be isolated in the filter structure. Examples are Multiple Feedback (MFB) and Generalized Immittance Converters (GIC) Filters [2,3,4,55].

It is easy to show that in the first category, as the active functional building blocks behavior, approaches the ideal over a wider range, extended operating frequencies would be obtained. This can be explained in the following.

Let us assume an active biquadratic filter realizing a transfer function T using functional active building blocks, whose individual transfer functions are

$$G_1, G_2, \ldots G_n$$

Also let:

T_a = The actual realized biquadratic transfer

function using non-ideal (frequency dependent) active building blocks.

$G_1, G_2, \ldots G_n$ = The actually realized (non-ideal) transfer functions of the building blocks using frequency dependent active elements (OA's).

Also let τ_i, $G_{ij}, \ldots G_{ni}$ be the corresponding ideal transfer functions when the active elements (OA's) used, are frequency independent, i.e., the GBWP of the OA's used are ∞. ($\tau_i = 0$ where $\tau_i = 1/\text{GBWP} = 1/\omega_i$).

T_a can be written as

$$T_a = f\ (G_1, G_2, \ldots G_n) \tag{5.1}$$

and

$$G_j = g\ (\tau_{1j},\ \tau_{2j}, \ldots \tau_{Nj}) \tag{5.2}$$

$$j = 1, 2, \ldots, n$$

For simplicity, let $n = 1$, and $N = 2$. The following argument can be easily shown to be valid for any integer values of n and N.

The Taylor's series expansion of T_a about G_i is given by

$$T_a = T_a\ \Big|_{G=G_i} + \frac{\partial T_a}{\partial G}\ \Big|_{G=G_i}(G-G_i) + \frac{1}{2}\frac{\partial^2 T_a}{\partial G^2}\ \Big|_{G=G_i}(G-G_i)^2 + \ldots \tag{5.3}$$

(5.3) can be rewritten as

$$\Delta T = T_i' \, (\Delta G) + \frac{1}{2} \, T_i'' \, (\Delta G)^2 + \ldots \qquad (5.4)$$

$$\simeq T_i' \, \Delta G \text{ for } \Delta G \text{ very small}$$

where

$$\Delta T = T_a - T_i \text{ and } \Delta G = G - G_i$$

It is to be noted that ΔG is complex in general. Also, T_i', T_i'',... are dependent on the topology of the active filter as well as G_i but independent of the nonidealness of G. Thus, ΔG has to be minimized to minimize ΔT.

Similarly, from a Maclaurin series expansion of (5.2) in τ_1 & τ_2 about their ideal values of $\tau_1 = \tau_2 = 0$, it can be shown that

$$\Delta G = \frac{\partial G}{\partial \tau_1} \bigg|_{\tau_1=\tau_2=0} \tau_1 + \frac{\partial G}{\partial \tau_2} \bigg|_{\tau_1=\tau_2=0} \tau_1 + \frac{1}{2} \left[\frac{\partial^2 G}{\partial \tau_1^2} \bigg|_{\tau_1=\tau_2=0} \tau_1^2 + \frac{\partial^2 G}{\partial \tau_2^2} \bigg|_{\tau_1=\tau_2=0} \tau_2^2 + 2 \frac{\partial^2 G}{\partial \tau_1 \partial \tau_2} \bigg|_{\tau_1=\tau_2=0} \tau_1 \tau_2 \right] + \ldots$$

$$(5.5)$$

Equation (5.5) can be rewritten as

$$\Delta G = G_1' \tau_1 + G_2' \tau_2 + \frac{1}{2} \left[G_1'' \tau_1^2 + G_2'' \tau_2^2 + 2 G_{12}'' \tau_1 \tau_2 \right] + \ldots$$

$$(5.6)$$

Also G, G_i, T_a and T_i can be expressed in a polar form as

$$G = M_G e^{j\phi a}$$

$$G_i = M_{Gi} e^{j\phi i} \qquad\qquad (5.7)$$

$$T_a = M_{Ta} e^{j\theta a}$$

$$T_i = M_{Ti} e^{j\theta i}$$

where M represents the magnitude of the function represented by the subscript.

Using (5.4) and (5.7), it is easy to show that

$$T \simeq M_{Ti} e^{j\theta i} \left[\frac{\Delta M_T}{M_{Ti}} + j\Delta\theta\right] \qquad\qquad (5.8)$$

$$\simeq M_{Gi} e^{j\phi i} \left[\frac{\Delta M_G}{M_{Gi}} + j\Delta\phi\right] \cdot T_i'$$

where

$$\Delta M_T = M_{Ta} - M_{Ti}$$

$$\Delta\theta = \theta_a - \theta_i$$

and $\quad \Delta\phi = \phi_a - \phi_i$

From (5.8), if ΔT is to be minimized, both the phase and gain deviations of the functional building block are to be minimized appropriately.

In (5.6), one may be tempted to choose the structure for realizing G such that the lower order derivatives G_1', G_2', G_1'', can be set to zero. Great care should be taken in making this decision. The main reason is that the higher order derivatives in

(5.6) may be increased in a manner that offsets the reduction in ΔG obtained by nulling the lower order derivative terms, particularly as the frequency increases. It is to be noted that, for a given number of OA's, a realization that possesses the zero low order sensitivities may not be optimum and a structure may exist that has a lower ΔG over a wider frequency range without having the zero sensitivity property. This can be easily seen by comparing the performance of C2OA-4 with C2OA-1 in finite gain applications, Fig. 3.6.

In addition, to control the phase angle of G, none of the poles of G should be moved to the right half of the s-plane to cancel the phase shift contribution due to the other poles and zeroes. This is not tolerable in finite gain applications and very undesirable even when the active building block is embedded in a filter structures since it leads to local instabilities and the filter's performance depends on the dynamic behavior of the active elements. From (5.4) and (5.8) it is obvious that by replacing the active building blocks in an active filter by the proposed building blocks, which are less dependent on the active device parameters, extended operating frequencies should be obtained.

In the second category, T_a can be expressed directly as a function of the τ's of the OA's (whether single or composite) as follows:

$$T_a = f(\tau_1, \tau_2 \ldots, \tau_n) \tag{5.9}$$

For a composite amplifier constructed using N OA's, τ_j can be expressed as

$$\tau_j = g(\tau_{1j}, \tau_{2j}, \ldots, \tau_{Nj}) \tag{5.10}$$

where τ_{ij} is the GBWP of the ith OA used in constructing the jth CNOA. For simplicity, let n=1 and N=2. Hence

$$T_a = f(\tau_1) \tag{5.11}$$

and

$$\tau_1 = g(\tau_{11}, \tau_{21}) \tag{5.12}$$

Thus, the Maclaurin series expansion of (5.11) about its ideal value of $\tau_1 = 0$ is given by

$$T_a = T_a \bigg|_{\tau_1 = \tau_{1i} = 0} + \frac{\partial T_a}{\partial \tau_1}\bigg|_{\tau_1 = \tau_{1i} = 0} \cdot (\tau_1 - \tau_{1i}) + \frac{1}{2} \frac{\partial^2 T_a}{\partial \tau_1^2}\bigg|_{\tau_1 = \tau_{1i} = 0} \cdot (\tau_1 - \tau_{1i})^2 + \ldots$$

$$\tag{5.13}$$

Equation (5.13) can be rewritten as

$$\Delta T = \frac{\partial T_a}{\partial \tau_1}\bigg|_{\tau_1 = \tau_{1i}} \Delta \tau_1 + \frac{1}{2} \frac{\partial^2 T_a}{\partial \tau_1^2}\bigg|_{\tau_1 = \tau_{1i}} \cdot (\Delta \tau_1)^2 + \ldots \tag{5.14}$$

$$= T_i' \Delta \tau_1 + \frac{1}{2} T_i'' (\Delta \tau_1)^2 + \ldots \tag{5.15}$$

$$\approx T_i' \Delta \tau$$

also $\Delta \tau_i$ is given by

$$\Delta\tau_1 = \left.\frac{\partial\tau_1}{\partial\tau_{11}}\right|_{\tau_{11}=\tau_{21}=0} \tau_{11} + \left.\frac{\partial\tau_1}{\partial\tau_{21}}\right|_{\tau_{11}=\tau_{21}=0} \tau_{21} + \cdots \qquad (5.16)$$

$\Delta\tau$ in (5.14) is generally complex. Also from (5.14), one has to minimize $\Delta\tau$ appropriately to minimize ΔT. This is shown to be achievable using the proposed CNOA's in filters of the second category.

5.3 EXAMPLE I - IMPROVING THE PERFORMANCE OF AN ACTIVE FILTER IN THE FIRST CATEGORY (A MULTIPLE AMPLIFIER BIQUAD) USING C2OA'S

In this section, it is shown how the operating frequencies of the first category of filters can be extended through the novel practical active functional building blocks that were presented in Chapters III and IV. These blocks allow the minimization of ΔG (5.6) and the trade-off between gain and phase deviations to achieve stable high frequency operation with low sensitivity to the trade-off compensation elements.

A biquadratic active filter, using those functional building blocks, is designed and tested. The filter is a multiple-amplifier biquad, that is well known as the state variable filters [32], and is shown in fig. 5.1.a. It uses two inverting integrators and a differential finite gain amplifier. These were constructed using a C2OA-4 for each integrator and a C2OA-2 for the differential amplifier. Its transfer functions $T_i(s)$ (at the bandpass output) is given by

$$T_i(s)_{BP} = \cfrac{\dfrac{1+R_6/R_5}{1+R_3/R_4} \cdot \dfrac{s}{R_1 C_1}}{s^2 + \dfrac{s}{R_1 C_1} \cdot \dfrac{1+R_6/R_5}{1+R_4/R_3} + \dfrac{R_6/R_5}{R_1 R_2 C_1 C_2}} \qquad (5.17)$$

The elements are chosen as

$$C_1 = C_2 = C, \quad R_1 = R_2 = R_3 = R_5 = R_6 = R$$

and $\omega_o = \dfrac{1}{RC}$

Referring to Chapter III, these design values correspond to

$$X = 2Q_p - 1 = R_4/R_3 \qquad (5.18)$$

and $K = R_6/R_5 = 1$ $\qquad (5.19)$

For maximally flat response $(Q_p = 1/\sqrt{2})$ of the differential amplifier, $\alpha = (\sqrt{1+K}/\sqrt{2}) - 1 = 0$ independent of X and Q_o. α equals 1 (maximally flat) was used in the C20A-4's.

The experimental results are given in Figs. 5.1.b and 5.1.c, compared with those obtainable using single OA's. The appreciable improvement in the useful operating frequencies is obvious. The excellent theoretical sensitivity, stability and dynamic range performance were also verified. Total Harmonic Distortion (THD) of much less than one percent at any of the filter outputs was measured over a wide range of frequencies and signal levels. E.g., the THD was found less than 50 dB below
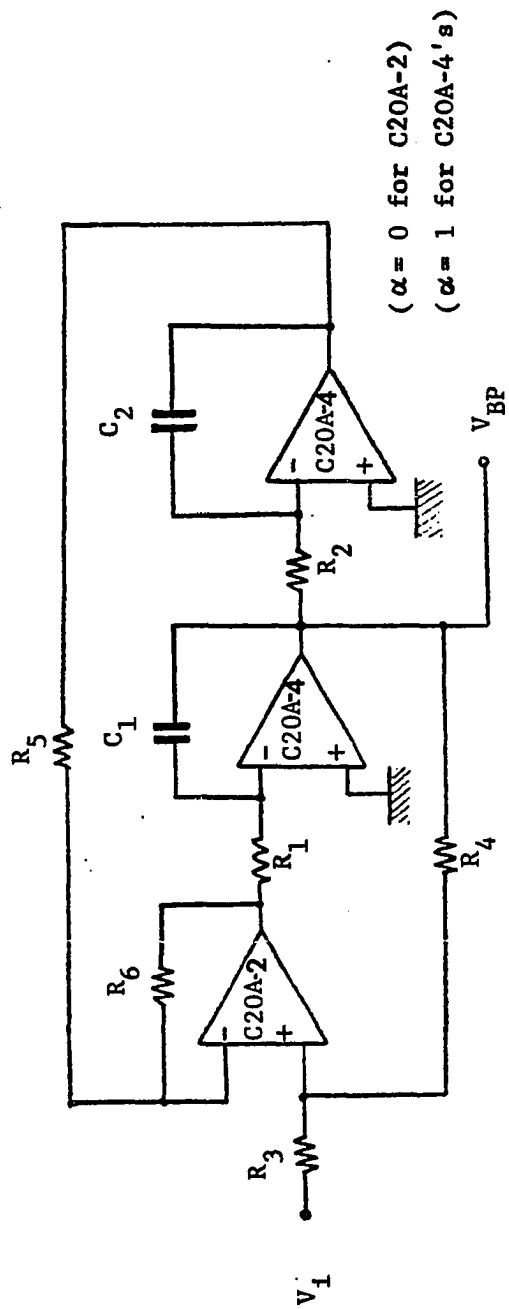
Fig. 5.1.a. The State Variable BP Filter (Two Integrator Loop) Using C20A-2 and C20A-4

$(\alpha = 0 \text{ for C20A-2})$

$(\alpha = 1 \text{ for C20A-4's})$

$$\frac{\Delta Q_o}{Q_o} = \left[1 - \frac{4Q_o W_o}{B} \right]^{-1} - 1$$

Calculated for single OA

$\omega_o = 30.8$ K rad/sec.

$\omega_o = 50$ K rad/sec.

measured using C20A's
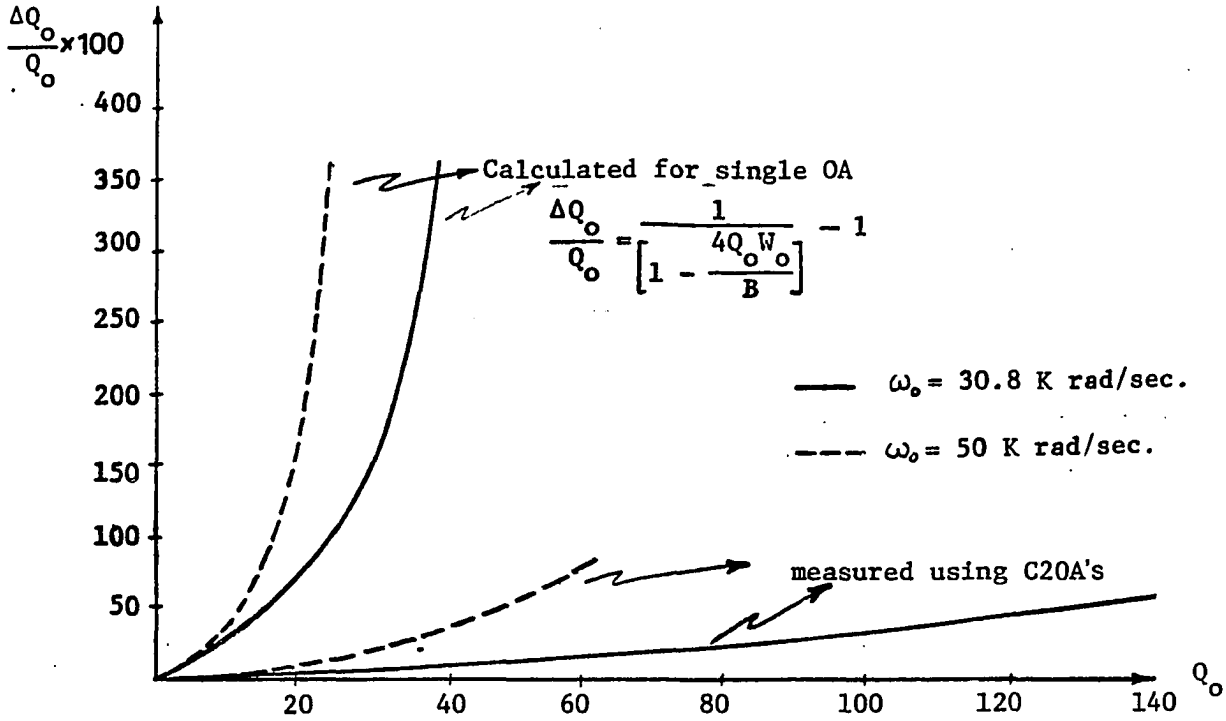
Fig. 5.1.b. Percentage Variation of Q_p as a Function of Q_p for the BP Filter of Fig. 5.1.a. ($\omega_p = 30.8$ & 50 K rad/sec) .

single OA $Q_o = 30$

single OA $Q_o = 10$

calculated

C20A's $Q_o = 30$

measured

C20A's $Q_o = 10$
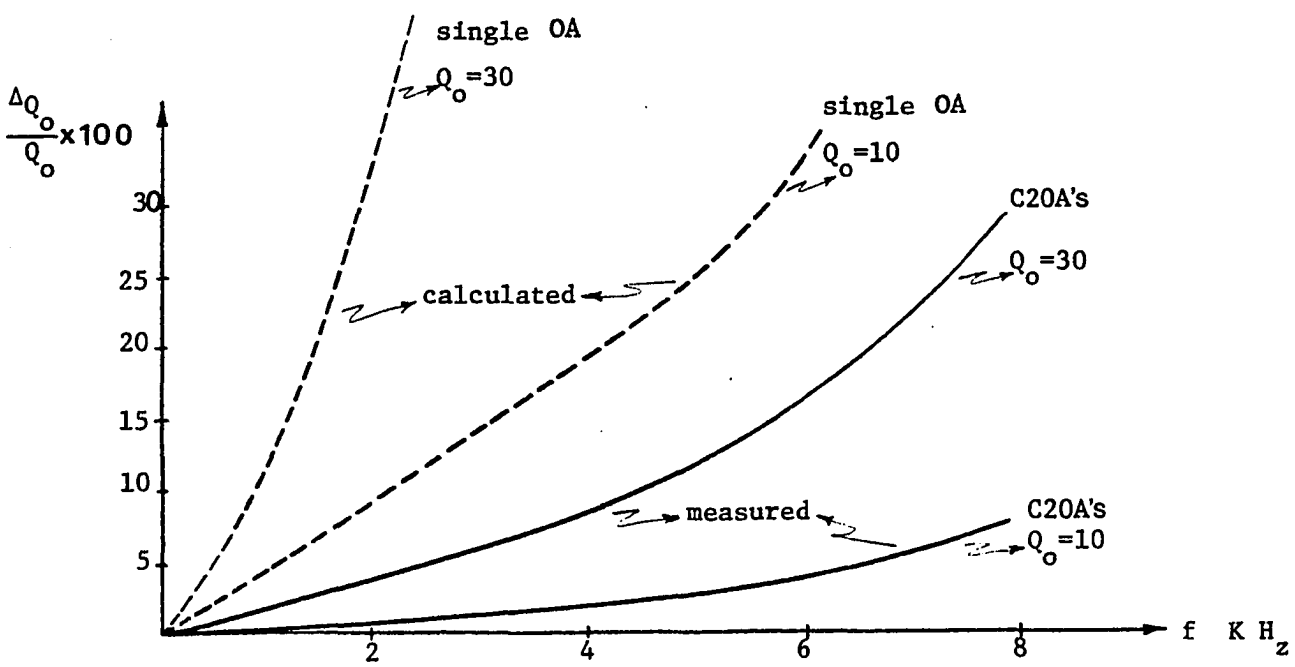
Fig. 5.1.c. Percentage Variation of Q_p as a Function of f_o for the BP Filter of Fig. 5.1.a.

Fig. 5.1. Experimental Results of the Two Integrator Loop BP Filter Using C20A-2 and C20A-4 (LM 7470A) .

the fundamental of f_o for an output voltage swing of twelve volts peak to peak, $V_{power\ supply}$ = ± 12 V, f_o = 16 kHz, and Q_p = 10. It is very interesting to note that as α in the integrator was set tc zero, resulting in a previously reported integrator [19,22,51], the filter became unstable in practice as predicted from the stability analysis in Chapter IV.

5.4 EXAMPLE II - IMPROVING THE PERFORMANCE OF ACTIVE FILTERS IN THE SECOND CATEGORY (MULTIPLE FEEDBACK BIQUADS) USING C2OA'S AND C3OA'S

In this section, two Multiple Feedback (MFB) single-biquadratic bandpass filters are considered to show the perfor-mance improvements of filters of the second categories using C2OA's and C3OA's.

The first filter section which is a single amplifier biquad, is shown in Fig. 5.2.a [7]. It realizes the bandpass transfer function $T_i(s)$ given by

$$T_i(s) = \frac{k}{1+k} \cdot \frac{1}{R_1 C_1} \cdot \frac{s}{s^2 + s\frac{1}{1+k}(\frac{1}{R_1 C_1} + \frac{1}{R_2 C_2} + \frac{1}{R_2 C_1}) + \frac{1}{1+k} \cdot \frac{1}{R_1 R_2 C_1 C_2}}$$

$$(5.20)$$

For R_1 = R_2 = R & C_1 = C_2 = C & ω = $\frac{1}{RC}$

$$\frac{V_o}{V_{in}} = k \frac{s/\omega}{1+3\ s/\omega_o + (1+k)s^2/\omega_o^2}$$

$$(5.21)$$

$$\text{and } \omega_o = \omega/\sqrt{1+k} \tag{5.22}$$

$$Q_p = \sqrt{1+k}/3 \tag{5.23}$$

$$BW = 3\omega_o/\sqrt{1+k} \tag{5.24}$$

where ω_o and Q_p are the filter poles resonant frequency and

quality factor respectively.

The filter is designed for $\omega_p = 3$ (resulting in k = 80). R

equals 1 kΩ is chosen. C20A-1 is used to replace the single OA of

the negative finite gain amplifier in the filter. α is designed

for maximally flat response given in Table 3.1 which yields

$$\alpha = (\sqrt{1+k}/\sqrt{2}) -1 = 5.3 \text{ (for k = 80)} \tag{5.25}$$

ω_o is varied by changing C. Experimental results of the band-

pass characteristics of the filter using C20A-1 as well as the

single OA are given in Figs. 5.2.b to 5.2.e. The results show the

considerable extension in the useful operating frequencies and the

improvement of the filter sensitivity to passive components and

power supply variations, due to the use of C20A-1. It is worth-

while to note that the peaks of the different bandpass responses

in Fig. 5.2.b follow a curve similar in shape to that of a finite

gain amplifier of gain-80 using C20A-1. This can be explained by

using (5.14) where $\Delta T \simeq T_i' . \Delta\tau$. Also these results verified

the stability and low sensitivity properties of the new design.

In addition, the dynamic range and harmonic distortion character-

istics were found similar to those obtained using a single OA.
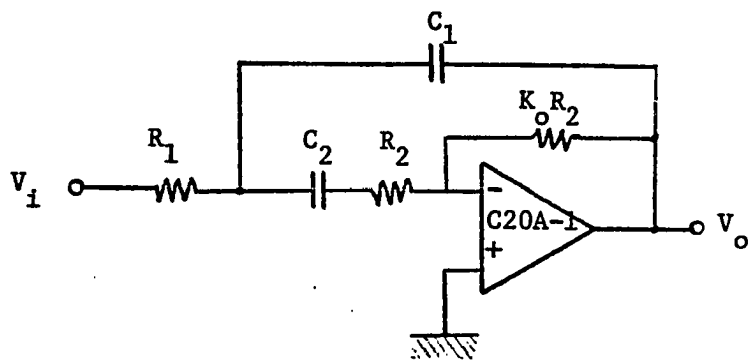
Fig. 5.2.a. The MFB Single-Biquad BP Filter Using
C20A-1 .

$\text{Log} \left| \dfrac{V_o/V_1}{K} \right|$

dB

0

-2

-4

-6

-8

-10

-12

-14

-3dB

$f_o=6.25$ $f_o=15$ $f_o=26.2$ $f_o=54$ $f_o=91$ $f_o=136$ $\dfrac{f}{KH_z}$

K = 80 $Q_p = 3$ R = 1 k
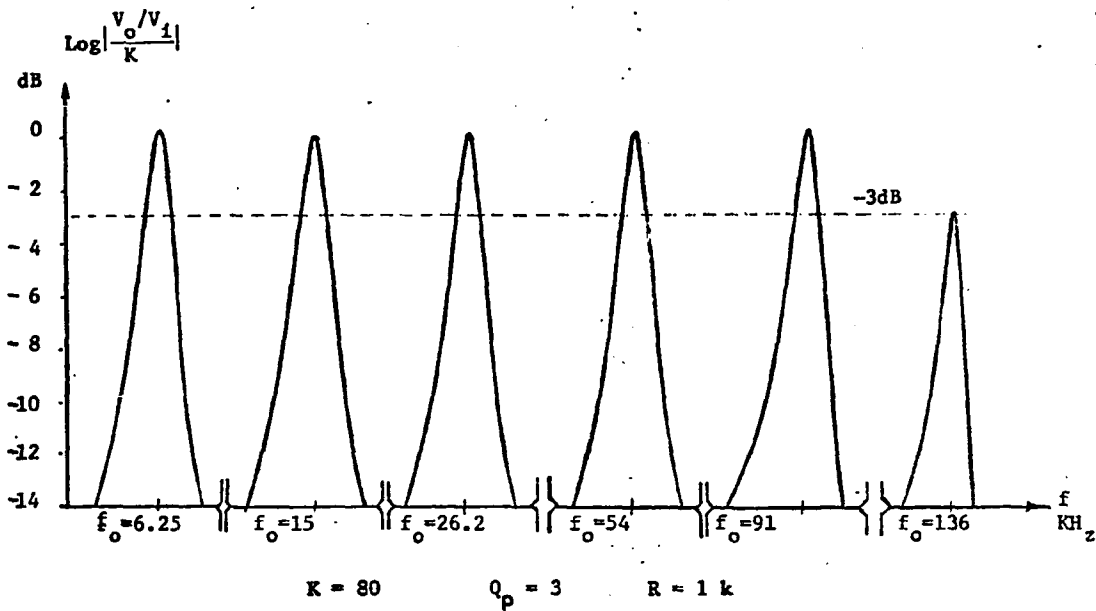
Fig. 5.2.b.   Frequency Responses of the MFB BP Filter
Using C20A-1 for Different ω_o .

$\text{Log} \left| \dfrac{V_o/V_1}{K} \right|$

dB

0

-2

-4

-6

-8

-10

-12

-14

-3dB

$f_o=6.25$ $f_o=15$ $f_o=26.2$ $f_o=54$ $f_o=91$ $f_o=136$ $\dfrac{f}{K\,H_z}$

K =80 $Q_p=3$ R = 1KΩ
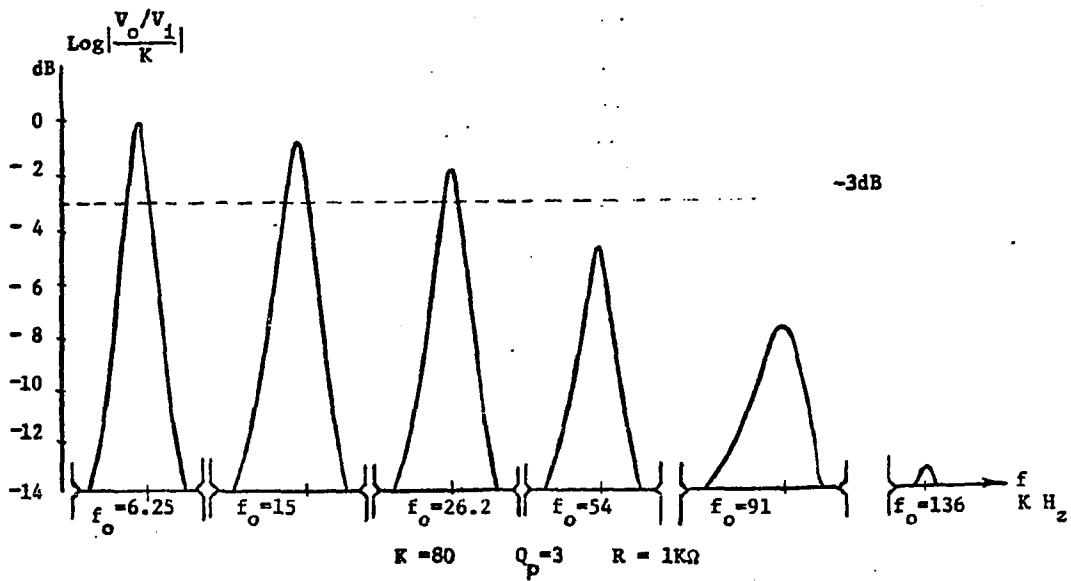
Fig. 5.2.c.   Frequency Responses of the MFB BP Filter
Using Single OA for Different ω_o .
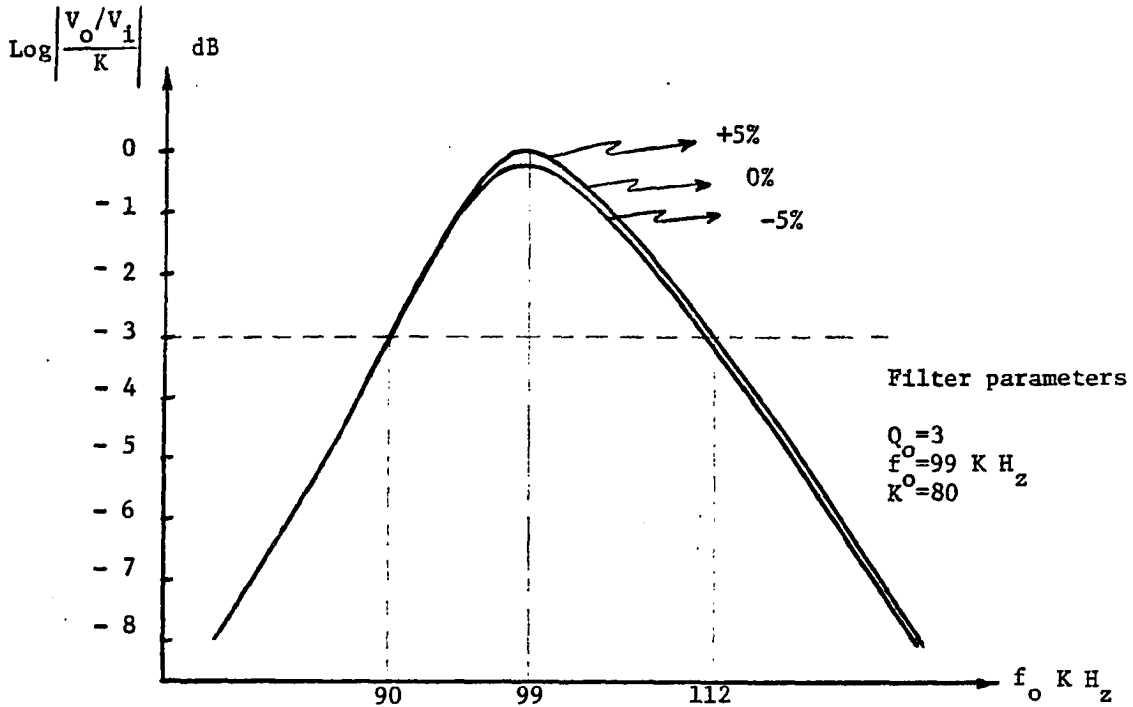
Fig. 5.2.d.   Effect of 5% Variation of Active Compensation Elements on the Frequency Response of the MFB Filter Using C20A-1 .
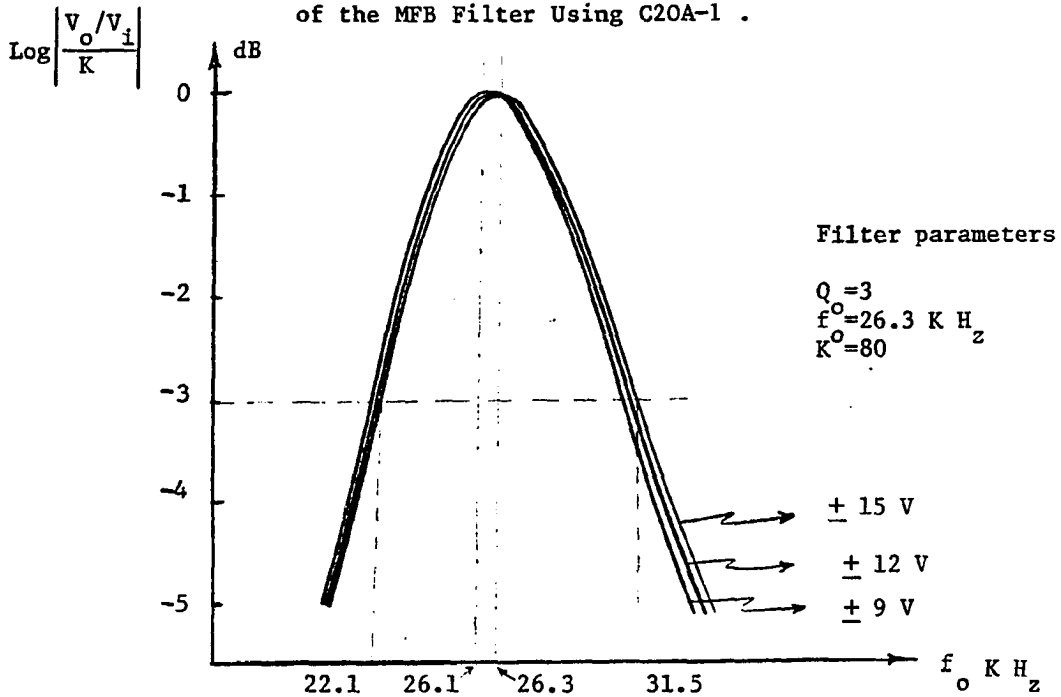
Fig. 5.2.e.   Effect of Power Supply Variations of the Frequency Response of the MFB Filter Using C20A-1 .

Fig. 5.2.   Experimental Results of the Multiple Feedback (MFB) Single-Biquad BP Filter Using C20A-1 (LM 747 OA) .

The second filter section is another MFB single-biquadratic bandpass active filter shown here in Fig. 5.3, as an example to illustrate the improved filter performance using one of the proposed C3OA's, namely, C3OA-1. For ideal OA's, i.e., $A_i \rightarrow \infty$ (i=1,2,3) the filter transfer function T_i is given by:

$$T_i = V_o/V_i$$
$$= - R_3 Cs/1+2R_1 Cs + R_1 R_3 C^2 s^2 \qquad (5.26)$$

Assuming finite gain amplifiers, the realized transfer function T_a is given by:

$$T_a = - R_3 Cs/\{1+[2RC+ \frac{1}{\omega(1+\alpha)}]s+[R_1 R_3 C^2+ \frac{(2R_1+R_3)C}{\omega(1+\alpha)} + \frac{1}{\omega^2}]s^2$$

$$+ [\frac{(2R_1+R_3)C}{\omega^2} + \frac{R_1 R_3 C^2}{\omega(1+\alpha)}] s^3 + [\frac{R_1 R_3 C^2}{\omega^2}]s^4\} \qquad (5.27)$$

Again, it can be easily shown that the dynamic range of this filter is identical, to that obtained, if a single OA replaces the C3OA. Also, neither OA gain matching is required, nor differences appear in any of the transfer function T_a coefficients.

To illustrate extended frequency performance, a BP filter with f_o = 37.95 kHz, and Q_p = 10, was designed and tested. The design values are:

C = 1 n.f.

R_i = 250 Ω

R_1 = 210 Ω

$R_2 = 1.3 \ k\Omega$

$R_3 = 84 \ k\Omega$

$\alpha R' = 0$

$R' = \infty$

$R = 0$

$\beta R = \infty$

The OA's used are LM747 with GBWP = 1 MHz ± 10%. Applying Routh-Hurwitz stability criterion, it can be easily shown that the necessary and sufficient conditions are well satisfied with a wide margin. Ideal and experimental results are shown in Fig. 5.4.

Performance comparisons are made with one of the best available high frequency designs [44]. Fig. 5.5 shows the theoretical amplitude responses of the BP filter using the design given here, and the design in [44] for $Q_p = 10$ and $\omega_o/\omega_i = 0.1$.

Also the experimental results using the two designs obtained from the BP filters are given in Fig. 5.6. The compensation remained fixed for the results in Fig. 5.6.

In the C3OA design, $\alpha = 0$, $\beta = \infty$

In the [44] design, $\Theta = 0.2$, $\beta = 1$

Fig. 5.6.a, shows the percentage deviation in f_o as a function of f_o for $Q_p = 5$, 10, and 20. Fig., 5.6.b, shows the percentage deviation in Q_p as a function of f_o for $Q_p = 5$, 10, and 20. The comparison in Figs. 5.5 and 5.6 show the

$$C = 1 \text{ n.f.}$$
$$R_i = 250 \ \Omega$$
$$R_1 = 210 \ \Omega$$
$$R_2 = 1.3 \text{ k}\Omega$$

$$R_3 = 84 \text{ k}\Omega$$
$$\alpha R' = R = 0$$
$$\beta R = R' = \infty$$

$$R_1 = R_i \ // \ R_2$$
$$\omega_o = 1/c \ \sqrt{R_1 R_3}$$
$$Q_p = \tfrac{1}{2} \cdot \sqrt{R_3 \ / \ R_1}$$

Fig. 5.3. Multiple Feedback (MFB) BP Filter Using C30A-1 (Using LM 747 OA) .

$$f_o = 37.95 \text{ KHz.}$$
$$Q_p = 10.1$$
$$\alpha = 3.5$$
$$\beta = 20$$

$$\alpha = -5\%$$
$$\beta = -5\%$$

Ideal MFB filter (ideal OA's)

C30A experimental

$$Q_{experimental} = 9.7$$
$$f_{o\,experimental} = 37.2$$
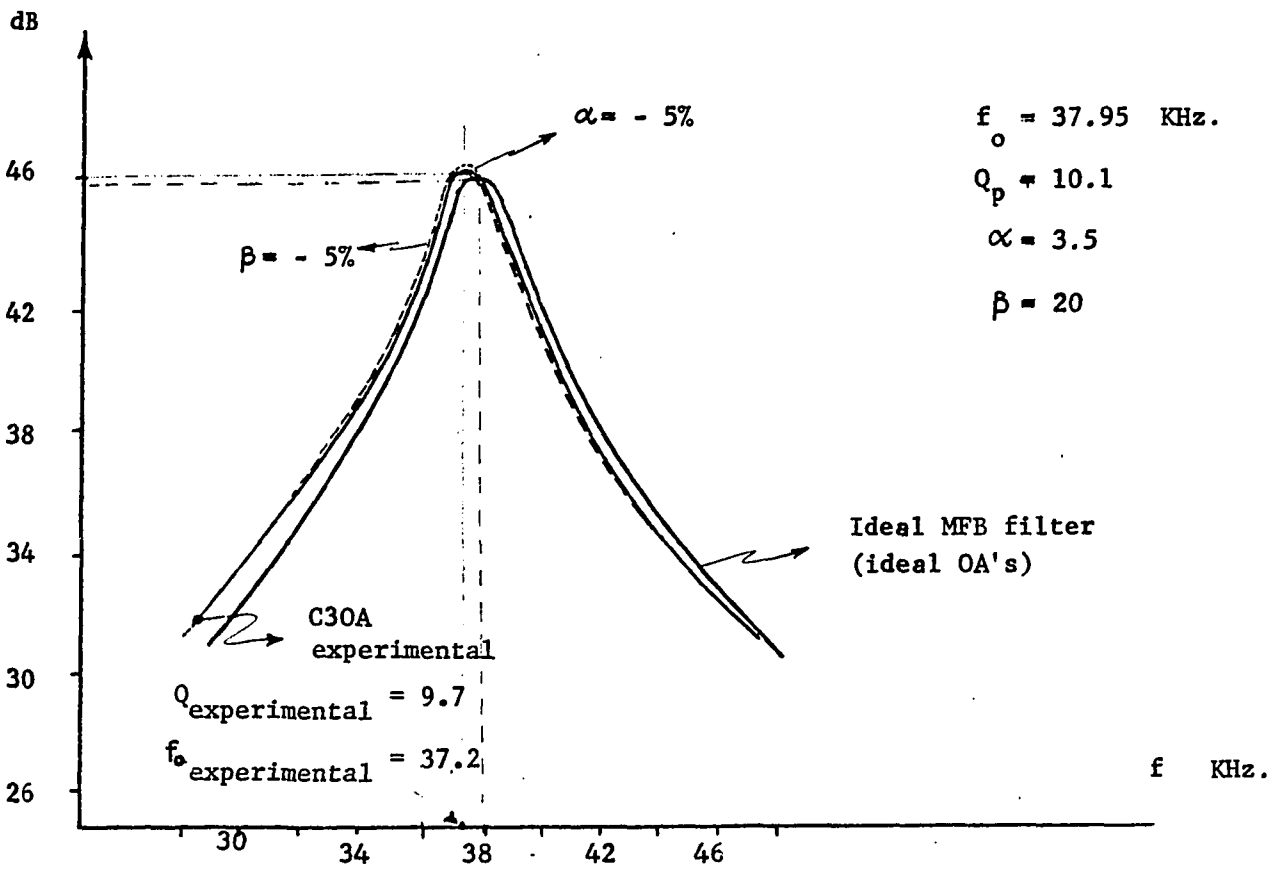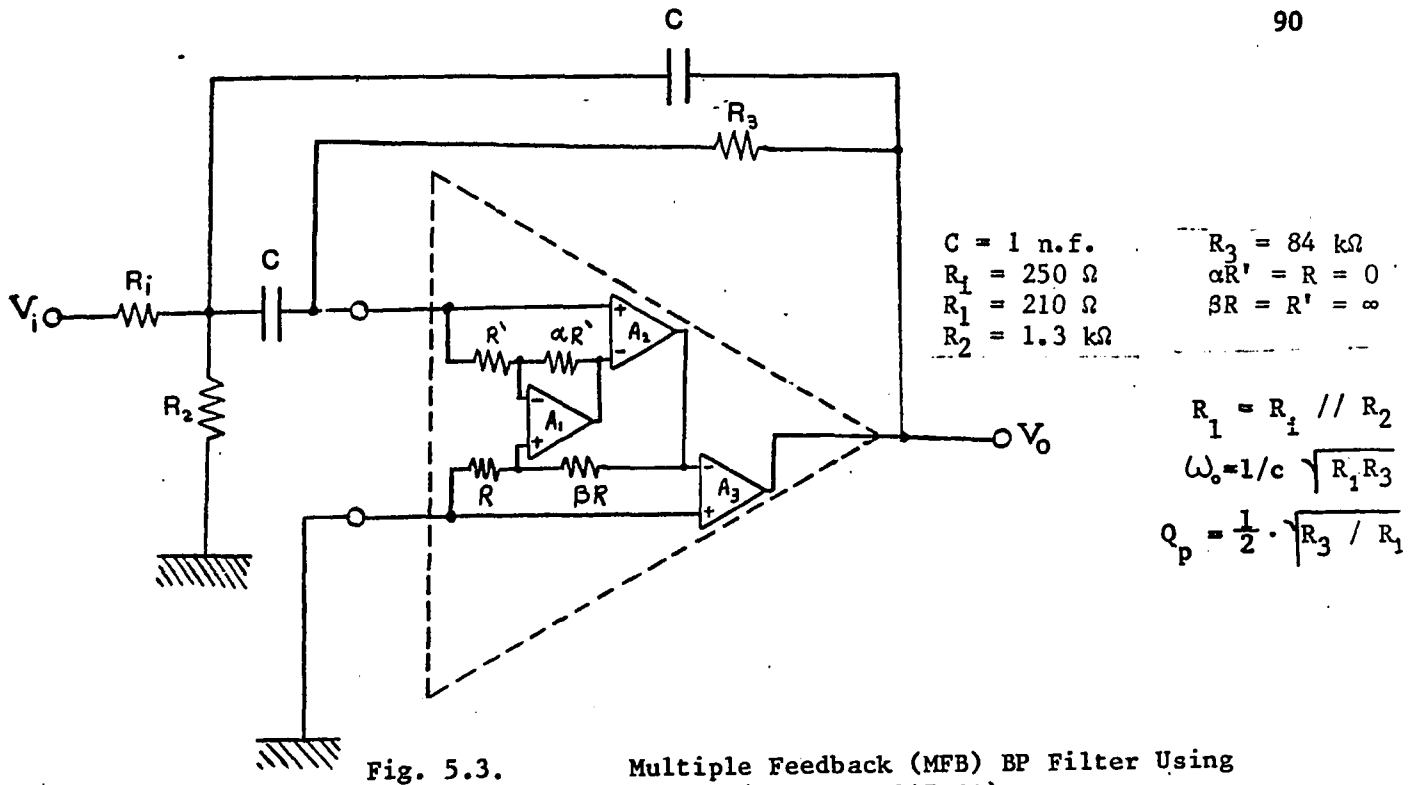
Fig. 5.4. Experimental Amplitude Response of the MFB BP Filter Using C30A, and its Variations due to Passive Elements Variations .
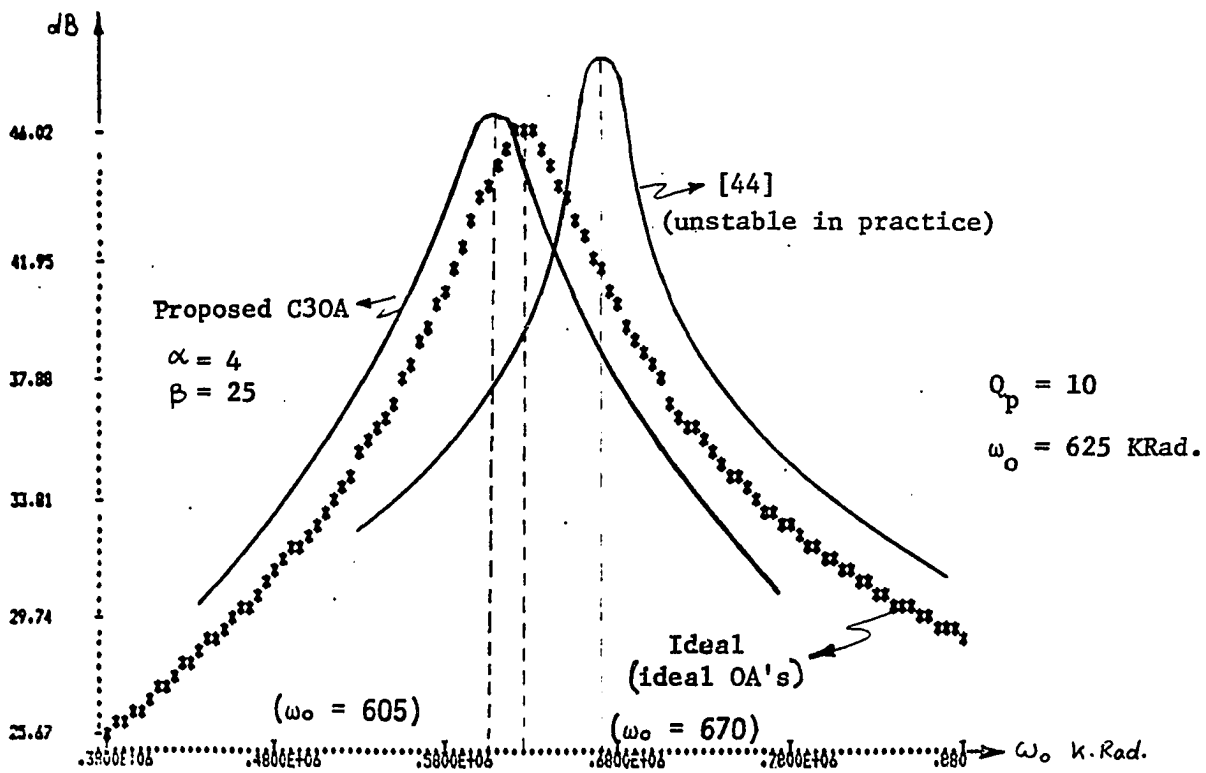
Fig. 5.5. Ideal Amplitude Response of the MFB BP Filter, and Theoretical Responses Using C30A, and [44] .

$\left|\frac{\Delta\omega_o}{\omega_o}\right| \times 100$ %

* Testing was only possible up to the * point.

---- Trapezoidal oscillations were encountered
and limiting diodes were necessary before *.

C30A $\alpha = 0$, $\beta = \infty$

[44] $\theta = 0.2$, $\beta = 1$
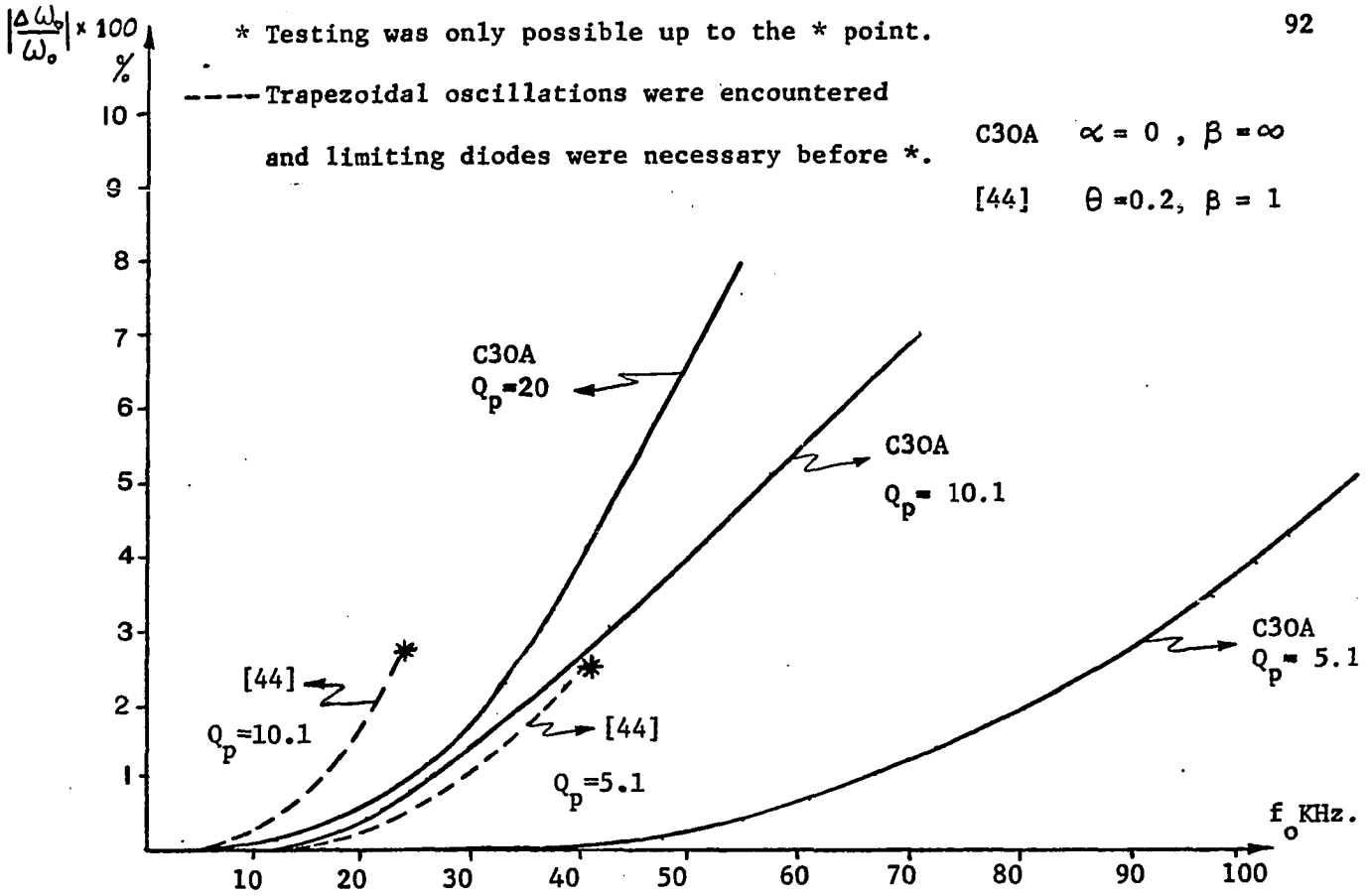
Fig. 5.6.a. Percentage Variations in ω_o of the MFB Filter for Q_p = 5, 10, 20 .
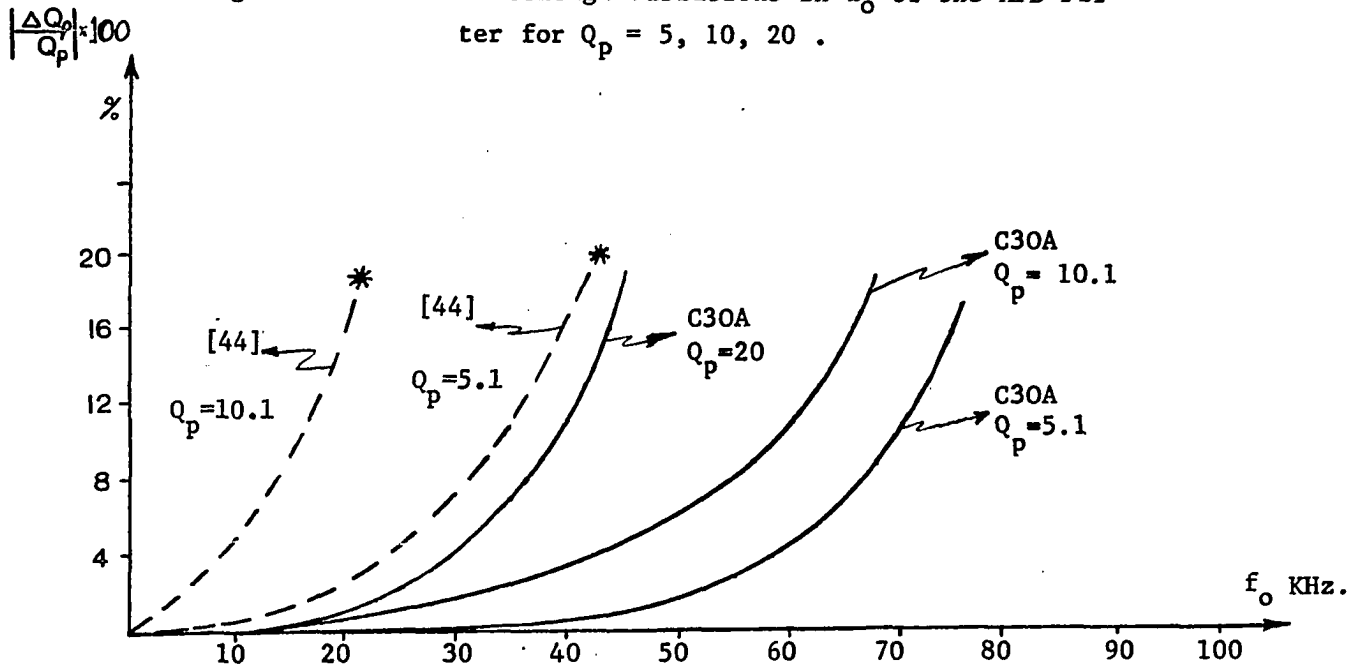
Fig. 5.6.b. Percentage Variations in Q_p of the MFB Filter for Q_p = 5, 10, 20 .

Fig. 5.6. Experimental Results fo the MFB BP Filter Using C30A and the Design Proposed in [44]

performance improvements in the proposed filter design.

5.5 CONCLUSIONS

In this chapter a new method for reducing the limiting effect of the OA's GBWP on active filters is presented. A detailed analysis of magnitude and phase compensation effects on the active filters led to the classification of these filters into two main categories. One that employs active functional building blocks, namely, inverting integrators and finite gain amplifiers, while the other category contains those filters where the functional building blocks cannot be isolated from the filter structure.

Practical examples of filters of both categories are given. The experimental performance of such filters designed using CNOA's is shown to be extremely close in agreement with theory. Performance comparison of the theoretical and experimental results of these filters with the state of the art designs, as well as with the designs using single OA's, show clearly the exceptional improvements of the filters characteristics.

In other words, active filters can be successfully operated at higher frequencies, if the filter structure is designed using compensated OA's such as CNOA's.

In conclusion, we have shown that in precision applications of OA's, such as in the field of active-RC filters, the use of actively compensated OA's (CNOA's) is not only possible but highly desirable. We have demonstrated theoretically the

advantage of such techniques, and have confirmed the results by actual measurements. These new techniques allow the limited GBWP effects of the OA's to be minimized and extend the useful operating frequency range of active filters designed, as well as improving the stability and sensitivity of these designs even at high Q values.

CHAPTER VI

HIGH FREQUENCY GENERALIZED IMMITTANCE CONVERTERS (GIC's) USING

CNOA'S AND THEIR APPLICATIONS IN INDUCTANCE SIMULATIONS AND

PROGRAMMABLE FILTERS:

6.1 INTRODUCTION

In the previous chapter, we discussed an alternative tech-
nology for improving the performance of a given filter transfer
function. The technique proposed, makes use of active devices
(OA's) as well as RC components, with the resulting filters termed
Active-RC filters or simply, Active filters.

The motivation behind the use of active-RC filters lies in
the desire to have inductorless filter realizations. It is well
known that of the three passive RLC elements, the inductor is the
most nonideal one. More over, with the rapidly increasing
interests in developing active filters in the integrated form,
inductors become an obvious obstacle. So far, it has not been
possible to fabricate inductors with reasonable values of
inductance and quality factor by integrated circuit techniques.
On the other hand, conventional inductors when miniaturized to be
consistent in size with other integrated circuit components, are
extremely poor in quality to be of any use for many applications
[2,32].

Probably, the major difficulty in the use of inductors arises
in the case of low frequency applications, like control systems
and analog computers. At these frequencies (less than 1 kHz),

practical inductors of reasonable Q tend to become unrealistically bulky and expensive.

A promising way to overcome the above diffulties is to design inductorless filters, using active elements and only resistors and capacitors as passive elements which are easily integrable. One of the methods of active-RC filter design consists of simulating the inductances in the LC Ladder by active-RC networks. The objective, therefore, is to find an active-RC network having an input impedance Z_{in} = SL where L is the value of the simulated inductance. A variety of networks have been proposed [26,55,56]. One of the most promising designs was the introduction of the Generalized Immittance Converter (GIC) [55]. In this chapter, a brief introduction to the GIC is presented. The effect of using the proposed CNOA's (N=2) in the GIC networks is also presented showing the considerable improvements of the GIC performances. Applications of GIC's in different filtering configurations is illustrated. Considerable bandwidth extension of the GIC filters is achieved through the use of C2OA's.

Two major applications of these improved GIC networks are discussed. The first is realizing a continuous time signal processing device using linear elements and switches controlled by logic signals to achieve fully programmable filters. The filter can be digitally programmed to realize different filtering topologies, as well as different transfer function parameters.

The second application is realizing simulated inductances using the improved GIC networks.

6.2 HIGH FREQUENCY GIC'S USING C2OA'S

6.2.1 The GIC

The Generalized Immittance Converter (GIC) is an active two-port network in which $Y_i = h(s) Y_L$ where Y_i and Y_L are the input and load admittances respectively, and $h(s)$ is referred to as the (admittance conversion function). There are two types of GIC's namely, voltage inversion type and current inversion type. The later can be implemented using two OA's [55]. This type is going to be considered throughout the work in this chapter and will be referred to simply as the GIC.

Let us now consider the GIC circuit [55] shown in Fig. 6.1. Assuming ideal OA's, the chain matrix [a] of the GIC can be obtained as

$$[a] = \begin{bmatrix} 1 & 0 \\ 0 & h(s) \end{bmatrix} \tag{6.1}$$

where $h(s)$, the admittance conversion function, is given by

$$h(s) = Y_2 Y_3 / Y_1 Y_4 \tag{6.2}$$

In the following sections we are going to show the applications of these GIC network in different practical active networks.

6.2.2 Active Filters Using GIC's

In a major contribution proposed in the literature [55], it has been shown that RC-active networks with low sensitivity to element variations can be designed by using GIC's. Several procedures using GIC's has been proposed to synthesis and realize different transfer functions. One major procedure is the proposed cascade synthesis, in which the basic active element is taken to be the GIC of Ref [55], shown in Fig. 6.2. In all, twelve second-order sections are obtained which are found to have the following features:

i) Low sensitivity to passive element variations.

ii) Low sensitivity to DC gain variations.

ii) With the exception of one configuration, isolation amplfiers are unnecessary.

iv) Each configuration uses one GIC and, therefore only two OA's per section are required.

By using combinations of the various sections proposed, Butterworth, Chebychev, Bessel, elliptic, all pass transfer functions, etc. can be realized.

Using the configuration of Fig. 6.2, the transfer functions between the input terminal and the output terminals 1,2,3 were obtained as

$$T_1 = V_1/V_i = \{Y_5 + h(s) \left[Y_7(1+Y_6/Y_2) - Y_5Y_8/Y_2\right]\} /D(s) \quad (6.3)$$

$$T_2 = V_2/V_i = \{Y_5(1+Y_8/Y_4) - Y_6Y_7/Y_4 + h(s)Y_7\} / D(s) \quad (6.4)$$
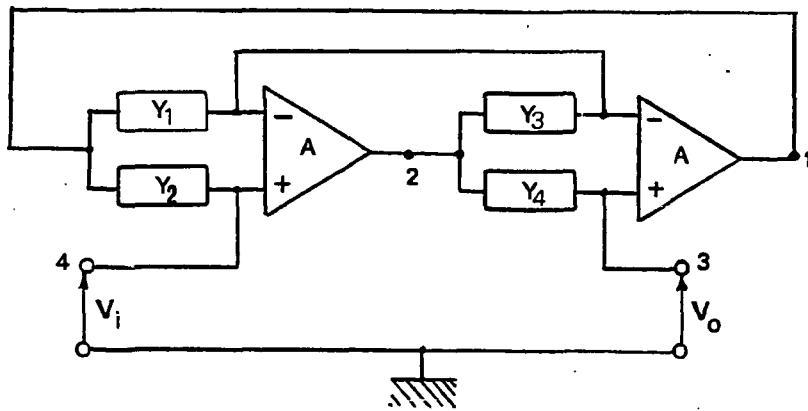
Fig. 6.1.   The Generalized Immittance Converter (GIC)
              Implementation Using OA's .
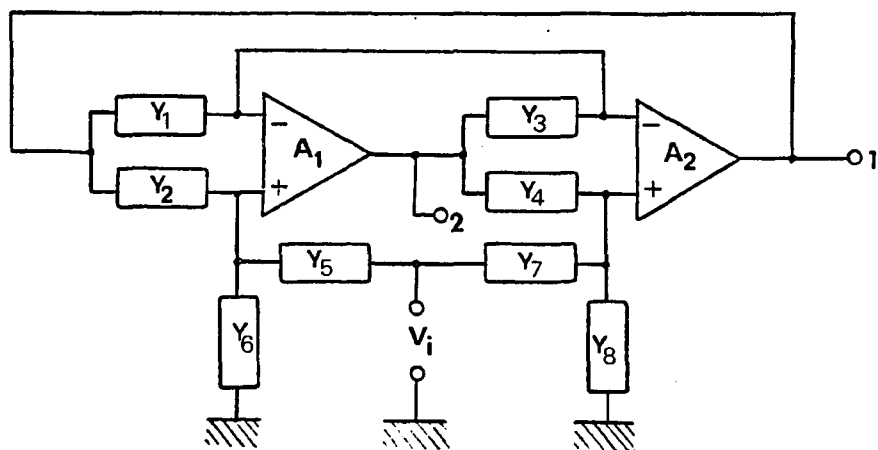
Fig. 6.2.   Active Filter Configuration Using the GIC
              of Fig. 6.1.

$$T_3 = V_3/V_i = \{Y_5 + h(s)Y_7\}\ /D(s) \tag{6.5}$$

where $D(s) = Y_5 + Y_6 + h(s)\ (Y_7 + Y_8)$. $\tag{6.6}$

The conversion function $h(s)$ and $Y_5 - Y_8$ can be selected in many ways and it is found that any second-order transfer function can be realized. By assuming $Y_i = SC_i + G_i$, where $i = 1, 2, 3$ or 4, and using (6.2) we have

$$h(s) = (SC_2 + G_2)(SC_3 + G_3)/(SC_1 + G_1)(SC_4 + G_4) \tag{6.7}$$

It is obvious, by omitting one or more conductances and/or capacitances, a number of specific conversion functions can be generated. A second-order transfer function can be expressed in the general form:

$$T(s) = (a_2 s^2 + a_1 s + a_o)/(b_2 s^2 + b_1 s + b_o) \tag{6.8}$$

where $a_1 = a_2 = 0$, $a_o = a_1 = 0$, $a_o = a_2 = 0$ or $a_1 = 0$ to realize a low pass (LP), high pass (HP), band pass (BP) or a notch (N) section, respectively. The coefficients a_i's and b_i's of $T(s)$ for these sections are all positive. These sections can be realized by choosing $h(s)$ in a simple manner such as $k_1 s$, $k_2 s$, $k_3 s^2 + k_4 s$ or their reciprocals. The different K_i's ($i=1,2,3$ or 4) are positive constants. By comparing (6.3-6.6) with (6.8),

different filtering topologies can be realized as simple RLC networks [55].

All pass (AP) transfer functions are often needed for delay equalization and these can be realized by using second-order transfer functions of the type given by (6.8), where $a_2 = b_2$, $a_1 = -b_1$ and $a_0 = b_0$. Using (6.3, 6.4) and Fig. 6.2, it is clear that the responses are obtained from an OA output, and because of the low output impedance of the OA, any number of sections can be cascaded without isolation amplifiers resulting in higher order active networks.

The pole Q factors and the undamped frequency of oscillation for the transfer function of (6.8) are defined as

$$Q_p = \sqrt{b_0 b_2}/b_1, \quad \omega_p = \sqrt{b_0/b_2} \qquad (6.9)$$

For a notch section, the notch frequency is defined by

$$\omega_n = \sqrt{a_0/a_2} \qquad (6.10)$$

and the multiplier constant can be taken to be

$$H_N = a_0/b_0 \text{ or } a_2/b_2 \qquad (6.11)$$

for $\omega_n > \omega_p$ or $\omega_n < \omega_p$, respectively.

Similarly for the LP, HP and Bp sections

$$H_{LP} = a_0/b_0, \quad H_{HP} = a_2/b_2, \quad H_{BP} = a_1/b_1 \qquad (6.12)$$

Finally, for all pass sections

$$Q_z = \sqrt{a_o a_2}/a_1, \quad \omega_z = \sqrt{a_o/a_2}, \quad H_{AP} = a_2/b_2 \qquad (6.13)$$

Using the above procedure, twelve different excellent transfer functions were proposed [55]. Most of the practical filter specifications can be realized using these designs. The sensitivities of Q_p, ω_p, Q_z, ω_z and also the multiplier constant of the realizations are found to be low with respect to the passive and active element variations. It was found that the realizations are free from low-frequency unstable modes of operation. Furthermore, the amplifier pole does not introduce any high frequency unstable mode. Also, Q_p is not affected by the amplifier pole ω_L, provided $A_o \, \omega_L \gg \omega_p$. Experimental results show close agreement between theory and practice, and these results indicate that these realizations are insensitive to temperature and power supply variations.

6.2.3 The New GIC Using C20A's

Although GIC filters proved to be a major breakthrough in active circuit designs, the same problems discussed in the previous chapter threaten and limit the use of these excellent designs, especially at higher operating frequencies. These problems arises from the finite and complex gain nature of the OA's that degrades the performance of RC-active filters (in general) significantly. This means that active filters based on ideal OA's result in actual characteristics that depart from the

ideal particularly when high pole - ω_p and pole - Q_p's are to be realized. The main thrust in dealing with these problems is to decrease the dependence of active networks on the GBWP's of the OA's used.

In this chapter we are going to follow the same technique used in the previous chapters to improve the performance of active filters. That is, by replacing the single OA's used in designing the GIC's with the composite OA C2OA's, one can obtain a GIC structure that is less dependent on the OA's GBWP's. Consequently, these improved GIC structures will be expected to provide better performance at higher ω_p's and/or Q_p's.

All possible combinations of the four C2OA's structures were used to replace the two OA's in the GIC network of Fig. 6.2. This resulted in sixteen different composite GIC networks. Each of these sixteen GIC networks was implemented in the band pass filter configuration shown in Fig. 6.3a. The filter design values were chosen to realize a BP filter with pole frequency f_p = 49.75 kHz and pole Q_p = 9.97 $\approx$ 10. The gain of this configuration at the pole frequency f_p is fixed at the value of 2.

The best tested combination that was found to provide filter characteristics matches as close as possible the designed values is shown in Fig. 6.3b. This is a GIC BP filter with C2OA-4 and C2OA-3 replacing the first and second single OA's respectively in the GIC structure. The values of α_1 and α_2 ratios used for
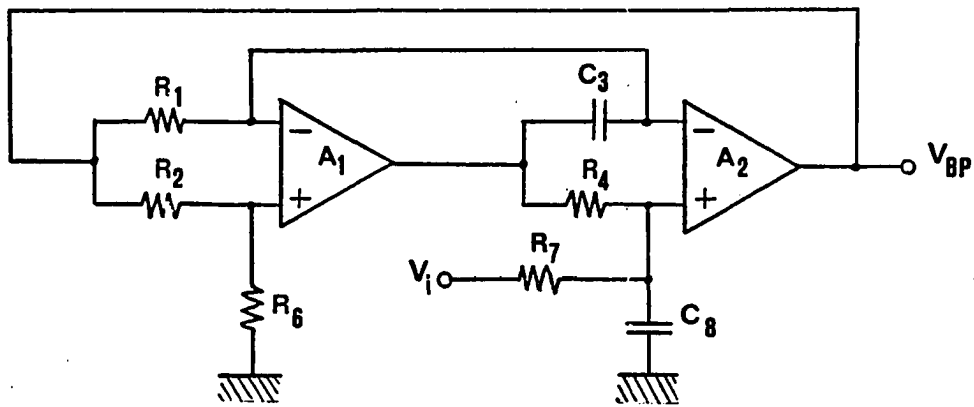
Fig. 6.3.a.   Practical BP Filter Realization Using Single
               OA GIC .
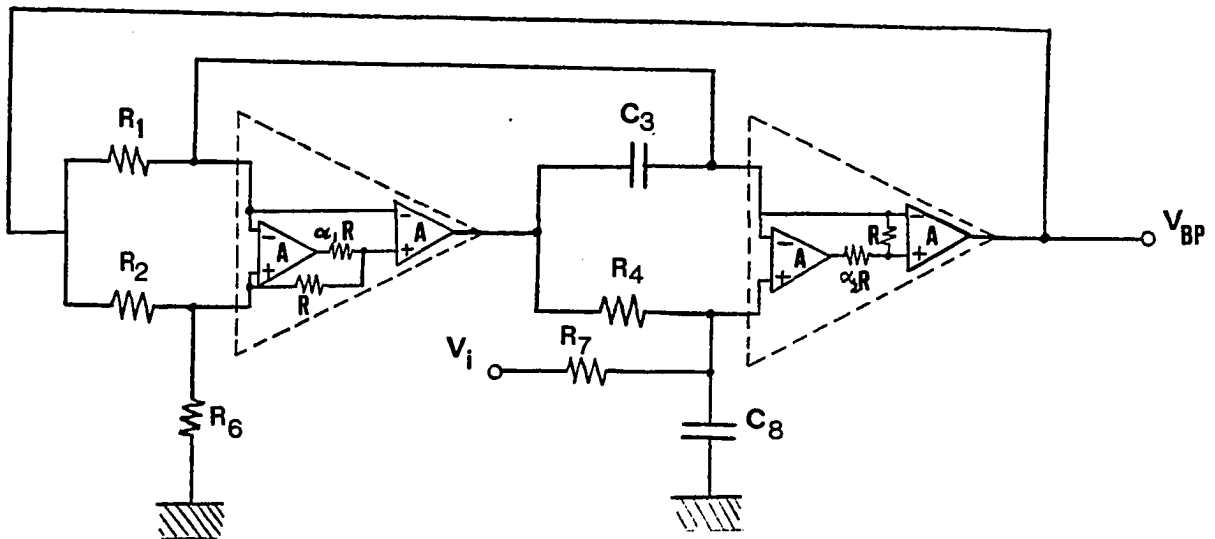
Fig. 6.3.b.   Practical BP Filter Realization of the Com-
               posite GIC Using C2OA-4 and C2OA-3 .

Fig. 6.3.   Practical BP Filter Realization Using the
              GIC .

the compensation of C2OA-4 and C2OA-3 are given in Fig. 6.3b, as well as the different design values of the GIC structure. Fig. 6.4 shows the experimental results of the composite GIC BP filter of Fig. 6.3b and the regular single GIC BP filter of Fig. 6.3a, both for the same ω_p and Q_p. The comparison clearly illustrates the considerable improvements obtained when using the C2OA's in place of the single OA's in the GIC structures. Fig. 6.4 also shows the effect of the compensating ratios α_1 and α_2 variations on the filter response. The same BP filter structure was tested at higher pole frequency of 100 kHz and higher Q_p of 20. The results were extremely, as close as possible to the designed values using the compensating resistor ratios as controlling parameters. Furthermore, no instability problems were encountered in any of these experimental results. By changing some of the GIC passive elements other filtering functions can be obtained as mentioned in the previous section. Fig. 6.5 show the experimental results of different filtering functions using the new high frequency version of the GIC network employing C2OA-4 and C2OA-3.

To capitalize on the successful experimental results using the new proposed composite GIC configuration, it was necessary to verify these results theoretically. The ideal transfer function of the GIC BP filter of Fig. 6.3a (assuming ideal OA's) is given by:
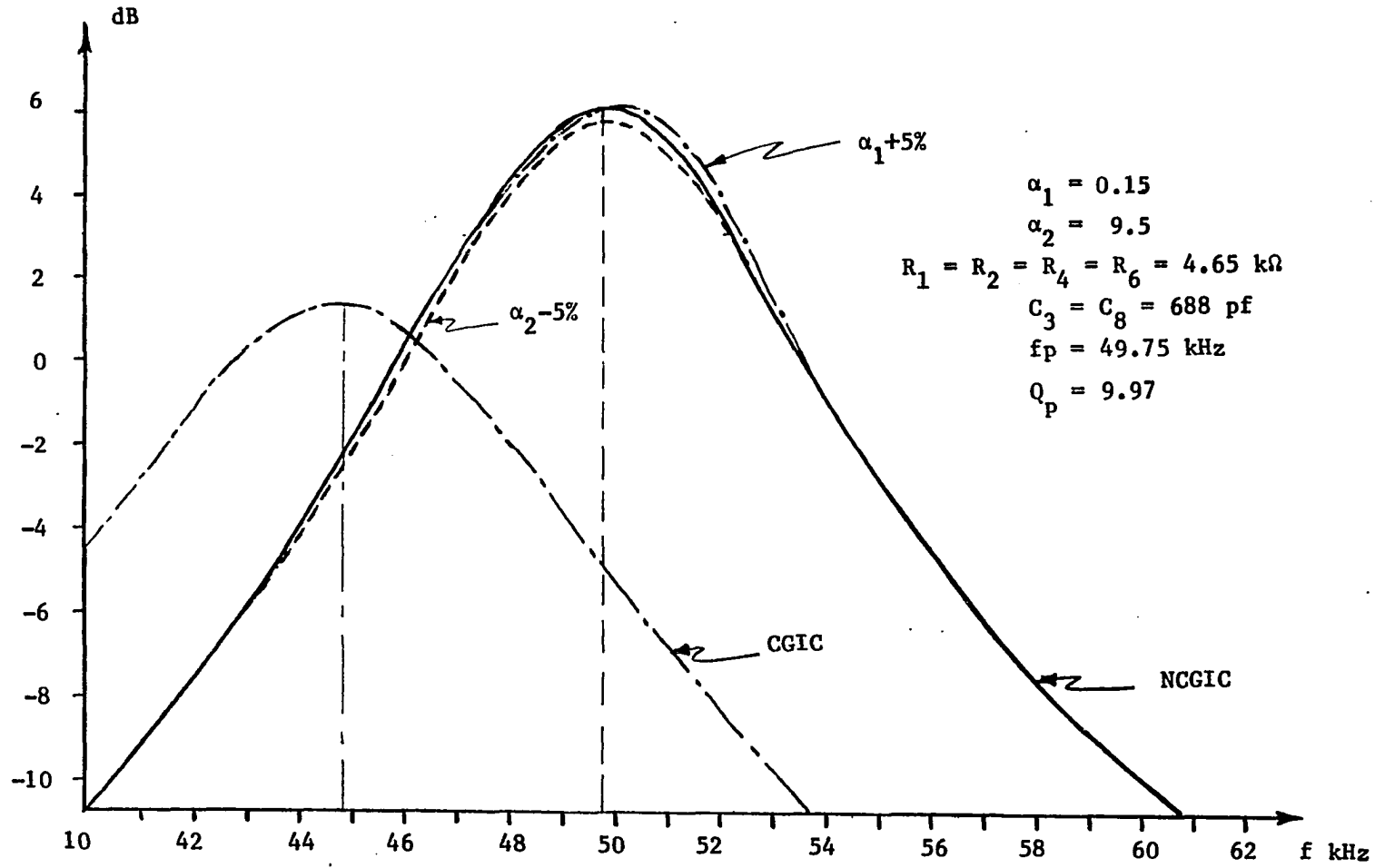
Fig. 6.4. Experimental Results of Single and Composite GIC BP Filters of Fig. 6.3, and the Response Sensitivity for α_1 & α_2 Variations (f_o = 50 kHz, Q_p = 10) .

$\alpha_1 = 0.15$

$\alpha_2 = 9.5$

$R_1 = R_2 = R_4 = R_6 = 4.65$ kΩ

$C_3 = C_8 = 688$ pf

fp = 49.75 kHz

$Q_p = 9.97$
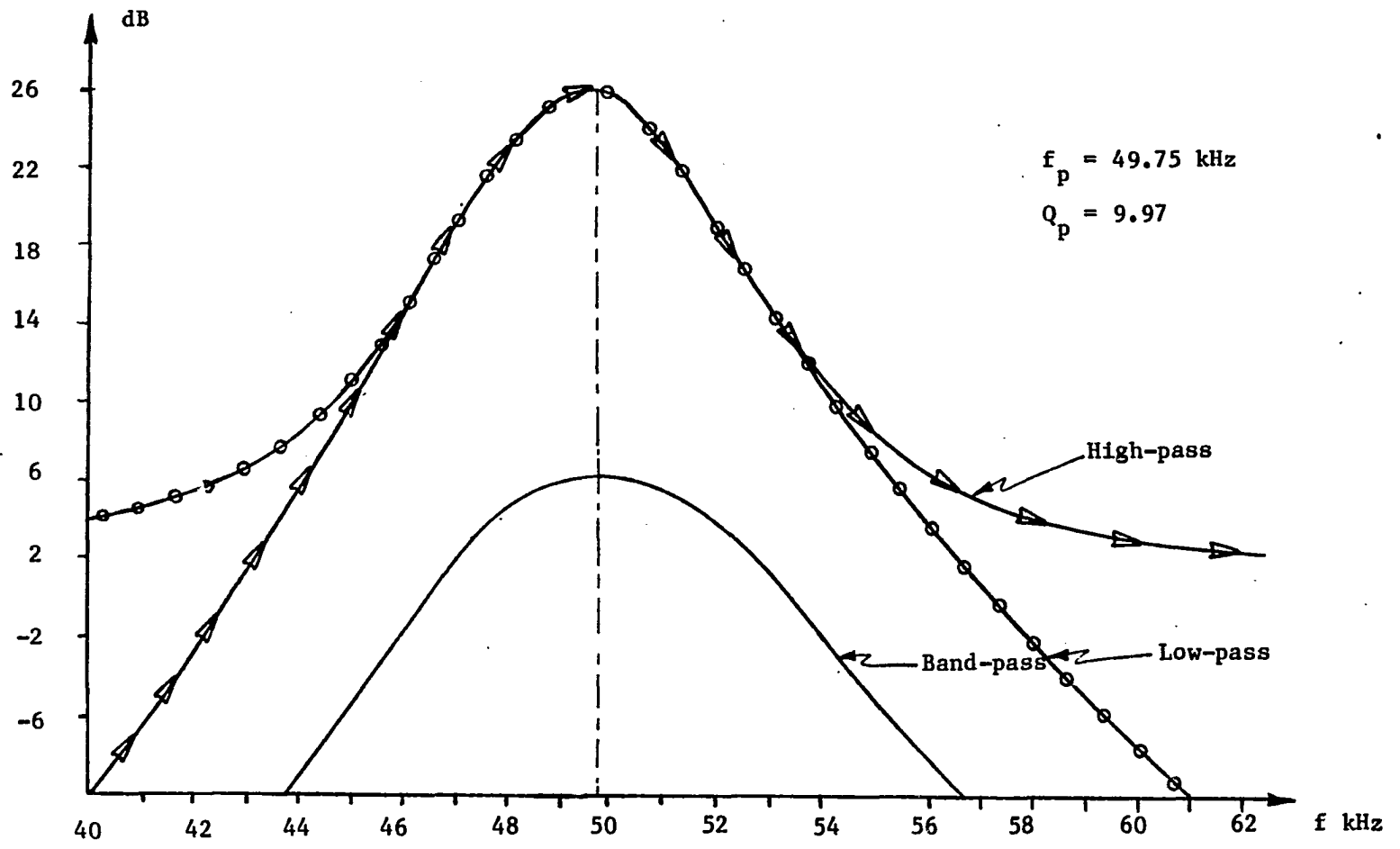
Fig. 6.5.   Experimental Results of the Composite GIC
Filter Response in BP, LP & HP Realizations
$(f_o = 50$ kHz, $Q_p = 10)$.

$f_p = 49.75$ kHz

$Q_p = 9.97$

$$T_i(s) = V_o/V_{in} = sC_3(G_2+G_6)G_7/[s^2C_3C_8G_2+sC_3G_2G_7+G_1G_4G_6] \quad (6.14)$$

Assuming the OA single pole model of (2.2), the above ideal transfer function yields the following single pole GIC BP expression:

$$T_s(s) = V_o/V_{in} = N_s/D_s \quad (6.15)$$

where $N_s = s^2 C_3 G_7/\omega + s[C_3G_7+(G_1G_7/\omega)]$

and $D_s = s^4\{C_3C_8/\omega^2\} + s^3\{[C_3C_8/\omega] + [C_8G_1/\omega^2] + [C_3G_7/\omega^2]\}$

$$+ s^2\{[C_3C_8G_2/(G_2+G_6)]+[C_8G_1/\omega]+[C_3(G_4+G_7)/\omega]+[G_1G_7/\omega^2]\}$$

$$+ s\{[C_3G_2G_7/(G_2+G_6)]+[G_1(G_4+G_7)/\omega]\}+\{G_1G_4G_6/(G_2+G_6)\}.$$

Also using the single pole OA model of (2.2), the composite GIC BP filter of Fig. 6.3b will have the transfer function given by:

$$T_c(s) = V_o/V_{in} = N_c/D_c \quad (6.16)$$

where $N_c = s^3\{(1+\alpha_1)C_3G_7/\omega^2\}+s^2\{[(1+\alpha_1)G_1G_7/\omega^2]+[(1+\alpha_1)C_3G_7/\omega]\}$

$$+s\{C_3G_7\}$$

and $D_c = s^6\{(1+\alpha_1)(1+\alpha_2)C_3C_8/\omega^4\}$

$$+s^5\{[(1+\alpha_1)(1+\alpha_2)C_3C_8/\omega^3]+[(1+\alpha_1)(1+\alpha_2)C_3(G_4+G_7)/\omega^4]\}$$

$$+[(1+\alpha_1)(1+\alpha_2)C_8G_1/\omega^4]\}$$

$$+s^4\{[(1+\alpha_2)C_3C_8/\omega^2]+[\alpha_1C_3C_8G_2/(G_2+G_6)\omega^2]$$

$$+[(1+\alpha_1)(1+\alpha_2)C_3(G_4+G_7)/\omega^3]$$

$$+[(1+\alpha_1)C_8G_1/\omega^3]+[(1+\alpha_1)(1+\alpha_2)G_1(G_4+G_7)/\omega^4]\}$$

$$+s^3\{[(1+\alpha_1)C_3C_8G_2/(G_2+G_6)\omega]+[(1+\alpha_2)C_3(G_4+G_7)/\omega^2]$$

$$+[(1+\alpha_1)C_8G_1/\omega^2]$$

$$+[\alpha_1C_3G_2(G_4+G_7)/(G_2+G_6)\omega^2]+[(1+\alpha_1)G_1(G_4+G_7)/\omega^3]\}$$

$$+s^2\{[C_3C_8G_2/(G_2+G_6)]+[\alpha_1C_3G_2G_7/(G_2+G_6)\omega]$$

$$+[C_3G_2(G_4+G_7)/(G_2+G_6)\omega]$$

$$+[(1+\alpha_1)G_1(G_4+G_7)/\omega^2]\}$$

$$+s\{[C_3G_2G_7/(G_2+G_6)]+[\alpha_1G_1G_4G_6/(G_2+G_6)\omega]+[G_1G_4/\omega]\}$$

$$+\{G_1G_4G_6/(G_2+G_6)\}.$$

where the GBWP of all the OA's used assumed to be equals for

simplicity i.e. $A_1=A_2=A_3=A_4 \cong \dfrac{\omega}{s}$.

Note that the ideal transfer function (6.14) can be obtained from either (6.15) or (6.16) by letting $\omega \to \infty$.

Computer plots of the three BP transfer functions (6.14)–(6.16) are shown in Fig. 6.6, for a pole frequency f_p = 49.75
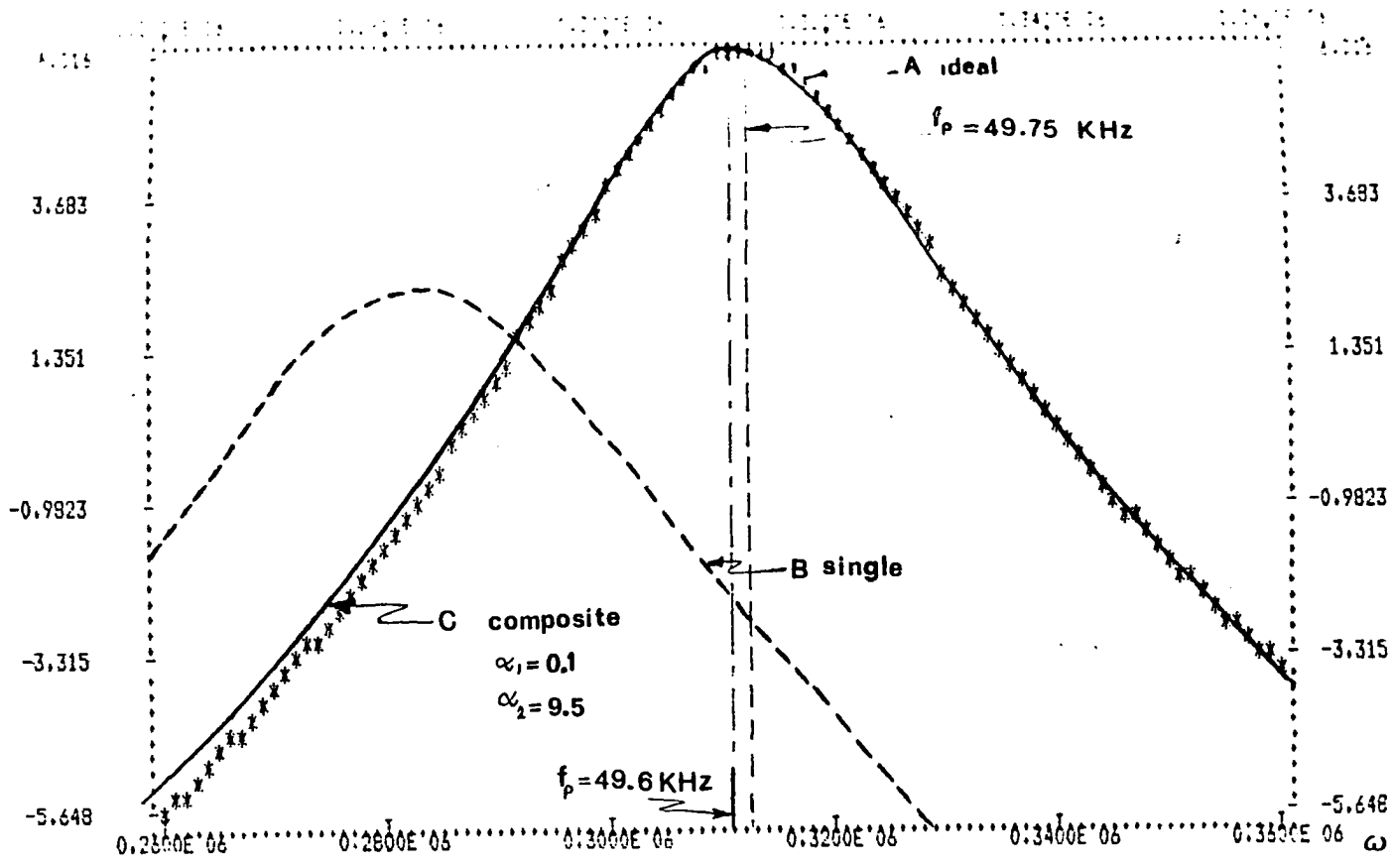
Fig. 6.6.   Computer Plots of the Theoretical Frequency
Responses of Ideal, Single and Composite GIC
(f_o = 50 kHz, Q_p = 10) .

110

kHz, and a pole $Q_p \simeq 10$. The figure shows clearly the considerable improvements in the filter response when using C2OA's in the GIC structure over that of a single GIC of this high ω_p and Q_p. Figs. 6.7a and 6.7b illustrate. the passive and active sensitivities of the composite GIC structures with respect to variations in the compensating ratios α_1 and α_2 as well as the OA GBWP's. The computer frequency response plots of Figs. 6.6 and 6.7 are in close agreement with the experimental results of Fig. 6.4.

To verify the experimental results of the wide BW applications of the new composite GIC filter, Figs. 6.8a and 6.8b show the computer plots of the filter frequency responses at $f_p \doteq$ 49.75 kHz and Q_p's = 10, 20, 40, as well as responses at $f_p =$ 100 kHz and Q_p's = 10, 20, 40. Similar results were previously obtained experimentally and were found in close agreement with the ideal responses.

Another verification of the theoretical and experimental results obtained for the new composite GIC design was through the use of Electronic Circuit Analysis Program (ECAP) to simulate the responses of the structure. Fig. 6.9 shows the OA model used to simulate each single OA in the filter structure. The complete ECAP program used is listed in Appendix D.2. Again the results obtained using this simulation were in close agreement with both the theoretical and experimental responses.
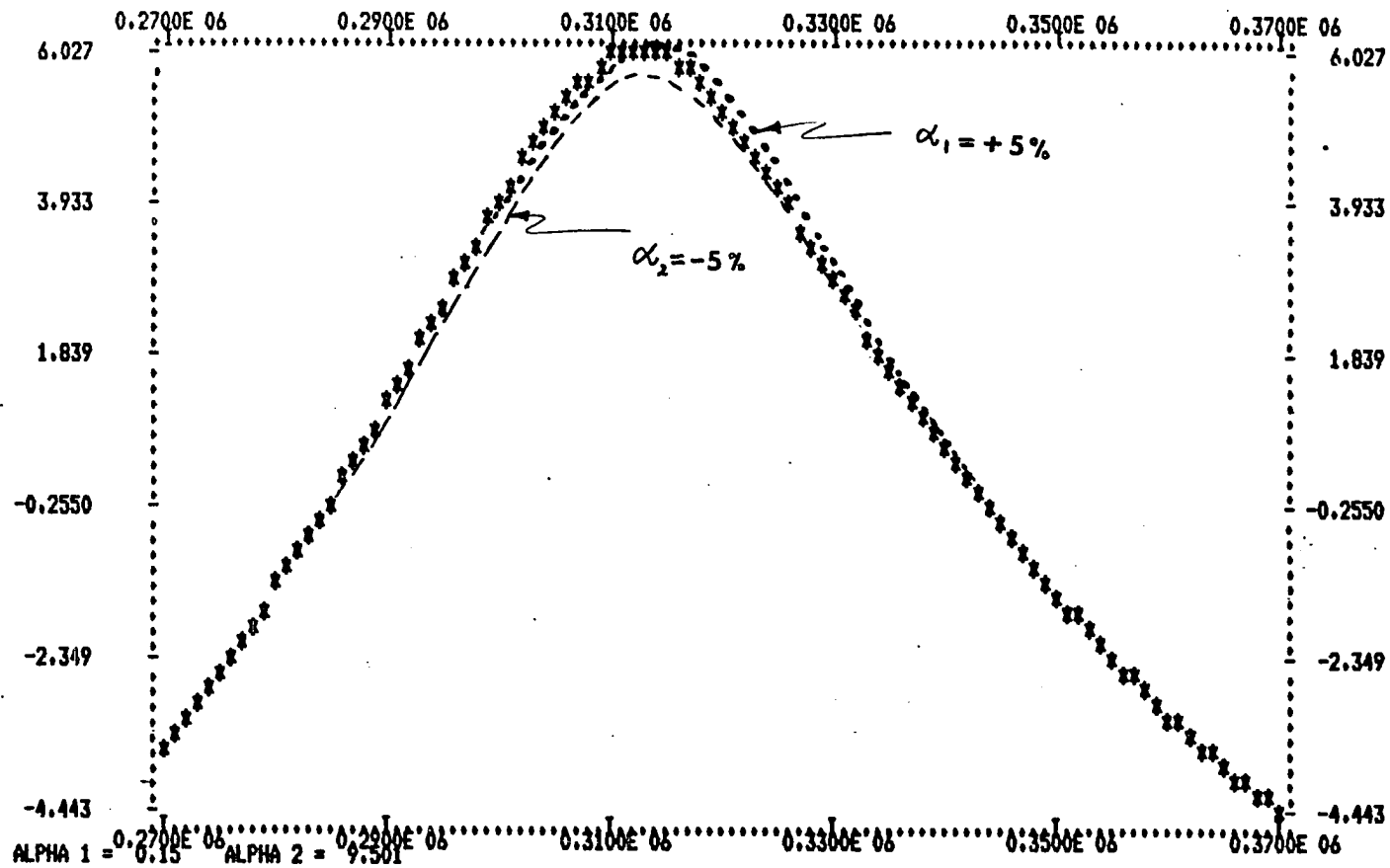
Fig. 6.7.a.   Computer Plots of the Composite GIC BP Filter
Responses with Compensating Elements Varia-
tions Effects

112

| | 0.2700E 06 | 0.2900E 06 | 0.3100E 06 | 0.3300E 06 | 0.3500E 06 | 0.3700E 06 |

GBWP = −5 %

GBWP = +5 %

$\alpha_1 = 0.15$

$\alpha_2 = 9.5$
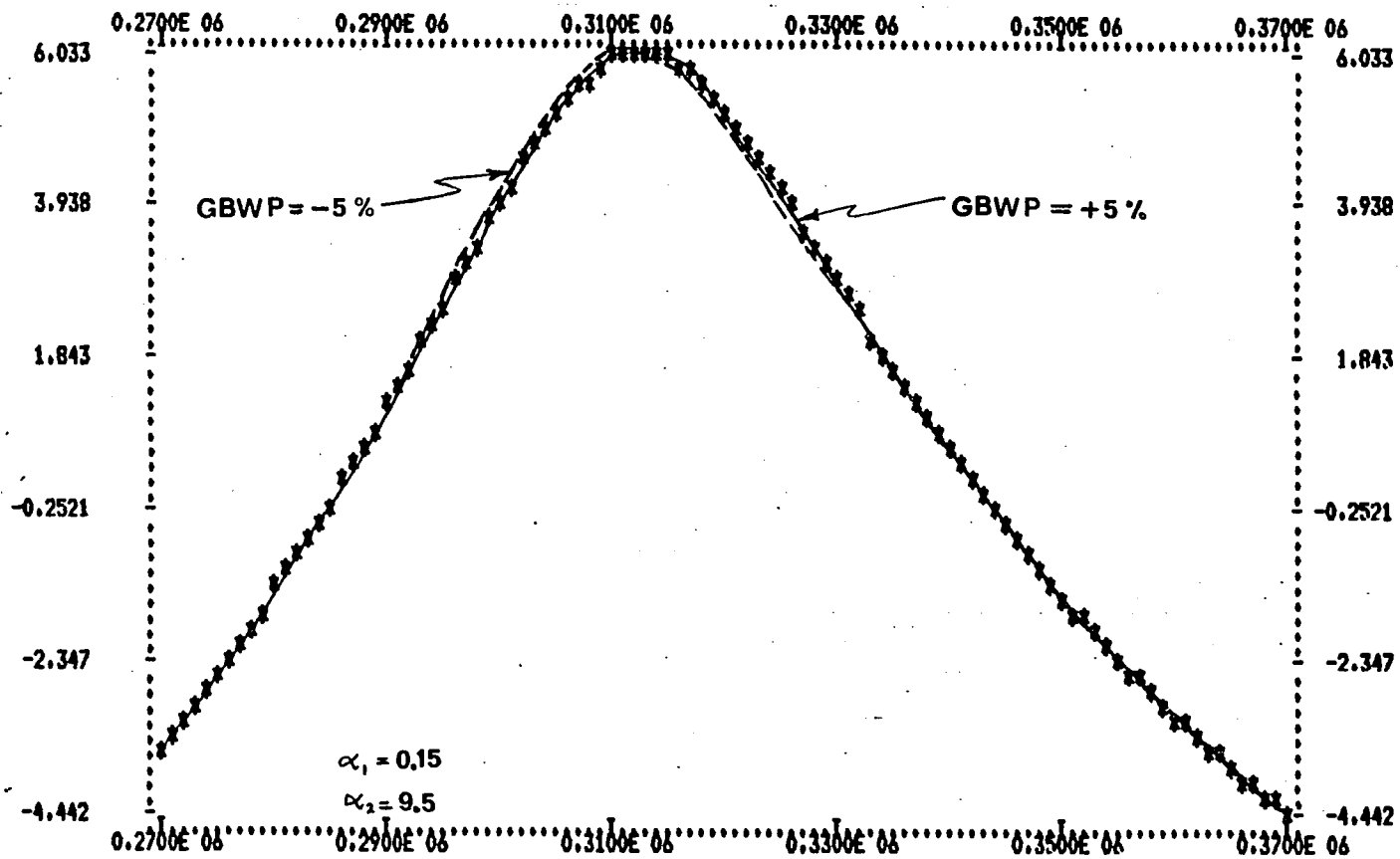
Fig. 6.7.b. Computer Plots of the Composite GIC BP Filter Responses with GBWP Variations Effects .

Fig. 6.7. Computer Plots of the Composite GIC BP Filter Responses with Element Variations Effects ($f_o = 50$ kHz, $Q_p = 10$) .
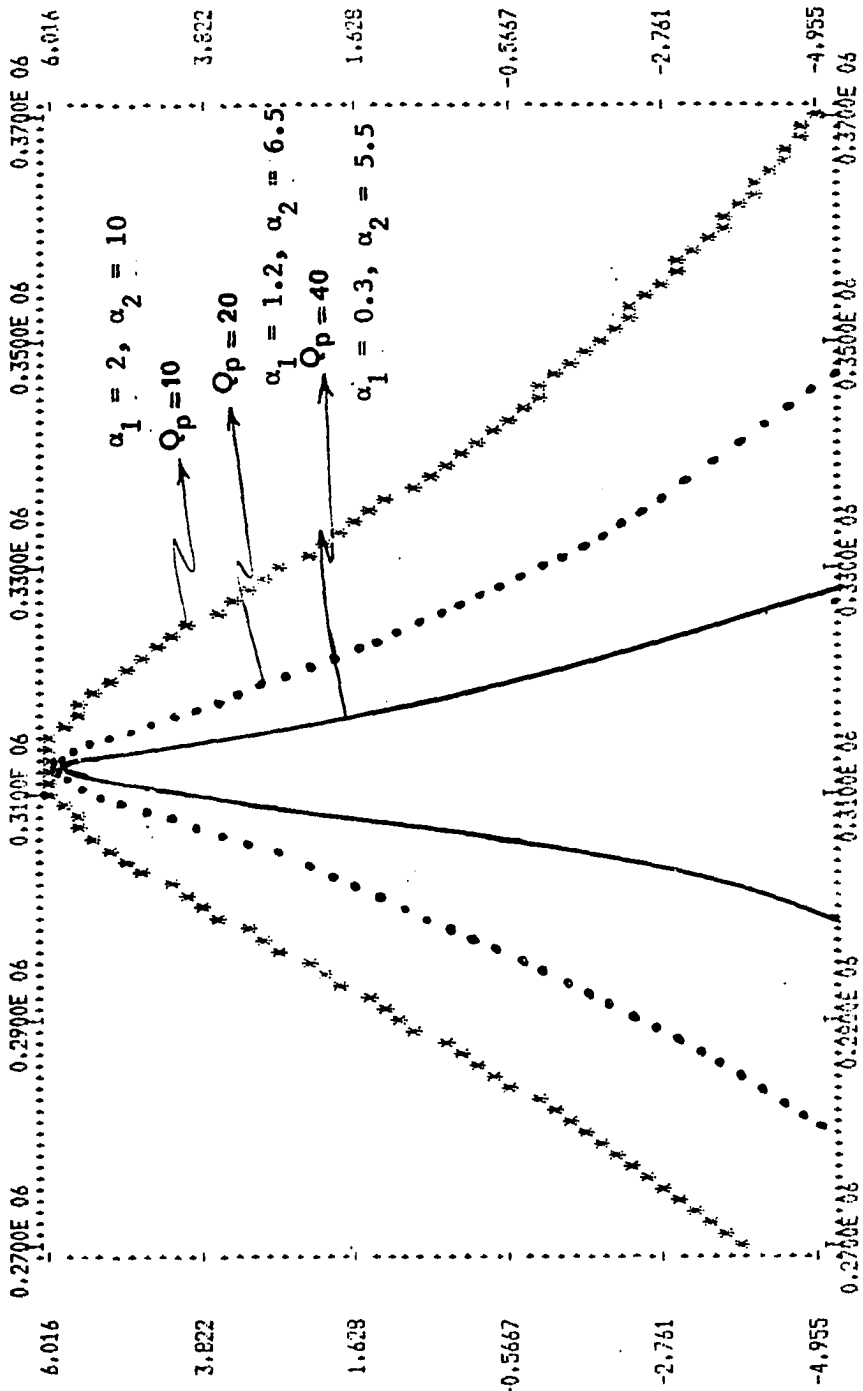
Fig. 6.8.a.   Computer Plots of the Composite GIC BP Fil-
ter Frequency Responses for f_o = 50 kHz & Q_p
= 10, 20, 40 .
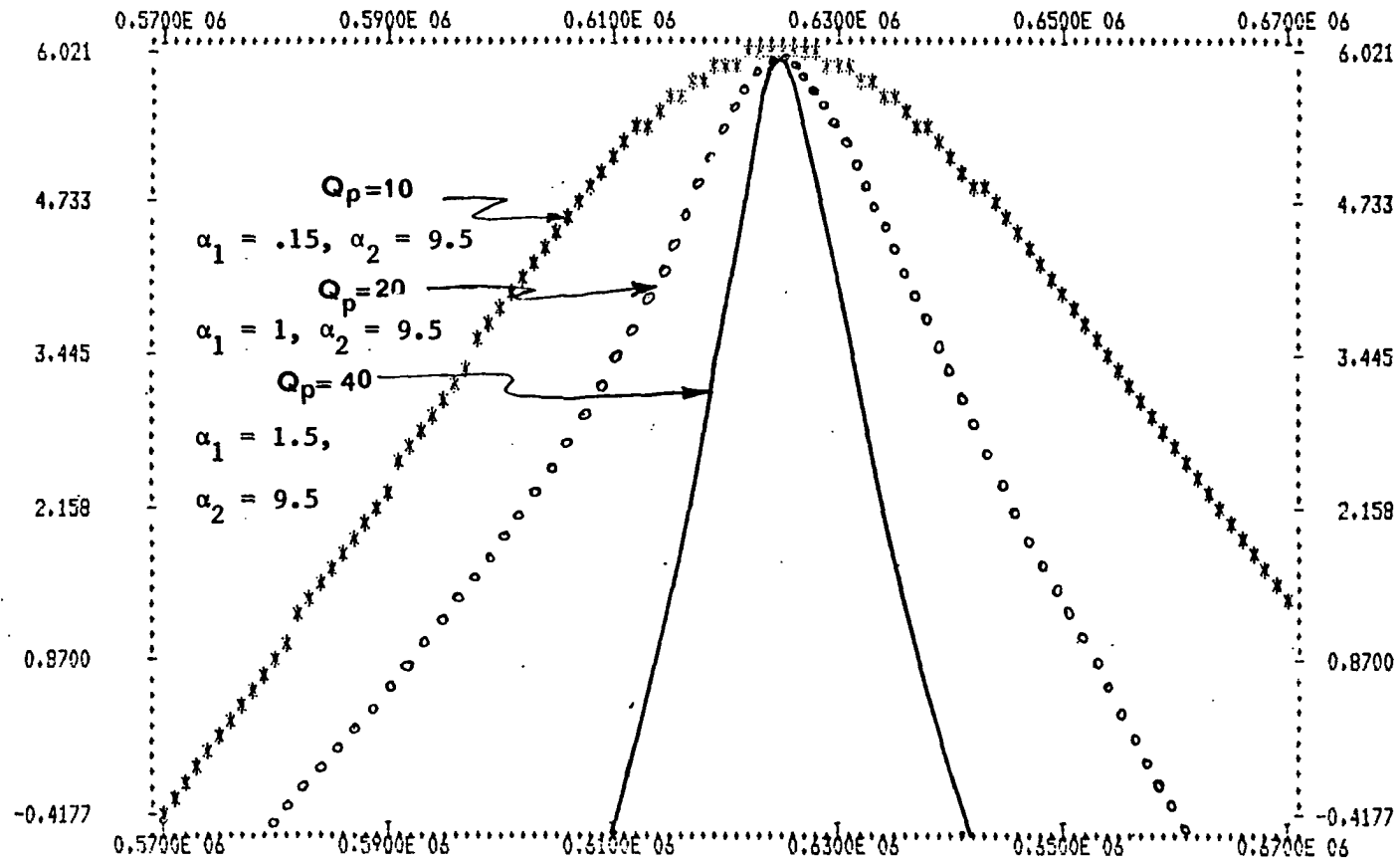
Fig. 6.8.b. Computer Plots of the Composite GIC BP Filter Frequency Responses for f_o = 100 kHz & Q_p = 10, 20, 40 .

Fig. 6.8. Computer Plots of the Composite GIC BP Filter Frequency Responses for Different ω_o's and Q_p's .

115
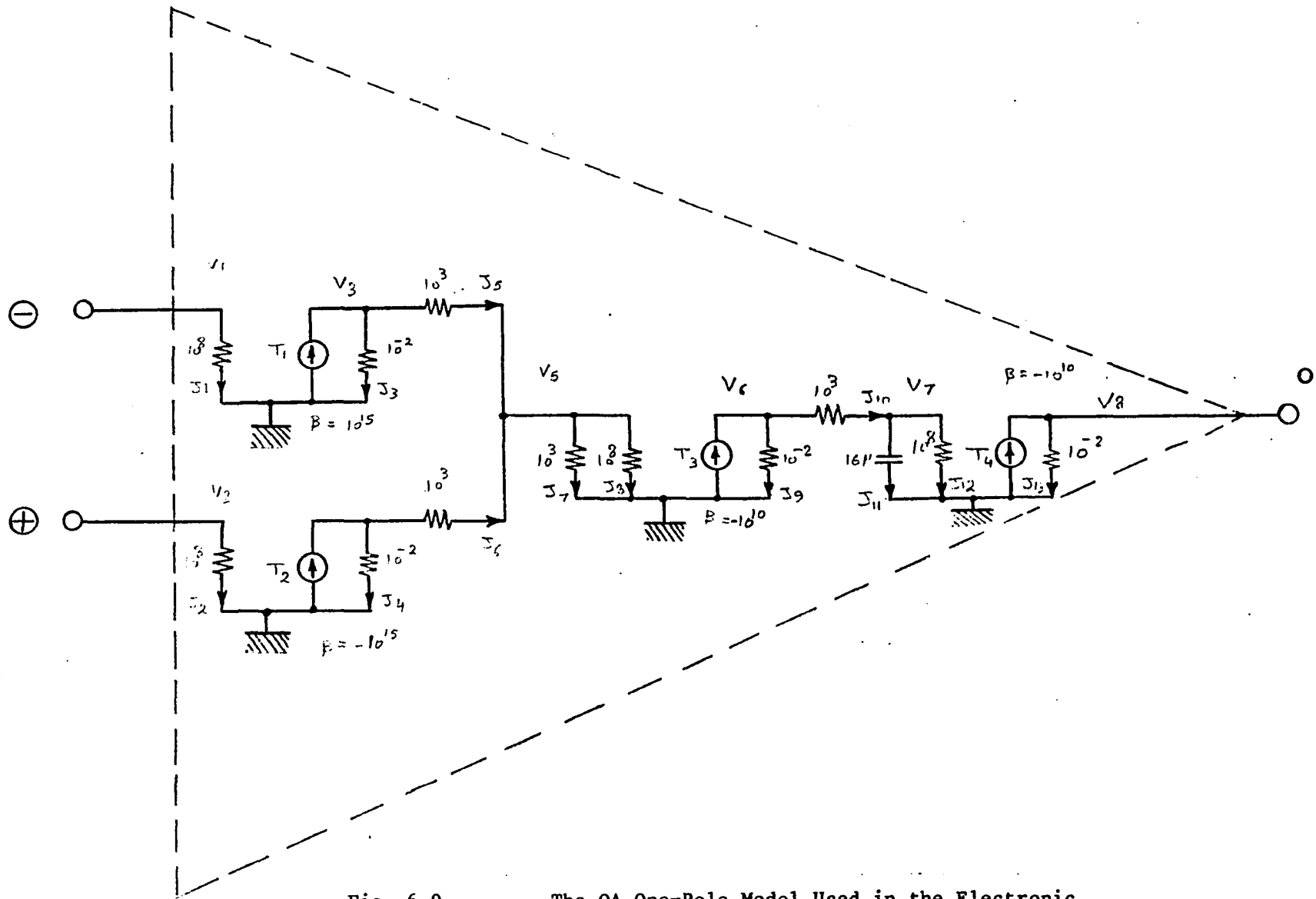
Fig. 6.9.   The OA One-Pole Model Used in the Electronic
Circuit Analysis Program to Simulate the
Filter Responses .

6.3 APPLICATIONS OF THE GIC NETWORKS IN PROGRAMMABLE FILTERS

6.3.1 Programmable Filters

Signal processing devices evolved considerably over the last several years. The progress was motivated by the advancement in film and semiconductor technologies, as well as the continuous upgrading of systems specifications to take advantage of the available technologies to the limits.

Linear filtering finds many applications, such as speech processing (recognition or synthesis), geology, instrumentation, communications, process control, adaptive balancing, etc. There has been much emphasis on performing the filter function digitally, largely because of the ease of varying and optimizing the transfer function. However, for many reasons, such as cost, size signal processing complexity, and bandwidth, it would be desirable to perform the filter function with linear components, yet retain the flexability of varying the filter parameters digitally.

Recently, several advantages of combining linear components (amplifiers and capacitors) and nonlinear elements (switches) have been demonstrated using MOS switched capacitor techniques [57,58]. Here, we are presenting the results of realizing a continuous active device using linear elements and switches controlled by digital signals to achieve fully programmable filters [30].

Our research addressed two different aspects of programma-
bility, namely:

1. Programming the filter's topology using a minimal set of
   elements to obtain any type of filtering function
   desired, e.g., LP, HP, BP, N, AP., etc.

2. Programming the transfer function parameters, e.g., pole
   resonant frequency ω_p and quality factor Q_p for a
   chosen type of filtering function.

6.3.2 The Proposed GIC Programmable Filter

The basic active network considered here as the heart of the
programmable filter is the GIC structure [55] of Fig. 6.2, whose
superior performance was established in the literature [59] and in
the previous section. The transfer function realized was given in
(6.8).

Table 6.1, illustrates that for any of the LP, HP, BP and N
realizations, five resistors, two capacitors and two OA's are
required. The passive elements are connected to different nodes,
shown in Fig. 6.10a, for the different realizations. A set of MOS
bilateral switches controlled by a digital binary word, are used
to interchange the elements to achieve the different types of
filter realizations as shown in Fig. 6.10b. The truth table of
the switch control logic is shown in Table 6.2, while Fig. 6.11
illustrates the minimum CMOS logic circuit used to realize this
table.

While four of the resistors are equal and of value R each,
the fifth resistor is the Q_p determining resistor and of value

Filter Type	Y_1	Y_2	Y_3	Y_4	Y_5	Y_6	Y_7	Y_8	Transfer Function
LP	G	C	$C+\dfrac{G}{QP}$	G	G	0	0	G	$T_2 = 2Wp^2/D(s)$
HP	G	G	C	G	0	G	C	$\dfrac{G}{QP}$	$T_1 = 2S^2/D(s)$
BP	G	G	C	G	0	G	$\dfrac{G}{QP}$	C	$T_1 = 2(Wp/Qp)^S/D(s)$
N+	G	G	C	G	G	0	C	$\dfrac{G}{QP}$	$T_2 = (S^2+W_n^2)/D(s)$

where $T(s) = N(s)/D(s)$ and. $D(s) = S^2 + (Wp/Qp)S + Wp^2$

+The other output T_1 realizes all-pass for the same elements.

TABLE 6.1.   The Elements Identification for Different
            Realizations of the GIC Filter .

119
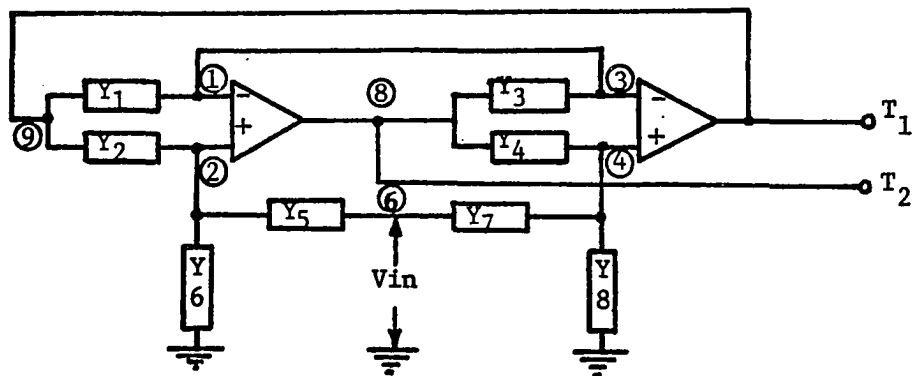
Fig. 6.10.a. Schematic Diagram of the Programmable GIC Filter Showing the Controlled Nodes .

To be Connected in Case of	Component Represented Realized	Node in Fig.1	Component & Switches	Node in Fig.1	Component Represented Realized	To be connected in case of
L, H, B, N	R_2, R_5	②	R — S_1, S_2	⑨ ⑥	R_2 R_5	H, B / L, N
N / L, H, B	R_2 / R_6, R_8	⑨	S_{15}, S_{16} — R — S_3, S_4	② ④	R_6, R_2 / R_8	H, B, N / L
L / H, B, N	C_2 / C_7, C_8	② ④	S_{13}, S_{14} — C — S_5, S_6, S_7 — GND	⑨ ⑥	C_2 / C_7 / C_8	L / H, N / B
L / H, B, N	RQ_3 / RQ_7, RQ_8	⑧ ④	S_{11}, S_{12} — RQ — S_8, S_9, S_{10} — GND	③ ⑥	RQ_3 / RQ_7 / RQ_8	L / B / H, N
H, B / L, N	T_1 / T_2	⑨ ⑧	S_{29}, S_{30} — Output		Output	L, H, B, N

Fig. 6.10.b.   Different Elements Realizations and the Corresponding Switches Used for Digitally Selecting the Filtering Type .

121

Binary Input fa fb	Filter (Switch)	S_1	S_2	S_3	S_4	S_5	S_6	S_7	S_8	S_9	S_{10}	S_{11}	S_{12}	S_{13}	S_{14}	S_{15}	S_{16}	S_{29}	S_{30}
0 0	Low Pass	0	1	0	1	1	0	0	1	0	0	1	0	1	0	0	1	0	1
1 0	High Pass	1	0	1	0	0	1	0	0	0	1	0	1	0	1	0	1	1	0
0 1	Band Pass	1	0	1	0	0	0	1	0	1	0	0	1	0	1	0	1	1	0
1 1	Notch	0	1	1	0	0	1	0	0	0	1	0	1	0	1	1	0	0	1

TABLE 6.2.   The Truth Table of the Switches Logic Used to Select the Filtering Function .
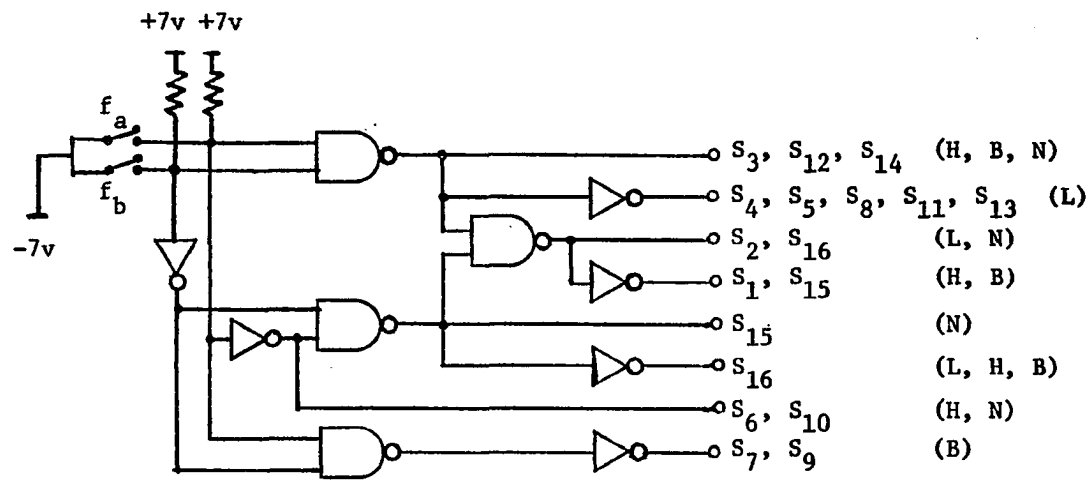
Fig. 6.11.   The CMOS Logic Diagram Used to Control the
Analog CMOS Switches of Fig. 6.10.b and to
Realize the Truth Table 6.2 .

$R_q = RQ_p$. The two capacitors are equal and of value c = $(1/\omega_p R)$ each. Two equal banks of capacitors are used to control ω_p. Each bank contains n binary weighted capacitors connected in parallel through analog CMOS switches as shown in Fig. 6.12. Using a digital binary word of n bits to control ω_p, different values of c will result at the 2 terminals of both capacitor banks that correspond to 2^n different values of ω_p. Using a similar technique the value of R_q can be controlled through a bank of m binary weighted resistors connected in series through analog CMOS switches as shown in Fig. 6.13. Using a digital binary word of m bits to control Q_p, different values of R_q can be achieved that correspond to 2^m different values of Q_p. Thus, full independent control of the pole pair ω_p and Q_p are achieved by programming the digital words controlling the switches to obtain the corresponding c and R_q. It can be easily shown that with minor modifications, an additional programmable element can be added for the control of the notch frequency.

The experimental results obtained using two-bit world to select the type of transfer function and two words four-bits each to determine ω_p and Q_p independently are given in Tables 6.2 and 6.3. Figs. 6.14a - 6.14d illustrates the different responses of the filter for different digital words to program the filtering function, Q_p and ω_p in different configurations.

Using the composite GIC network in this programmable filter design provides a better performance and extends the filter

digital word controlling Wp

$a_n \cdot \cdot a_2 \, a_1 \, a_0$

(For linear Wp control $C_{i+1}=2C_i$, consequently $C=\sum\limits_{i=0}^{n} C_0 A_i$)
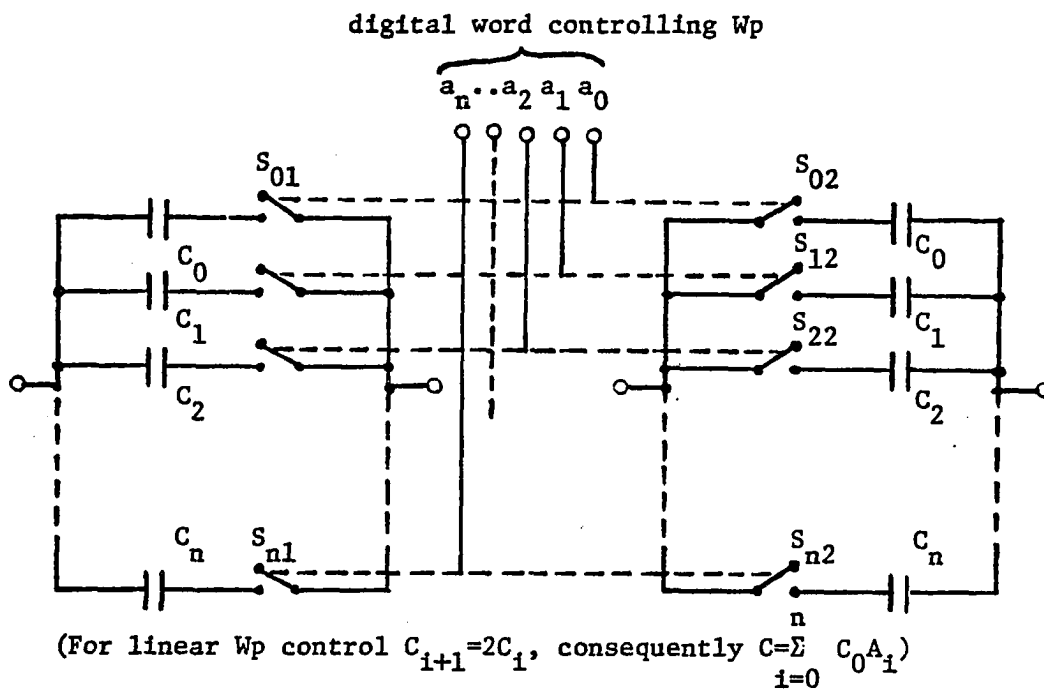
Fig. 6.12.　　The Two Capacitor Banks Realizations for the Programming of ω_p .

digital word controlling Qp

$b_m \quad b_2 \quad b_1 \quad b_0$

(For linear Qp control, $R_{j+1}=2R_j$ resulting in $RQp=\sum\limits_{j=0}^{m} R_0 b_j$)
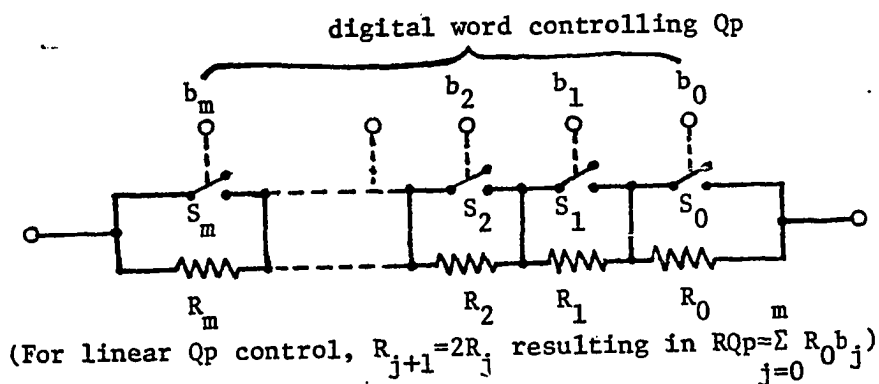
Fig. 6.13.　　The Resistor Bank Used to Realize R_q Needed for the Programming of Q_p.

f_p					Q_p				
a_3	a_2	a_1	a_0	f_p realized (kHz)	b_3	b_2	b_1	b_0	Q_p realized
0	0	0	1	7.96	0	0	0	1	0.5
0	0	1	0	3.98	0	0	1	0	1
0	0	1	1	2.65	0	0	1	1	1.5
0	1	0	0	1.99	0	1	0	0	2
0	1	0	1	1.59	0	1	0	1	2.5
0	1	1	0	1.33	0	1	1	0	3
0	1	1	1	1.14	0	1	1	1	3.5
1	0	0	0	0.95	1	0	0	0	4
1	0	0	1	0.88	1	0	0	1	4.5
1	0	1	0	0.80	1	0	1	0	5
1	0	1	1	0.72	1	0	1	1	5.5
1	1	0	0	0.66	1	1	0	0	6
1	1	0	1	0.61	1	1	0	1	6.5
1	1	1	0	0.57	1	1	1	0	7
1	1	1	1	0.53	1	1	1	1	7.5

Q_p (R=20KΩ, C_1=1nF, R_1=10KΩ)

TABLE 6.3.   The Two Four-Bit Words that Control f_p and Q_p
and their Corresponding Realized f_p and Q_p

126
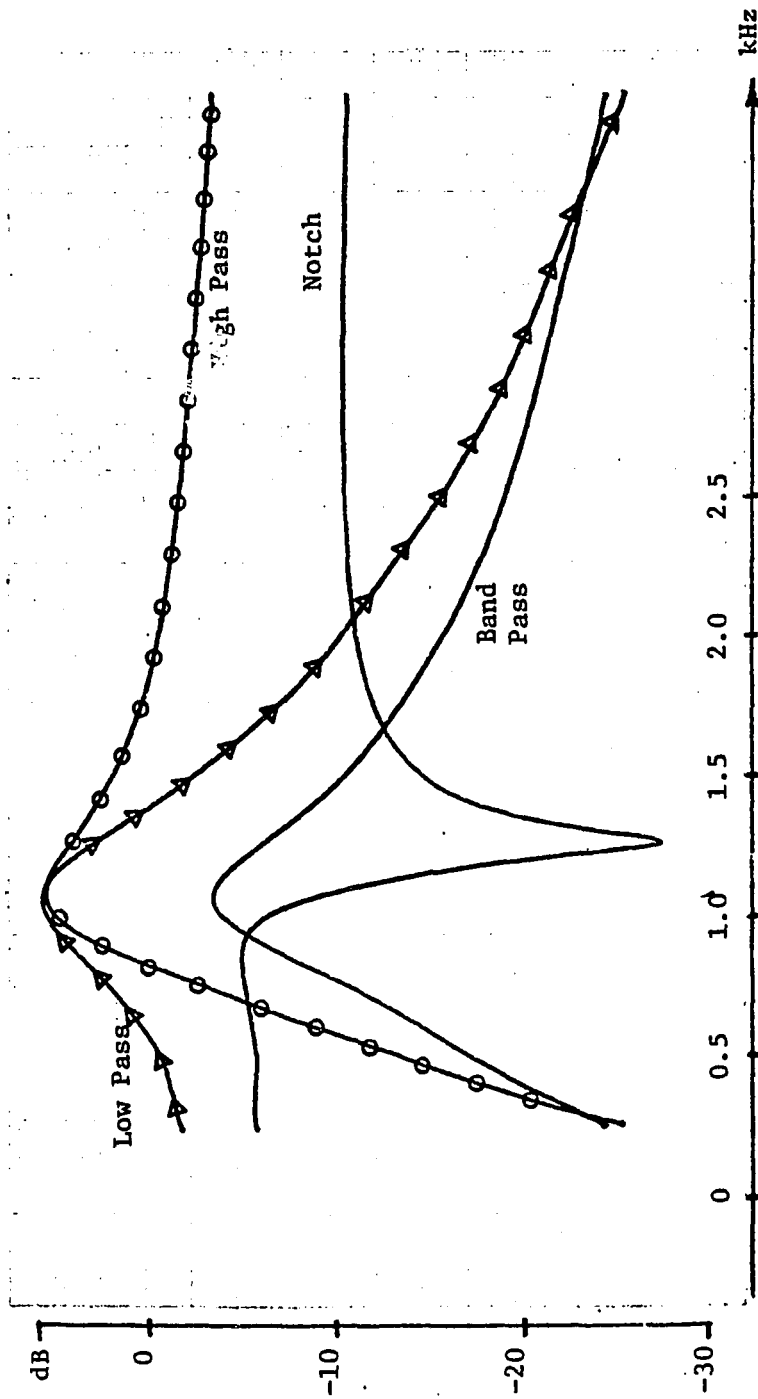
Fig. 6.14.a.   The Transfer Function Programming ($f_p = 1.15$ kHz, $Q_p = 3$).

Reproduced with permission of the copyright owner. Further reproduction prohibited without permission.
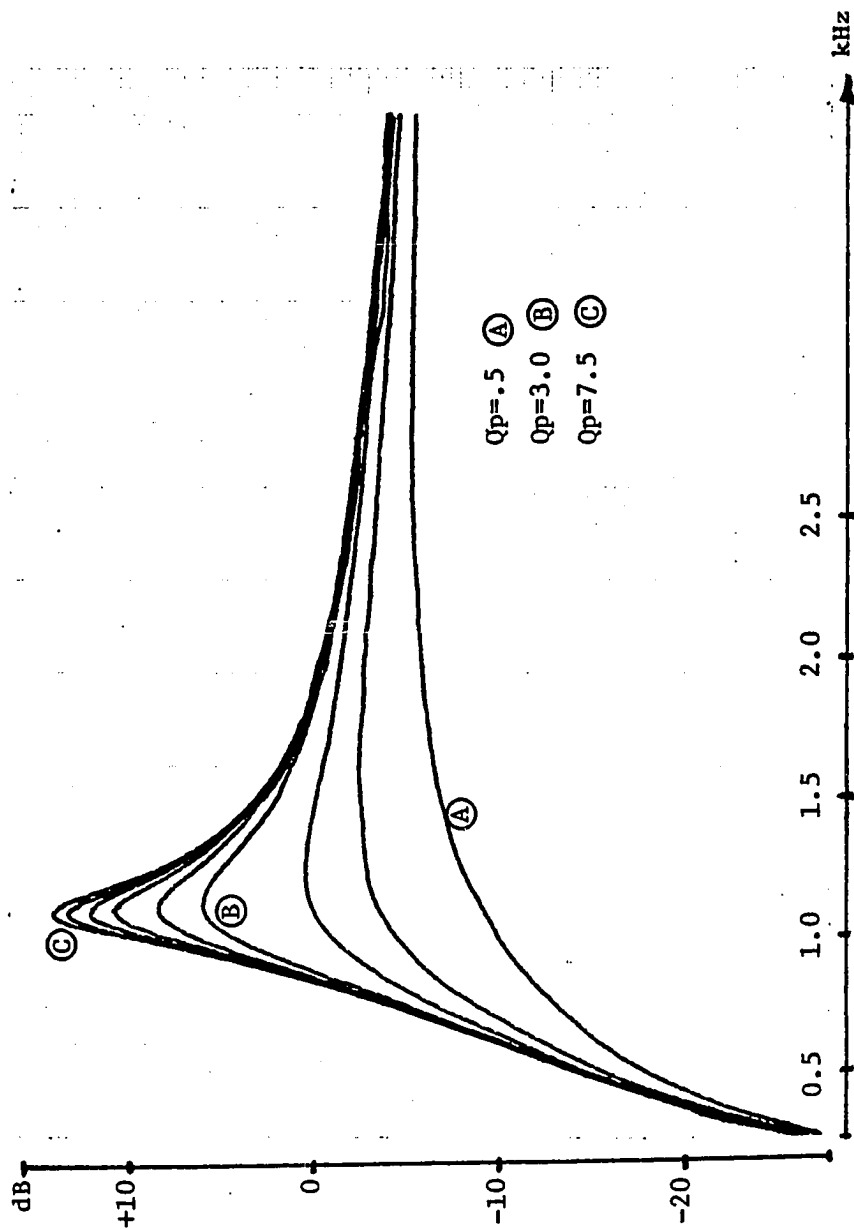
Fig. 6.14.b. Q_p Programming of a High-Pass Filter (f_p = 1.15 kHz)
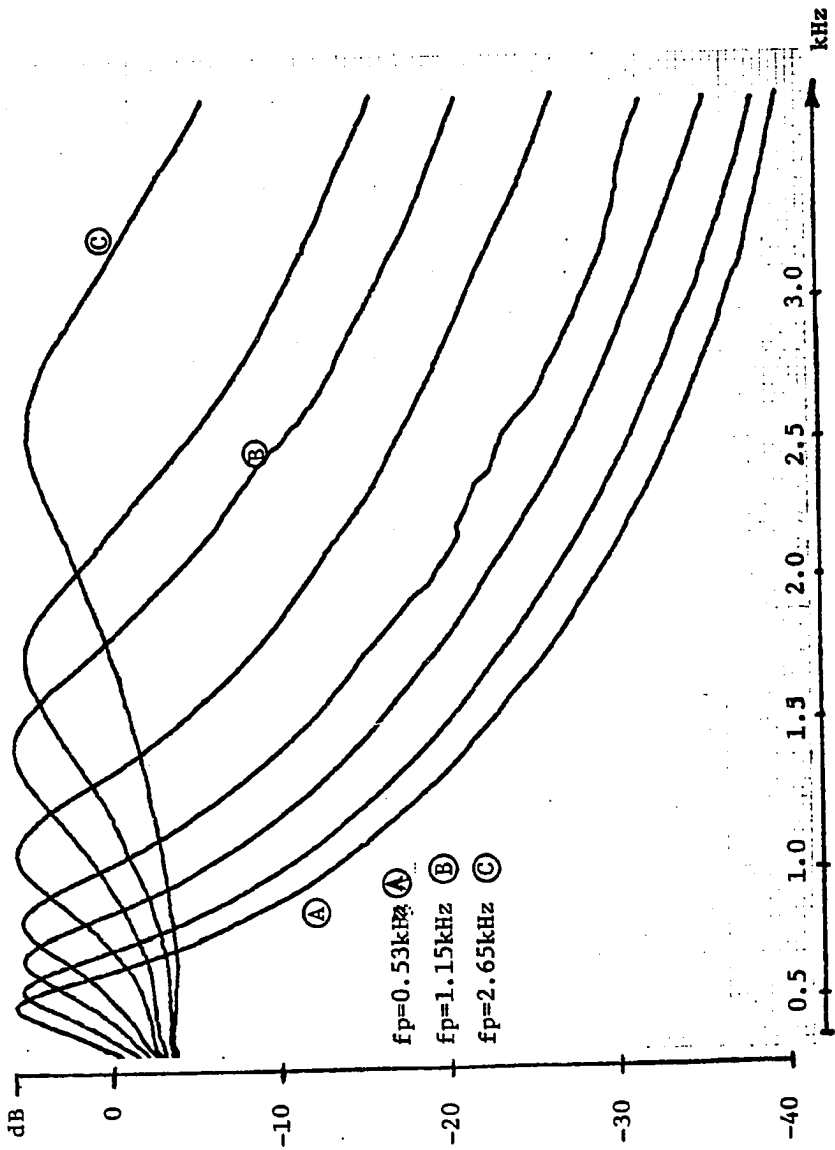
Fig. 6.14.c. ω_p Programming of a Low-Pass Filter ($Q_p = 3$).
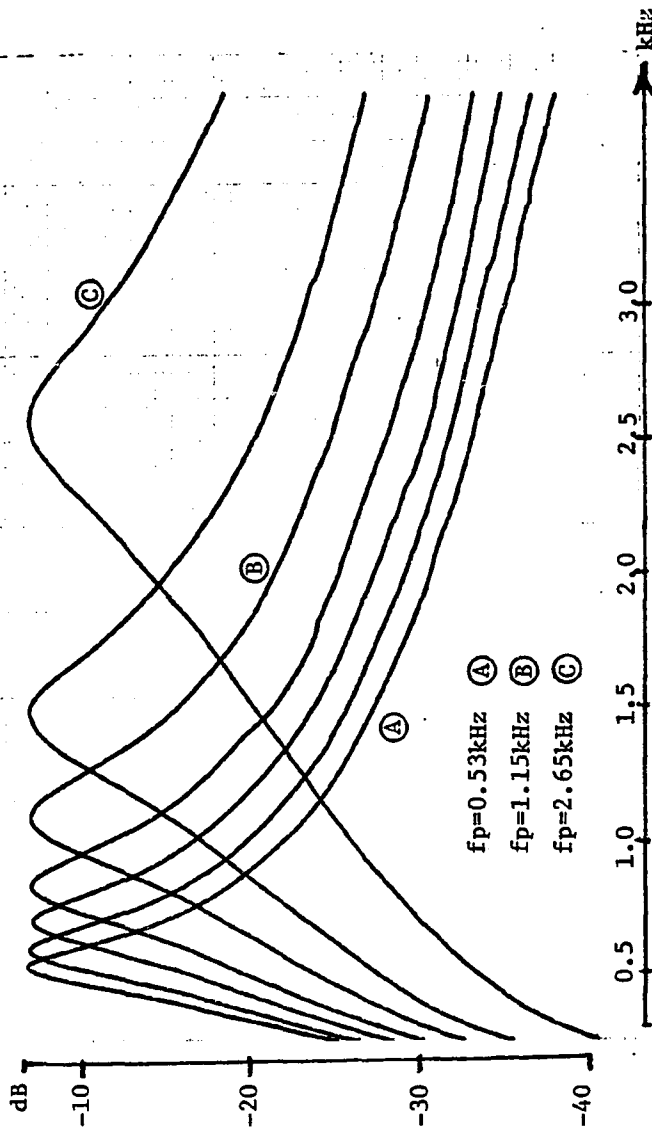
Fig. 6.14.d. ω_p Programming of a Bandpass Filter ($Q_p = 3$)

Fig. 6.14.   Programmable Filter Experimental Frequency
Responses .

bandwidth at higher Q. This can be easily shown from the results of the previous section in comparison to this results.

The availability of such compact, versatile, analog, programmable filter, opens up many novel and independent application areas.

6.4 APPLICATION OF THE GIC NETWORKS IN INDUCTANCES SIMULATIONS

The GIC network was initially proposed as the best OA inductance simulation circuit. This circuit is shown in Fig. 6.15a, where all resistors and capacitors have been replaced by general impedance branches. Analysis of this circuit yields the input impedance

$$Z_{11} = V_1/I_1 = Z_1 Z_4 Z_6/Z_2 Z_3 \qquad (6.17)$$

Thus for Z_{11} to be in the form $Z_{11} = SL$,

one possibility is when $Z_1 = R_1$, $Z_2 = R_2$, $Z_3 = \dfrac{1}{sc_3}$, $Z_4 = R_4$ and $Z_5 = R_5$ leading to the circit shown in Fig. 6.15b with

$$Z_{11} = sC_3 R_1 R_4 R_6/R_2 = SL \qquad (6.18)$$

$$\text{i.e. } L = C_3 R_1 R_4 R_6/R_2 \qquad (6.19)$$

In the above, we assumed ideal OA's for realizing the GIC and hence obtained ideal inductances. Let us now address the nonideal performance of the GIC due to the finite gain and BW of the OA's,
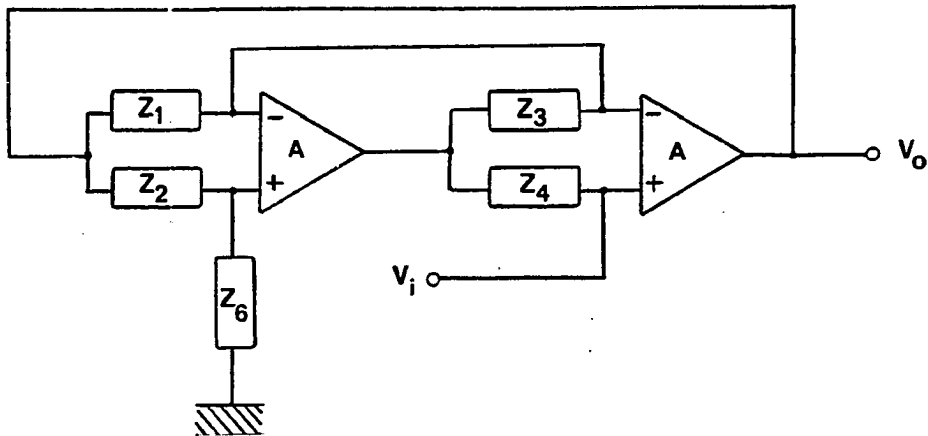
Fig. 6.15.a.   Practical Single GIC Configuration Used for
Inductance Simulation.
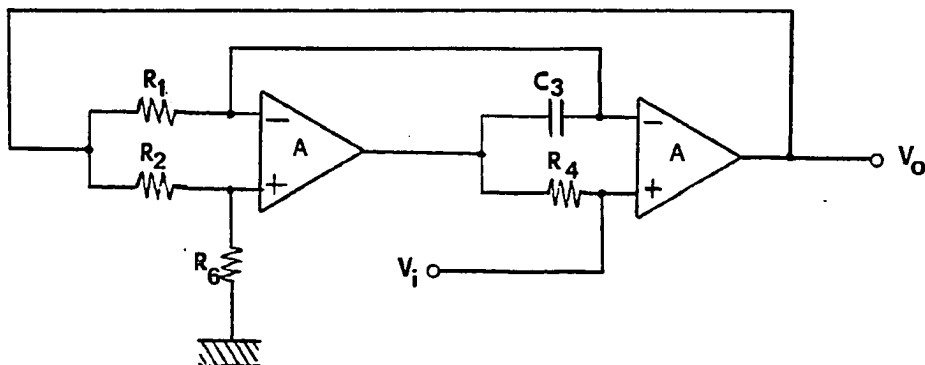
Fig. 6.15.b.   Single GIC Structure Simulating 0.1 H
Inductance .

the following expression for the simulated inductance can be easily derived using one pole OA model of (2.2):

$$L_s = V_i/I_i = N_s/D_s \qquad (6.20)$$

where $N_s = s^2[C_3/\omega^2] + s[(G_1/\omega^2) + (C_3/\omega)] + [(G_1/\omega) + G_2 C_3/(G_2 + G_6)]$

and $D_s = s^3[C_3 G_4/\omega^2] + s^2[(G_1 G_4/\omega^2) + (C_3 G_4/\omega)] + s[G_1 G_4/\omega]$

$$+ [G_1 G_4 G_6/(G_2 + G_6)]$$

Using the composite GIC structure proposed in Section 6.2 the following expression for the simulated inductance of the circuit of Fig. 6.16, can be obtained.

$$L_c = V_i/I_i = N_c/D_c \qquad (6.21)$$

where $N_c = s^4\{(1+\alpha_1)(1+\alpha_2)C_3/\omega^4\} + s^3\{(1+\alpha_1)(1+\alpha_2)G_1/\omega^4\}$

$$+ s^2\{C_3(1+\alpha_2)/\omega^2 + G_1(1+\alpha_1)\alpha_2/\omega^3\}$$

$$+ s\{[G_2 C_3 \alpha_2/\omega(G_2 + G_6)] + [G_1(1+\alpha_1)/\omega^2]\} + \{G_2 C_3/(G_2 + G_6)\}$$

and $D_c = s^5\{(1+\alpha_1)(1+\alpha_2)C_3 G_4/\omega^4\} + s^4\{(1+\alpha_1)(1+\alpha_2)G_1 G_4/\omega^4\}$

$$+ s^3\{[C_3 G_4(1+\alpha_2)/\omega^2] + [G_1 G_4(1+\alpha_1)\alpha_2/\omega^3]\}$$

$$+ s^2\{G_1 G_4(1+\alpha_1)\alpha_2/\omega^2\} + s\{G_1 G_4 G_6 \alpha_2/\omega(G_2 + G_6)\} + \{G_1 G_4 G_6/(G_2 + G_6)\}$$

This results in an excellent inductance simulation that will have performance very close to the ideal even at high frequency of
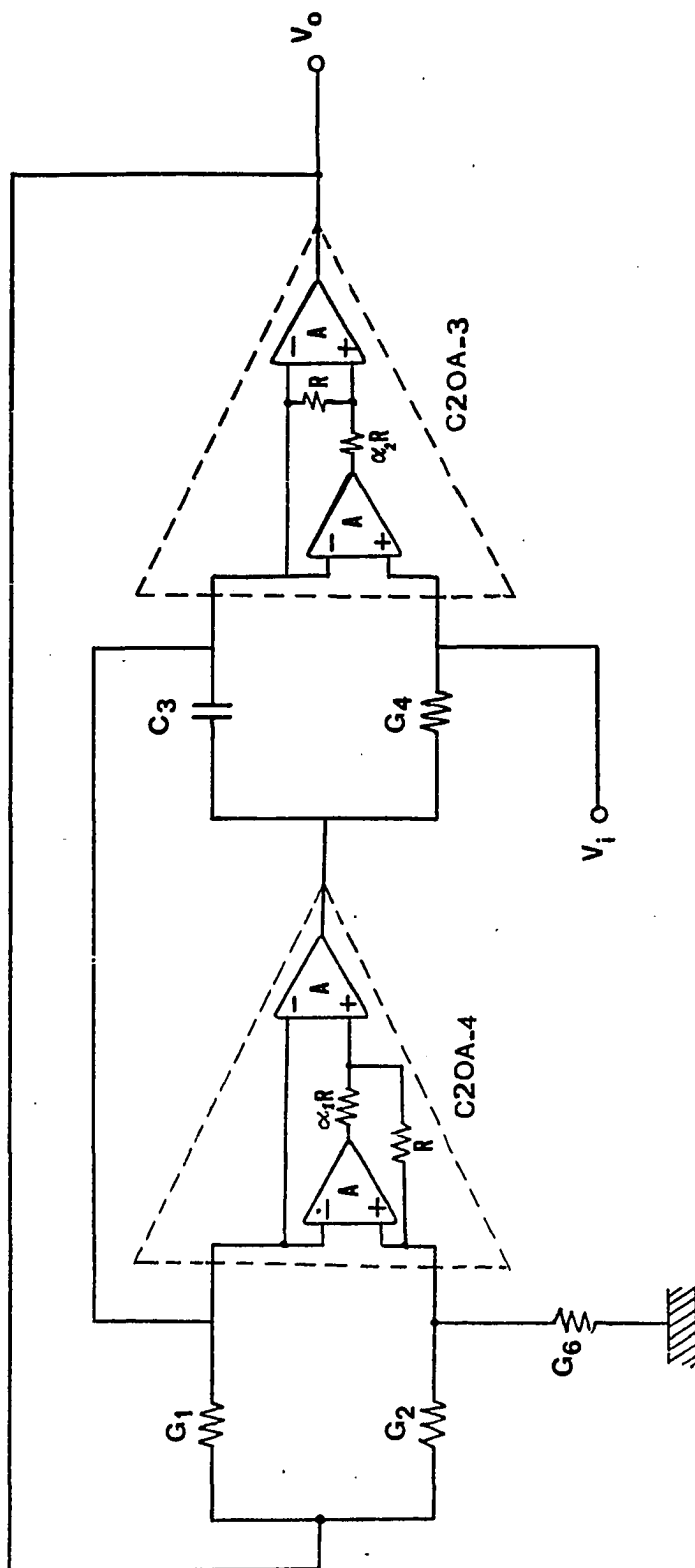
Fig. 6.16. New Practical Composite GIC Configuration
Simulating 0.1 H Inductance

operation. These results can be easily noted from Fig. 6.17 where the simulated inductance obtained using the structure of Fig. 6.16 is plotted and compared with the ideal realization and the circuit of Fig. 6.15b using single GIC.

6.5 CONCLUSIONS

At present, miniature inductors have small Q factors, the feasible inductance range is limited, and they are not compatible with either integrated circuit or thin film technology. In an effort to produce inductors with superior performance several types of active structures were proposed to simulate inductors using RC active networks. A major contribution in that effort was the introduction of GIC the networks. In this chapter, a brief presentation of the GIC structures were discussed along with important applications of the GIC's in active filters. A new composite GIC designs were proposed using the C2OA's to replace the single OA's in the GIC networks. The result were superior networks regarded for their high frequency and high Q applications. Applications of these GIC networks in programmable filters were discussed. A compact versatile analog network that can be controlled by digital signals to achieve fully programmable filters was presented. The filter topology as well as the transfer function parameters can be digitally controlled through the use of analog switches.
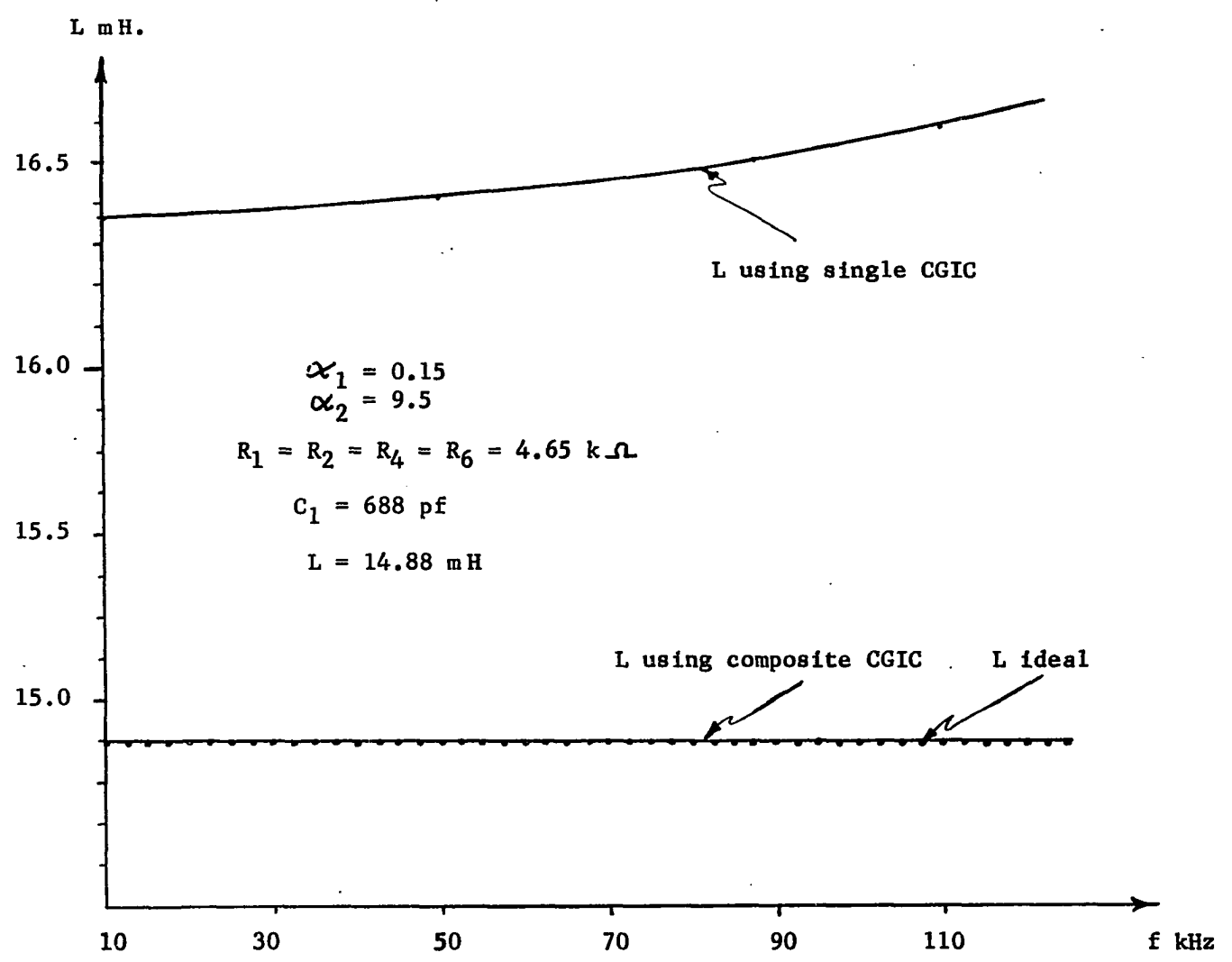
Fig. 6.17.a. Computer Plots of the Simulated Inductances
Using Single and Composite GIC Structures.

In the figure:

L mH.

16.5

16.0

$\alpha_1 = 0.15$
$\alpha_2 = 9.5$

$R_1 = R_2 = R_4 = R_6 = 4.65 \ k\Omega$

$C_1 = 688 \ pf$

L = 14.88 mH

15.5

L using single CGIC

L using composite CGIC   L ideal

15.0

10   30   50   70   90   110   f kHz
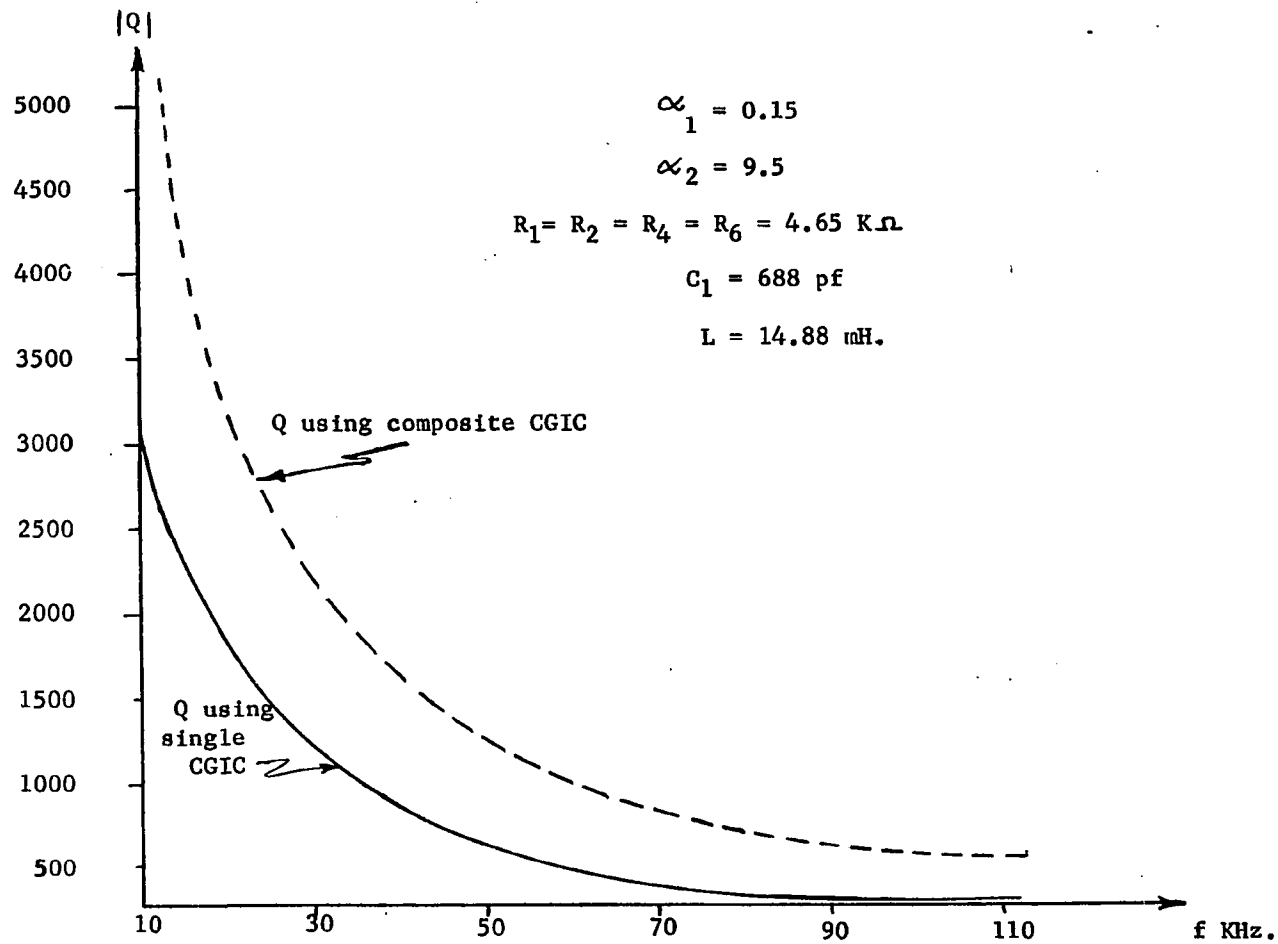
Fig. 6.17.b. Computer Plots of Q of the Simulated Inductances
Using Single and Composite GIC Structures.

Finally, the application of the new composite GIC in inductance simulations is also presented. The computer plots of the simulated inductor show clearly the considerable improvements contributed by the use of composite GIC and C2OA's.

CHAPTER VII

CONCLUSIONS

The main objective of this research was to introduce a general technique that helps solving the problem of high-frequency roll-off of the operational amplifiers, which imposes a practical limitation to their usefulness in RC-active filter design.

A new approach for extending the useful operating frequencies in a wide range of linear active networks, realized using OA's, has been presented. The BW extension is achieved by replacing each of the single OA's in the active realization by a composite OA (CNOA). A technique has been given for the generation of the CNOA's. Each CNOA is constructed using N single OA's and 2(N-1) active compensating resistors resulting in (N-1) resistor ratios. The CNOA is versatile since it has 3 terminals that resembles those of the single OA.

The suggested method generates a large number of CNOA's for a given N. For N = 2, 3 and 4, CNOA's were generated and examined according to a stringent performance criteria that considers stability, sensitivity, BW properties and the GBWP mismatch effect of the single OA's. Several of the CNOA's, namely C2OA-1 to C2OA-4, C3OA-1 to C3OA-6 and C4OA-1 to C4OA-5, have passed the performance criteria, and have been found very useful in the most frequently used applications. Each CNOA is constructed using N OA's, that do not require GBWP matching, and 2(N-1) low accuracy

and low spread resistors for active compensation. The ratio of these resistors can be used advantageously to minimize the gain and phase error in an appropriate manner, that depends on the application, to reduce the deviation of the active realization's response from ideal, and to guarantee stability. No extra high accuracy passive components are required compared to the single OA realization.

It is to be noted that the slew rate of the generated composite amplifiers is not any better than the slew rate of the OA's used for constructing the CNOA's themselves. On the other hand, using OA's with higher slew rate as an output stage in the CNOA construction, while using a high input impedance OA's in the input stage will result in a composite amplifier with high impedance and fast slew rate. Such an advantage can only be possible due to the fact that relatively large mismatch of the GBWP's of the OA's used to construct the CNOA's are tolerated within practical range. Consequently different types of OA's can be mixed in the design to achieve most of the required specifications.

The theoretical excellent performance properties of the realizations using the proposed CNOA's, including wide dynamic range, stability and low sensitivity, were verified in numerous applications. Different examples of the basic active building blocks, namely finite gain (inverting, non-inverting and differential) amplifiers, as well as inverting integrators

utilizing the proposed CNOA's are exhaustively studied. The theoretical and experimental results illustrates their superior performance compared to the best reported contributions with respect to stability and useful BW.

To illustrate the improvement contributed by the applications of CNOA's in active filters, a new classification of these filters into two major categories was discussed. The first filters category employs the above active building blocks, while the other one contains these filters where the functional blocks cannot be isolated from the filter structure. Practical examples of filters of both categories constructed using the proposed CNOA's were implemented. Theoretical and experimental results of these realizations compared favorably with the state of the art designs, as well as with these designs using single OA's.

Using the CNOA's to construct Generalized Immittance Converter Networks proved to be an excellent application to demonstrate the usefulness of the proposed composite amplifiers. The appreciable improvements of the new composite GIC performance was a major motivation that led to the introduction of two important applications. The first, is a new fully programmable linear active filter. The filter combines the use of linear element and analog CMOS switches to achieve a compact versatile analog network that can be controlled by digital signals to select the filter topology as well as the transfer function parameters.

The second application of the composite GIC is inductances simulations, where the excellent results obtained can be very beneficial in a broad range of applications.

In conclusion, solving the problem of the BW limitation resulting from the OA frequency dependence in the manner presented, resulted in a general solution with a wide range of useful applications as demonstrated theoretically and experimentally. As stated earlier this contribution has achieved two objectives. The main one was describing a new general technique for bandwidth extension of linear active networks using OA's while maintaining the other important properties such as stability, sensitivity and dynamic range. This resulted in several families of novel composite OA's. The second objective was to show that when these CNOA's are used in a wide range of important applications then, for a given number of OA's N, the realizations obtained were found superior to, or in a few cases as good as, the best available circuits which were reported for specific applications. The performance improvements in these realizations led to the introduction of two useful applications namely the programmable filter and the use of composite GIC's in inductance simulations.

In addition, it is worthwhile to mention that the generator method presented in this contribution is actually a composite dependent source generation technique, i.e., it is also applicable

to any of the four types of dependent sources, voltage (and current) controlled voltage (or current) sources. Novel composite dependent sources with considerably performance improvements are expected to result when the procedure described is applied to other linear active networks employing devices other than OA's, e.g. transistors.

The technique presented in this research, generated numerous new composite networks that might be useful in solving the problem of designing high performance non-inverting integrators. The availability of such high performance positive integrators will be a considerable contribution to active filters design.

The proposed designs and technique open the field to a broad range of applications for future research. One cannot deny the benefits of these ideas in switched capacitor networks, where researchers have started recently to investigate the limited effects imposed by the OA's on the performance of switched capacitor networks. It is also quite rewarding to see the recognition of this work in some recent contributions [60,61].

BIBLIOGRAPHY

[1] B. B. Bhattacharyya, Wasfy B. Mikhael and A. Antoniou, "Design of RC-Active Networks by Using Generalized Immittance Converters", IEEE International Symposium on Circuit Theory, pp. 290-294, Apr. 1973.

[2] A. Sedra and P. Brackett, "Filter Theory and Design: Active and Passive", Matrix Publishers, Inc., 1978.

[3] S. Mitra, "Analysis and Synthesis of Linear Active Networks", John Wiley & Sons, Inc. 1969.

[4] M. Ghausi and K. Laker, "Modern Filter Design Active-RC and Switched Capacitor", Prentice-Hall, Inc., 1981.

[5] Wasfy B. Mikhael and Sherif M. Nessim, "Actively Compensated Composite Operational Amplifiers," Midwest Symposium on Circuits and Systems, Albuquerque, New Mexico, pp. 374-378, June 1981.

[6] Wasfy B. Mikhael and Sherif Michael Nessim, "A Systematic General Approach for the Generation of Composite OA's With Some Useful Applications in Linear Active Networks", 25th Midwest Symposium on Circuits and Systems, Houghton, MI, Aug. 1982.

[7] Wasfy B. Mikhael and Sherif M. Nessim, "Active Filter Design for High Frequency Operation", Midwest Symposium on Circuits and Systems, Albuquerque, New Mexico, pp. 573-576, June 1981.

[8] Wasfy B. Mikhael and Sherif Michael Nessim, "Novel High Frequency Linear Active Networks Using Regular OA's", 25th Midwest Symposium on Circuits and Systems, Houghton, MI, Aug. 1982.

[9] G. Wilson, "Insensitive very-low frequency RC oscillator," Elec. Lett., vol. 10, no. 21, Oct. 1974.

[10] A. Budak and D. M. Petrela, "Frequency Limitations of Active Filters using Operational Amplifiers," IEEE Trans. Circuit Theory, Vol. CT-19, no. 4, July 1972.

[11] E. A. Faulkner and J. B. Grimbleby, "Active Filters and Gain Bandwidth Product," Elec. Lett., vol. 6, no. 17, August 1970.

[12] S. K. Mitra, and B. H. Shanta Pai, "Active Filters Using Amplifiers having Frequency Dependent Gain Characteristics," Proc. IEE Int. Symp. Network Theory, London, 1971.

BIBLIOGRAPHY (Continued)

[13] G. S. Moschytz, "FEN Filter Design Using Tantalum and Silicon Integrated Circuits," Proc. IEEE, vol. 58, no. 4, pp. 550-566, April 1970.

[14] G. Wilson, "Compensation of Some Operational Amplifier Based RC-Active Networks," IEEE Trans. Circuits Syst., vol. CAS-23, pp. 443-446, July 1976.

[15] A. Antoniou and K. S. Naidu, "A Compensation Technique for a Gyrator and its Use in the Design of a Channel-Bank Filter," IEEE Trans. Circuits Syst., vol. CAS-22, pp. 316-323, Apr. 1975.

[16] P. O. Brackett and A. S. Sedra, "Active Compensation for High-Frequency Effects in Op-Amp Circuits with Applications to Active RC Filters," IEEE Trans. Circuits Syst., vol. CAS-23, pp. 68-72, Feb. 1976.

[17] R. Geiger, "Amplifiers with Maximum Bandwidth," IEEE Trans. Circuits and Systems, Vol. CAS-24, pp. 510-512, Sept. 1977.

[18]. Ahmed M. Soliman, "Instrumentation Amplifiers With Improved Bandwidth," IEEE Circuits and Systems Magazine, Vol. 3, No. 1, pp. 7-9, 1981.

[19] M. A. Reddy, R. Ravishankar, B. Ramamurthy and K. R. Rao, "A High-Quality Double-Integrator Building-Block for Active-Ladder Filters," IEEE Trans. on Circuits and Systems, Vol. CAS-28, No. 12, pp. 1174-1177, December 1981.

[20] Aram Budak, Gerhard Wullink and Randall L. Geiger, "Active Filters with Zero Transfer Function Sensitivity with Respect to the Time Constant of Operational Amplifiers", IEEE Trans. on Circuits and System, Vol. CAS-27, No. 10, pp. 849-854, Oct. 1980.

[21] Randal L. Geiger and Aram Budak, "Active Filters with Zero Amplifier Sensitivity", IEEE Trans. on Circuits and Systems, Vol. CAS-26, No. 4, pp. 277-288, April 1979.

[22] K. R. Rao, M. A. Reddy, S. Ravichandran, B. Ramamurthy, and R. Ravi Sankar, "An Active-Compensated Double-Integrator Filter Without Matched Operational Amplifiers," IEEE Proceedings, Vol. 68, No. 4, pp. 534-538, APril 1980.

[23] Ahmed M. Soliman, "A Generalized Active Compensated Noninverting VCVS with Reduced Phase Error and Wide Bandwidth," IEEE Proceedings, Vol. 67, No. 6, pp. 963-965, June 1979.

BIBLIOGRAPHY (Continued)

[24] S. Natarajan and B. B. Bhattacharyya, "Design and Some
Applications of Extended Bandwidth Finite Gain Amplifiers," J.
Franklin Inst., Vol. 305, No. 6, pp. 320-341, June 1978.

[25] S. Natarajan and B. B. Bhattacharyya, "Design of Actively
Compensated Finite Gain Amplifiers for High-Frequency
Applications," IEEE Trans. Circuits Syst., Vol. CAS-27, pp.
1133-1139, Dec. 1980.

[26] A. Antoniou, "Realization of Gyrators Using Operational
Amplifiers, and Their Use in Rc-Active-Network Synthesis",
IEEE Proceedings, Vol. 116, No. 11, pp. 1838-1850, Nov. 1969.

[27] A. C. Davies, "The Significance of Nullators, Norators and
Nullors in Active-Network Theory," Radio Electron. Eng., Vol.
34, pp. 259-267, 1967.

[28] J. Braun, "Equivalent N.I.C. Networks with Nullators and
Norators," Ibid, CT-12, pp. 411-412, 1965.

[29] B. D. Tellegen, "On Nullators and Norators," IEEE Trans. on
Circuit Theory, Vol. CT-13, pp. 466-469, 1966.

[30] Wasfy B. Mikhael and Sherif Michael Nessim, "Electronically
Programmable Active Filters," Midwest Symposium on Circuits
and Systems, Toledo, Ohio, August 1980, pp. 109-113.

[31] J. Millman and C. Halkias, "Integrated Electronics; Analog and
Digital Circuits and Systems," McGraw-Hill, Inc., 1972, pp.
386.

[32] L. P. Huelsman and P. E. Allen, "Introduction to the Theory
and Design of Active Filters", McGraw-Hill Book Company, p.
217.

[33] R. Srinivasagopalan and G. O. Martens, "A Comparison of a
Class of Active Filters with Reference to the OA Gain Band-
width Product", IEEE Trans. Circuits and Systems, Vol. CAS-21,
pp. 377-381, 1974.

[34] R. Tarmi and M. S. Ghausi, "Very High Q Insensitive Active RC
Networks", IEEE Trans. Circuit Theory, Vol. CT-17, pp. 358-
366, 1970.

[35] W. B. Mikhael and B. B. Bhattacharyya, "A Practical Design for
Insensitive RC Active Filters", IEEE Trans. Circuits and
Systems, Vol. CAS-22, pp. 407-415, 1975.

BIBLIOGRAPHY (Continued)

[36] M. A. Reddy, "OA Circuits with Variable Phase Shift and Their Application to High Q Active RC Filters and RC Oscillators", IEEE Trans. Circuits and Systems, Vol. CAS-23, pp. 384-389, 1976.

[37] R. Schaumann, "Low Sensitivity High Frequency Tunable Active Filter Without External Capacitors", IEEE Trans. Circuits and Systems, Vol. CAS-22, pp. 39-44, 1975.

[38] S. Srinivasan, "Synthesis of Transfer Functions Using OA Pole", Int. J. Electronics, Vol. 40, No. 7, pp. 5-13, 1976.

[39] K. R. Rao and S. Srinivasan, "A Bandpass Filter Using the Oa Pole", IEEE J. Solid State Circuits, Vol. 8, pp. 245-246, 1973.

[40] D. Akerberg, and M. Mossberg, "A Versatile Active RC Building Block with Inherent Compensation for the Finite Bandwidth of the Amplifier", IEEE Trans. Circuits and Systems, Vol. CAS-21, pp. 75-78, 1974.

[41] M. A. Reddy, "An Insensitive Active RC Filter for High Q and High Frequencies", IEEE Trans. Circuits and Systems, Vol. CAS-23, pp. 429-433, 1976.

[42] B. B. Bhattacharyya, M. S. Abougabal and M. N. S. Swamy, "An Optimal Design of RC Active Filters Using Grounded Capacitors", Int. Jnl. Circuit Theory & Applic. In press.

[43] Ahmed M. Soliman and Mohammed Ismail, "Active Compensation of Op-Amps," IEEE Trans. on Circuits and Systems, Vol. CAS-26, No. 2, pp. 112-117, Feb. 1979.

[44] Randall L. Geiger and Aram Budak, "Design of Active Filters Independent of First- and Second-Order Operational Amplifier Time Constant Effects," IEEE Trans. on Circuits and Systems, Vol. CAS-28, No. 8, pp. 749-757, August 1981.

[45] J. Tow, "Active-RC Filters-A State-Space Realization," Proc. IEEE, Vol. 56, pp. 1137-1139, June 1968.

[46] L. C. Thomas, "The Biquad: Part I - Some Practical Design Considerations," IEEE Trans. Circuit Theory, Vol. CT-18, pp. 350-357, May 1971.

[47] —, "The Biquad: Part II - A Multipurpose Active Filtering System," IEEE Trans. Circuit Theory, Vol. CT-18, pp. 358-361, May 1971.

BIBLIOGRAPHY (Continued)

[48] F. E. J. Girling and E. F. Good, "Active Filters," (Pts. 1, 12, 13, 14), Wireless World, Vol. 75, pp. 348-352, Aug. 1969; Vol. 76, pp. 341-345, July 1970; Vol. 76, pp. 445-450, Sept. 1970; Vol. 76, pp. 505-510, Oct. 1970.

[49] P. Brackett and A. Sedra, "Direct SFG Simulation of LC Ladder Networks with Applications to Active Filter Design," IEEE Trans. on Circuits and Systems, Vol. CAS-23, pp. 61-67, Feb. 1976.

[50] Texas Instruments, Inc., "The Linear and Interface Circuit Data Book for Design Engineers."

[51] G. Bailey, R. Geiger, "A New Integrator With Reduced Amplifier Dependence for Use in Active RC-Filter Synthesis," IEEE International Symposium on Circuits and Systems, pp. 87-90, 1980.

[52] Ahmed M. Soliman and Mohammed Ismail, "On the Active Compensation of Noninverting Integrators," IEEE Proceedings, Vol. 67, No. 6, pp. 961-963, June 1979.

[53] P. O. Brackett and A. S. Sedra, "Active Compensation for High-Frequency Effects in Ap. Amp Circuits with Applications to Active-Rc Filters," IEEE Trans. Circuits and Systems, Vol. CAS-23, pp. 68-73, Feb. 1976.

[54] G. C. Temes, and S. K. Mitra, "Modern Filter Theory and Design," Wiley, 1973.

[55] B. B. Bhattacharyya, Wasfy B. Mikhael and A. Antoniou, "Design of RC-Active Networks Using Generalized-Immittance Converters", Journal of The Franklin Institute, Vol. 297, No. 1, pp. 45-58, Jan. 1974.

[56] R. H. S. Riordan, "Simulated Inductors Using Differential Amplifiers", Electronic Letters, Vol. 3, pp. 50-51, Feb. 1967.

[57] R. W. Brodersen, P. R. Gray and D. A. Hodges, "MOS Switched Capacitor Filters", IEEE Proceedings, Volume 67, No. 1, pp. 61-75, January, 1979.

[58] D. J. Allstot, R. W. Brodersen, and P. R. Gray, "An Electrically-Programmable Switched Capacitor Filter", IEEE Journal of Solid State Circuits, Vol. SC-14, No. 6, pp. 1034-1041, December, 1979.

BIBLIOGRAPHY (Continued)

[59] A. K. Mitra and U. K. Aatre, "A Note on Frequency and Q Limitations of Active Filters", IEEE Transactions CAS, Vol. CAS-24, pp. 215-218, April, 1977.

[60] K. M. Reineck, F. W. Stephenson, R. Berstein, and R. Bokulic, "A Generalized Approach to Zero-Sensitivity in Active Networks", Midwest Symposium on Circuits and Systems, Houghton, MI, August 1982, pp. 464-468.

[61] R. Schaumann, "Designing Active RC Biquads with Improved Performance", IEEE Trans. on Circuits and Systems, Vol. CAS-30, No. 1, Jan. 1983, pp. 56-57.

[62] A. Budak, "Passive and Active Network Analysis and Synthesis," Boston, MA, Houghton Mifflin, 1974, pp. 248, 274, 381.

[63] Ahmed M. Soliman, "Classification and Generation of Active Compensated Non-Inverting VCVS Building Blocks," International Journal of Circuit Theory and Applications, Vol. 8, pp. 395, 405, 1980.

[64] George Wilson, "Compensation of Some Operational-Amplifier Based RC-Active Networks," IEEE Trans. on Circuits and Systems, Vol. CAS-23, No. 7, pp. 443-446, July 1976.

[65] Ashok Nedungadi, "A Simple Inverting-Noninverting Voltage Amplifier," IEEE Proceedings, Vol. 68, No. 3, pp. 414-415, March 1980.

[66] R. Nandi and A. K. Bandyopadhyay, "A High-Input Impedance Inverting/Noninverting Active Gain Block," IEEE Proceedings, Vol. 67, No. 4, pp. 690-691, April 1979.

[67] Ken Martin and Adel S. Sedra, "On the Stability of the Phase-Lead Integrator," IEEE Trans. on Circuit and Systems, Vol. CAS-24, No. 6, pp. 321-324, June 1977.

[68] Ahmed M. Soliman and Mohammed Ismail, "A Universal Variable Phase 3-Port VCVS and Its Application in Two-Integrator Loop Filters", IEEE International Symposium on Circuits and Systems, pp. 83-86, 1980.

[69] S. Ravichandran and K. Radhakrishna Rao, "A Novel Active Compensation Scheme for Active-RC Filters", IEEE Proceedings, Vol. 68, No. 6, pp. 743-744, June 1980.

BIBLIOGRAPHY (Continued)

[70] Sundaram Natarajan, "Active Sensitivity Minimization in SAB's With Active Compensation and Optimization", IEEE Trans. on Circuits and Systems, Vol. CAs-29, pp. 239-245, April 1982.

[71] S. Natarajan, "Synthesis of Actively Compensated Double-Integrator Filter Without Matched Operational Amplifiers", IEEE Proceedings, Vol. 68, No. 12, pp. 1547-1548, December 1980.

[72] A. K. Mitra and V. K. Aatre, "Low Sensitivity High-Frequency Active R Filters", IEEE Trans. on Circuits and Systems, Vol. CAS-23, No. 11, pp. 670-676, November 1976.

[73] A. K. Mitra and V. K. Aatre, "A Note on Frequency and Q Limitations of Active Filters", IEEE Trans. on Circuits and Systems, Vol. CAS-24, No. 4, pp. 215, 218, April 1977.

[74] A. S. Sedra and J. L. Espinoza, "Sensitivity and Frequency Limitations of Biquadratic Active Filters", IEEE Trans. on Circuits and System, Vol. CAS-22, pp. 122-130, Feb. 1975.

[75] J. J. Friend, A. Harris, and D. Hilberman, "Star: An Active Biquadratic Filter Section," IEEE Trans. on Circuits and Systems, Vol. CAS-22, pp. 115-121, 1975.

[76] A. Budak and D. M. Petrela, "Frequency Limitations of Active Filters Using Operational Amplifiers", IEEE Trans. Circuit Theory, Vol. CT-19, pp. 322-328, July 1972.

[77] Wasfy B. Mikhael and Sherif Michael Nessim, "Generation of Actively Compensated Composite Operational Amplifiers and their Use in Extending the Operating Frequencies of Linear Active Networks", IEEE Int. Symposium on Circuits and Systems, Newport Beach, California, May 1983, pp. 1290-1293.

```
**************************
*                        *
*     APPENDIX A         *
*                        *
**************************
```

```
*******************************************************************
*                                                                 *
*     THE  PROMISSING  C20A  DESIGNS  AND  THEIR                   *
*     CORRESPONDING  FINITE  GAIN  EXEPRESSIONSIER                 *
*                                                                 *
*******************************************************************
```

```
              *             C20A - 5          *

F   = NP / D
NP  = (1.+G)
D   = 1. + (1.+G) * (A-1.) * S * Y + (1.+G)*A*S*S*Y*Y
F   = NN / D
NN  = - G


              *             C20A - 6          *

F   = NP / D
NP  = (1.+G)
D   = 1. + A*(1.+G)*S*Y + A*(1.+G)*S*S*Y*Y
F   = NN / D
NN  = - G


              *             C20A - 7          *

F   = NP / D
NP  = (1.+G)*A
D   = 1. + (A+(1.+G))*S*Y + A*(1.+G)*S*S*Y*Y
F   = NN / D
NN  = -G * (1.+A*S*Y)
```

```
*              C20A - 8 ·           *

F  = NP / D
NP = (1.+G)*(A-1.)
D  = 1. + ((1.+G)+A)*S*Y + (1.+G)*A*S*S*Y*Y
F  = NN / D
NN = -G *(1.+A*S*Y)


*              C20A - 9            *

F  = NP / D
NP = (1.+G)
D  = 1. + A*S*Y + A*(1.+G)*S*S*Y*Y
F  = NN / D
NN = -G


*              C20A - 10           *

F  = NP / D
NP = (1.+G)*(1.+A*S*Y)
D  = 1. + (A-1.)*(1.+G)*S*Y + A*(1.+G)*S*S*Y*Y
F  = NN / D
NN = -G


*              C20A - 11           *

F  = NP / D
NP = (1.+G)
D  = 1. + S*Y + (1.+G)*S*S*Y*Y
F  = NN / D
NN = -G * (1.+S*Y)



F  =      TRANSFER FUNCTION
   =      N / D
Y  =      1 / GBWP
G  =      FINITE GAIN
A  =      ( ALPHA + 1 )
B  =      ( BETA  + 1 )
C  =      ( GAMMA + 1 )
W  =      1 / INEGRATOR TIME CONSTANT
```
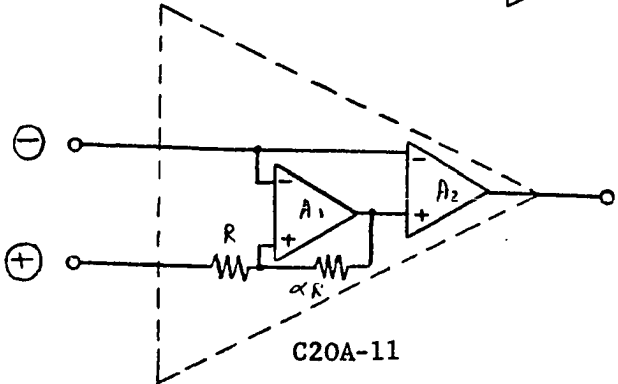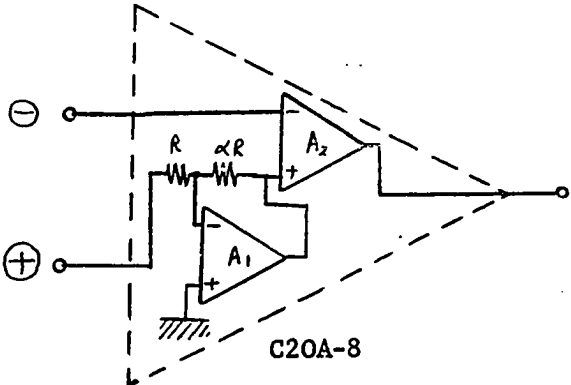
C20A-5

C20A-6

C20A-7

C20A-8

C20A-9

C20A-10

C20A-11
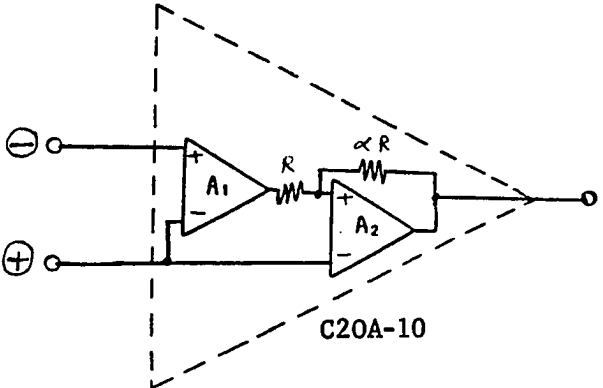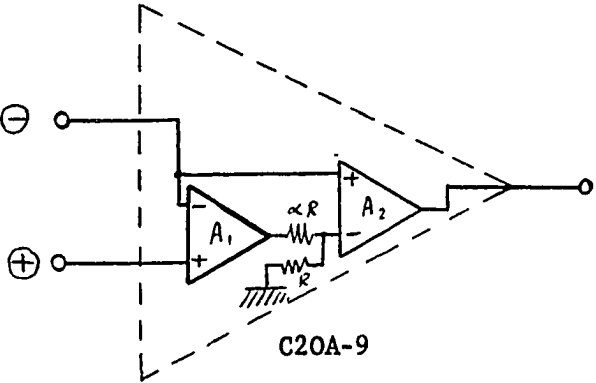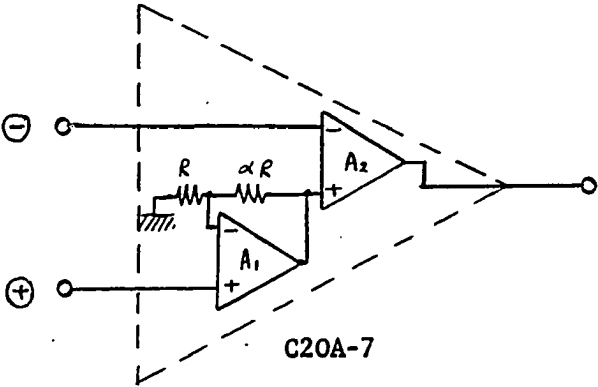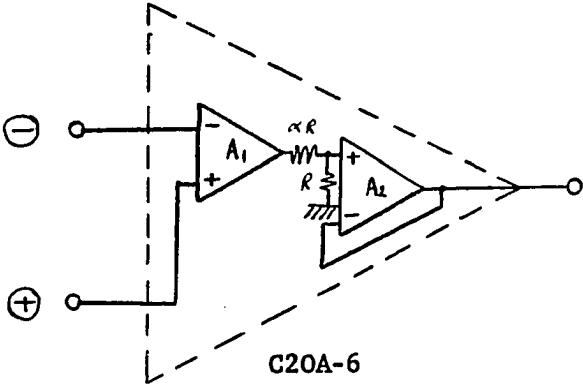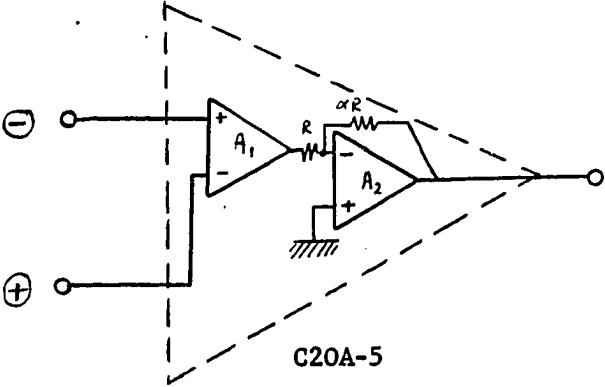
```
************************
*                      *
*    APPENDIX B-1      *
*                      *
************************
```

```
****************************************************************
*                                                              *
*    ThE  PROMISSING  C30A  DESIGNS  AND  THEIR                *
*    CORRESPONDING  FINITE  GAIN  EXEPRESSIONSIER              *
*                                                              *
****************************************************************
```

```
C                    *           C30A - 1           *
    F=(1.+G)*(1.+1./(1.+A)*S*Y+S*S*Y*Y)/
    K(1.+(1.+(1.+G)/(1.+B))*S*Y+(1.+G)/(1.+A)*S*S*Y*Y+(1.+G)*S**3*Y**3)
    F=-G*(1.+S*Y)/
    K(1.+(1.+(1.+G)/(1.+B))*S*Y+(1.+G)/(1.+A)*S*S*Y*Y+(1.+G)*S**3*Y**3)
C                    *           C30A - 7           *
    F=(1.+G)*(1.+(2.+B)/(1.+B)*S*Y+S*S*Y*Y)/
    K(1.+(1.+G)/(1.+A)/(1.+B)*Y*S+(1.+G)*(1./(1.+A)+1./(1.+B))*Y*Y*S*S+
    K(1.+G)*Y**3*S**3)
    F= - (G)/(1.+(1.+G)/(1.+A)/(1.+B)*Y*S+(1.+G)*(1./(1.+A)+1./(1.+B))
    K*Y*Y*S*S+(1.+G)*Y**3*S**3)
C                    *           C30A - 3           *
    F=(1.+G)*(1.+1./(1.+A)*S*Y+S*S*Y*Y)/
    K(1.+(1.+G)/(1.+B)*S*Y+(1.+G)/(1.+A)*S*S*Y*Y+(1.+G)*S**3*Y**3)
    F=-G/
    K(1.+(1.+G)/(1.+B)*S*Y+(1.+G)/(1.+A)*S*S*Y*Y+(1.+G)*S**3*Y**3)
C                    *           C30A - 8           *
    F=(1.+G)*(1.+S*Y)/(1.+(1.+G)/(1.+A)/(1.+B)*Y*S+(1.+G)*(1./(1.+A)+1
    K./(1.+B))*Y*Y*S*S+(1.+G)*Y**3*S**3)
C                    *           C30A - 5           *
    F=(1.+G)*(1.+(1.+A)*Y*S+(1.+A)*Y*Y*S*S)/(1.+(A+(1.+G)/(1.+B))*Y*S+
    K(1.+G)*(1.+A)/(1.+B)*Y*Y*S*S+(1.+G)*(1.+A)*Y**3*S**3)
    F= - (G)*(1.+A*Y*S)/(1.+(A+(1.+G)/(1.+B))*Y*S+((1.+A)*(1.+G)/(1.+B
    K))*Y*Y*S*S+(1.+A)*(1.+G)*Y**3*S**3)
C                    *           C30A - 10          *
    F=(1.+G)*(1.+(1.+A+B/(1.+B))*S*Y+A*S*S*Y*Y)/
    K(1.+(1.+A)*Y*S+(1.+G)*(1.+A)/(1.+B)*Y*Y*S*S+(1.+G)*(1.+A)*Y**3*S**
    K3)
```
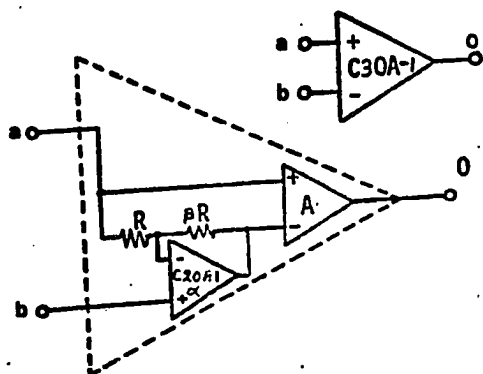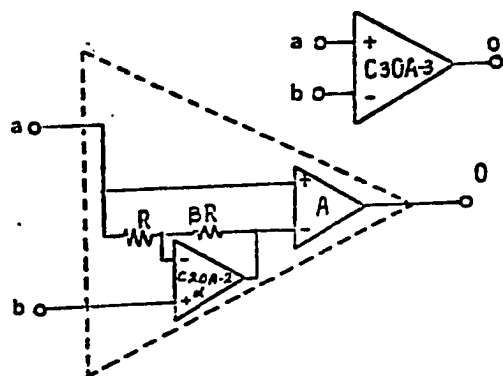
C30A-1
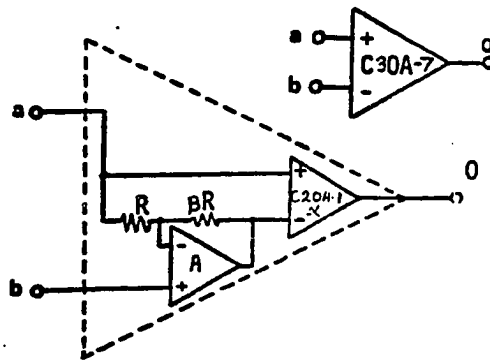
C30A-7

C30A-3
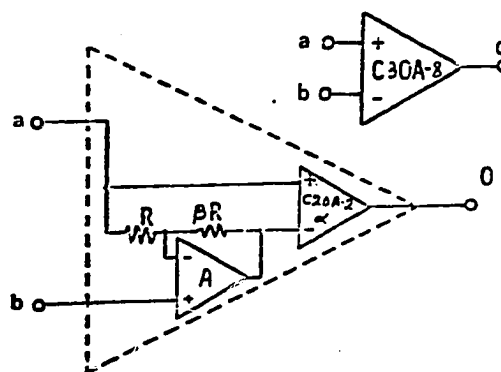
C30A-8
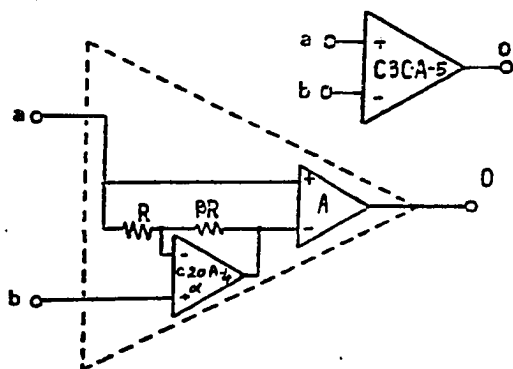
C30A-5
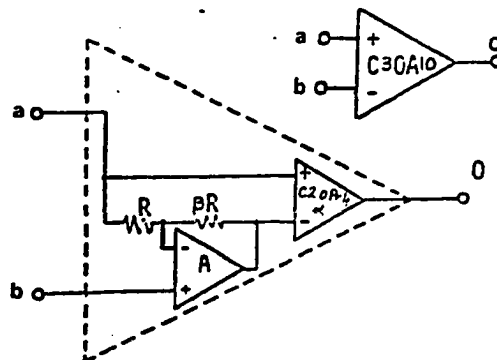
C30A-10

```
C                    *              C30A - 9           *
      F=(1.+G)/(1.+(1.+G)/(1.+A)/(1.+B)*Y*S+(1.+G)*(1./(1.+A)+1./(1.+B))
     K*Y*Y*S*S+(1.+G)*Y**3*S**3)
C                    *              C30A - 11          *
      F=(1.+G)*(1.+A*Y*S)/(1.+(1.+A)*Y*S+(1.+G)*(1.+A)/(1.+B)*Y*Y*S*S+(1
     K.+G)*(1.+A)*Y**3*S**3)
C                    *              C30A - 12          *
      F=(1.+G)*(1.+S*Y+B/(1.+A)*S*S*Y*Y)/
     K(1.+(1.+B)/(1.+A)*Y*S+((1.+B)+(1.+G)*(1.+B)/(1.+A))*Y*Y*S*S+(1.+B)
     K*(1.+G)*Y**3*S**3)
C                    *              C30A - 14          *
      F=(1.+G)*(1.+(1.+A)*Y*S+A*Y*Y*S*S)/(1.+(2.+A)*Y*S+(1.+G)*(1.+A)/
     K(1.+B)*Y*Y*S*S+(1.+G)*(1.+A)*Y**3*S**3)
      F=-G*(1.+(2.+A)*Y*S)/(1.+(2.+A)*Y*S+(1.+G)*(1.+A)/
     K(1.+B)*Y*Y*S*S+(1.+G)*(1.+A)*Y**3*S**3)
C                    *              C30A - 13          *
      F=(1.+G)*(1.+B/(1.+A)*Y*S+B*Y*Y*S*S)/
     K(1.+(1.+B)/(1.+A)*Y*S+((1.+B)+(1.+G)*(1.+B)/(1.+A))*Y*Y*S*S+(1.+B)
     K*(1.+G)*Y**3*S**3)
      F=-G*(1.+(1.+B)/(1.+A)*Y*S+(1.+B)*Y*Y*S*S)/
     K(1.+(1.+B)/(1.+A)*Y*S+((1.+B)+(1.+G)*(1.+B)/(1.+A))*Y*Y*S*S+(1.+B)
     K*(1.+G)*Y**3*S**3)
C                    *              C30A - 15          *
      F=(1.+G)*(1.+A*S*Y+B*(1.+A)*S*S*Y*Y)/
     K(1.+(1.+A)*S*Y+(1.+A)*(1.+B)*S*S*Y*Y+(1.+A)*(1.+B)*(1.+G)*S**3*Y**
     K3)
      F=(-G)*(1.+(1.+A)*S*Y+(1.+A)*(1.+B)*S*S*Y*Y)/
     K(1.+(1.+A)*S*Y+(1.+A)*(1.+B)*S*S*Y*Y+(1.+A)*(1.+B)*(1.+G)*S**3*Y**
     K3)
C                    *              C30A - 16          *
      F=(1.+G)*(1.+A*(1.+(1.+A)**2/(1.+A+2.*B+2.*A*B))*S*Y+
     K(A*B*(1.+A)**2/(1.+A+2.*B+2.*A*B))*S*S*Y*Y)/
     K(1.+(1.+A)*(1.+A*(1.+A)/(1.+A+2.*B+2.*A*B))*S*Y+
     K((1.+A)**3*(1.+B)+(1.+A)**2*B)/(1.+A+2.*B+2.*A*B)*S*S*Y*Y+
     K((1.+A)**3*(1.+B)*(1.+G)+B*(1.+A)**2*(1.+G))/(1.+A+2.*B+2.*A*B)
     K*S**3*Y**3)
      F=-G*(1.+(1.+A)*(1.+A*(1.+A)/(1.+A+2.*B+2.*A*B))*S*Y+
     K((1.+A)**3*(1.+B)+(1.+A)**2*B)/(1.+A+2.*B+2.*A*B))*S*S*Y*Y)/
     K(1.+(1.+A)*(1.+A*(1.+A)/(1.+A+2.*B+2.*A*B))*S*Y+
     K((1.+A)**3*(1.+B)+(1.+A)**2*B)/(1.+A+2.*B+2.*A*B)*S*S*Y*Y+
     K((1.+A)**3*(1.+B)*(1.+G)+B*(1.+A)**2*(1.+G))/(1.+A+2.*B+2.*A*B)
     K*S**3*Y**3)
```

```
F  =    TRANSFER FUNCTION
   =    N / D
Y  =    1 / GBWP
G  =    FINITE GAIN
A  =    ( ALPHA + 1 )
B  =    ( BETA  + 1 )
C  =    ( GAMMA + 1 )
W  =    1 / INEGRATOR TIME CONSTANT
```

C30A-9
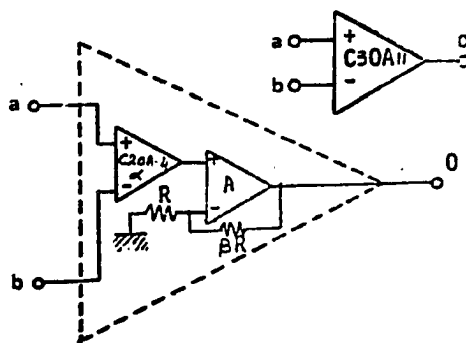
C30A-11
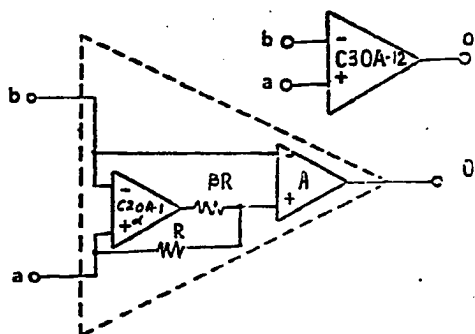
C30A-12
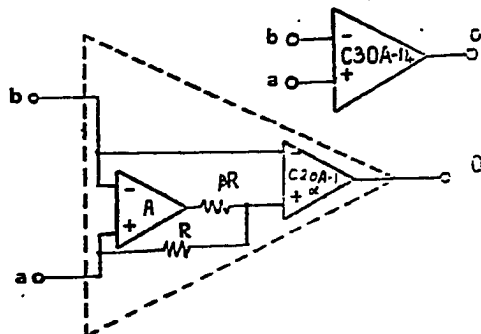
C30A-14

C30A-13

C30A-15

```
*****************************
*                           *
*       APPENDIX B-2         *
*                           *
*****************************
```

```
****************************************************************
*                                                              *
*       THE   PROMISSING   C30A   INTEGRATORS                  *
*              TRANSFER  FUNCTIONS                             *
*                                                              *
****************************************************************
```

AC30A- 1
F = T*(1.+S*Y)/
&((1.+W/B)+(1.+1./B+W/A)*S*Y+(1./A+W)*S*S*Y*Y+S**3*Y**3)
AC30A- 3
F = T/
&((1.+W/B)+(1./B+W/A)*S*Y+(1./A+W)*S*S*Y*Y+S**3*Y**3)
AC30A- 5
F = T*(1.+(A-1.)*S*Y)/
&((1.+W/B)+((A-1.)+1./B+W*A/B)*S*Y+
&(A/B+W*A)*S*S*Y*Y+A*S**3*Y**3)
AC30A- 7
F = T/
&((1.+W/A/B)+(1./A/B+W/A+W/B)*S*Y+(1./A+1./B+W)*S*S*Y*Y+
&S**3*Y**3)
AC30A- 10
F = T*(1.+A*S*Y)/
&(1.+(A+W*A/B)*S*Y+(A/B+W*A)*S*S*Y*Y+A*S**3*Y**3)
AC30A- 12
F = T*(1.+B/A*S*Y+B*S*S*Y*Y)/
&(1.+(B/A+W*B/A)*S*Y+(B+B/A+W*B)*S*S*Y*Y+B*S**3*Y**3)
AC30A- 14
F = T*(1.+(A+1.)*S*Y)/
&(1.+(A+1.+W*A/B)*S*Y+(A/B+W*A)*S*S*Y*Y+A*S**3*Y**3)
AC30A- 15
F = T*(1.+A*S*Y+A*B*S*S*Y*Y)/
&(1.+A*S*Y+(A*B+W*A*B)*S*S*Y*Y+A*B*S**3*Y**3)

```
F =     TRANSFER FUNCTION
  =     N / D
Y =     1 / GBWP
G =     FINITE GAIN
A =     ( ALPHA + 1 )
B =     ( BETA  + 1 )
C =     ( GAMMA + 1 )
W =     1 / INEGRATOR TIME CONSTANT
```
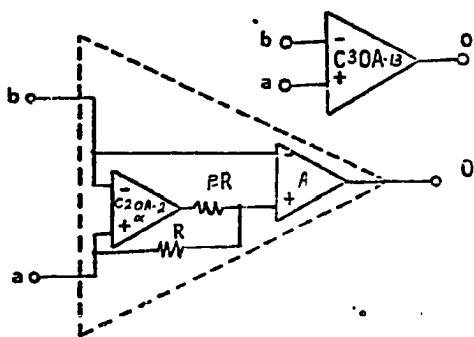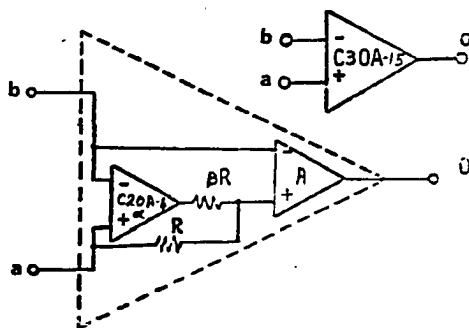
```
**************************
*                        *
*      APPENDIX C         *
*                        *
**************************
```

```
***********************************************************
*                                                         *
*     THE   PROMISSING   C40A   DESIGNS   AND   THEIR      *
*     CORRESPONDING   FINITE   GAIN   EXEPRESSIONSIER      *
*                                                         *
***********************************************************
```

```
C                       *            C40A - 1            *
     F=G*(1.+(1./B+1./C)*S*Y+(B+1.)/B*S*S*Y*Y+S**3*Y**3)/
     %(1.+(1.+G/A/C)*S*Y+(G/C+G/A/B)*S*S*Y*Y+(G/A+G/B)*S**3*Y**3+
     %G*S**4*Y**4)
     F=-(G-1.)*(1.+S*Y)/
C                       *            C40A - 2            *
     F=G/
     %(1.+G/B/C*S*Y+(G/C+G/A/B)*S*S*Y*Y+(G/A+G/B)*S**3*Y**3+G*S**4*Y**4)
     F=-(G-1.)/
C                       *            C40A - 3            *
     F=G*(1.+S*Y)/
     %(1.+(1.+G/B/C)*S*Y+(G/A/B+G/C)*S*S*Y*Y+(G/A+G/B)*S**3*Y**3+
     %G*S**4*Y**4)
     F=-(G-1.)*(1.+S*Y)/
C                       *            C40A - 4            *
     F=G*(1.+(1./A+1./B)*S*Y+(1.+1./B)*S*S*Y*Y+S**3*Y**3)/
     %(1.+G/A/C*S*Y+(G/C+G/A/B)*S*S*Y*Y+(G/A+G/B)*S**3*Y**3+G*S**4*Y**4)
     F=-(G-1.)/
C                       *            C40A - 5            *
     F=G*(1.+1./B*S*Y+S*S*Y*Y)/
     %(1.+G/A/C*S*Y+(1.+1./B)*G*C*S*S*Y*Y+(1.+A/B)*G*C*S**3*Y**3+
     %G*S**4*Y**4)
     F=-(G-1.)/
```

C40A-1

C40A-2

C40A-4

C40A-3
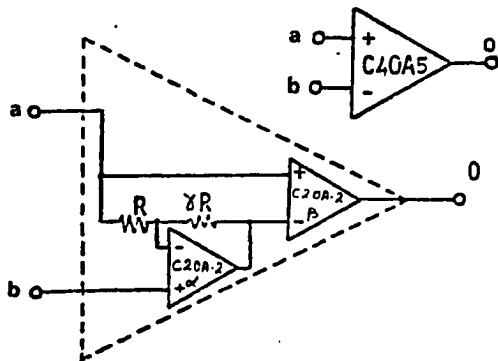
C40A-5
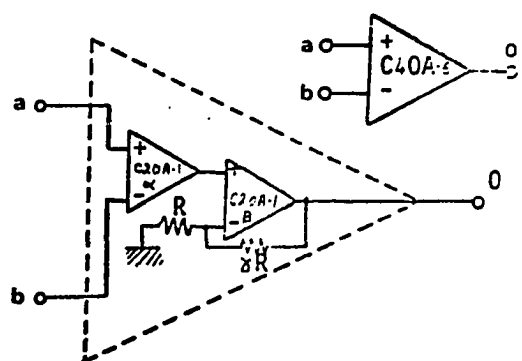
C40A-6

```
C                        *           C40A - 6            *
      F=G*(1.+2.*S*Y+S*S*Y*Y)/
     1(1.+(1.+G/B/C)*S*Y+(G*A*B+G*C)*S*S*Y*Y+G*C*(A+B)*S**3*Y**3+
     1G*S**4*Y**4)
      F=-(G-1.)*(1.+S*Y)/
C                        *           C40A - 7            *
      F=G*(1.+S*Y)/
     1(1.+G/B/C*S*Y+(G/A/B+G/C)*S*S*Y*Y+(G/B+G/A)*S**3*Y**3+G*S**4*Y**4)
      F=-(G-1.)/
C                        *           C40A - 8            *
      F=G*(1.+1./B*S*Y+S*S*Y*Y)/
     1(1.+(1.+G/A/C)*S*Y+(G/A/B+G/A/C)*S*S*Y*Y+(G/A+G/B)*S**3*Y**3+
     1G*S**4*Y**4)
      F=-(G-1.)*(1.+S*Y)/
C                        *           C40A - 17           *
      F=G*(1.+(B-1.)*S*Y)/
     1(1.+B*S*Y+B*G/C*S*S*Y*Y+B*G/A*S**3*Y**3+B*G*S**4*Y**4)
      F=-(G-1.)*(1.+B*S*Y)/
C                        *           C40A - 18           *
      F=G*(1.+(A-1.)*S*Y)/
     1(1.+((A-1.)+G/B/C)*S*Y+(G*A/B/C+G/C)*S*S*Y*Y+
     1(G*A/C+G*A/B)*S**3*Y**3+A*G*S**4*Y**4)
      F=-(G-1.)*(1.+(A-1.)*S*Y)/
C                        *           C40A - 19           *
      F=G*(1.+(C-1.)/B*S*Y+(C-1.)*S*S*Y*Y)/
     1(1.+1./A*S*Y+(1C+A*G/A/B)*S*S*Y*Y+(C*G/A+C*G/B)**3*Y**3+
     1C*G*S**4*Y**4)
      F=-(G-1.)*(1.+1./A*S*Y+S*S*Y*Y)/
C                        *           C40A - 20           *
      F=G*(1.+(A+B-2.)*S*Y+(A-1.)*(B-1.)*S*S*Y*Y)/
     1(1.+(A+B-1.)*S*Y+(B+B*G/C)*S*S*Y*Y+A*B*G/C*S**3*Y**3+
     1A*B*G*S**4*Y**4)
      F=-(G-1.)*(1.+(A+B-1.)*S*Y+B*S*S*Y*Y)/
C                        *           C40A - 22           *
      F=G*(1.+(B-1.)*S*Y+(C-1.)*B*S*S*Y*Y)/
     1(1.+B*S*Y+B*C*S*S*Y*Y+B*C/A*S**3*Y**3+B*C*S**4*Y**4)
      F=-(G-1.)*(1.+B*S*Y+B*C*S*S*Y*Y)/
C                        *           C40A - 23           *
      F=G*(1.+((A-1.)/C+(C-1.)*A/C+1./B)*S*Y+((A-1.)/B+1.)*S*S*Y*Y+
     1(A-1.)*S**3*Y**3)/
     1(1.+(A+1.)*S*Y+(A+A*G/C)*S*S*Y*Y+A*G/B*S**3*Y**3+A*G*S**4*Y**4)
      F=-(G-1.)*(1.+(A+1.)*S*Y+A*S*S*Y*Y)/
```
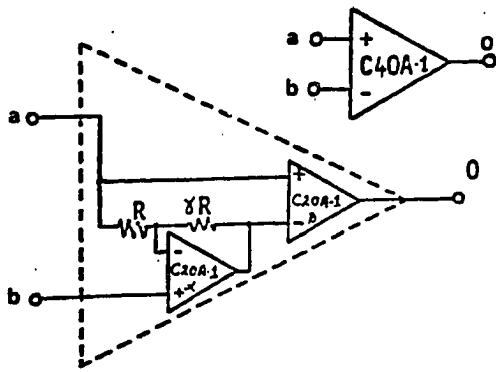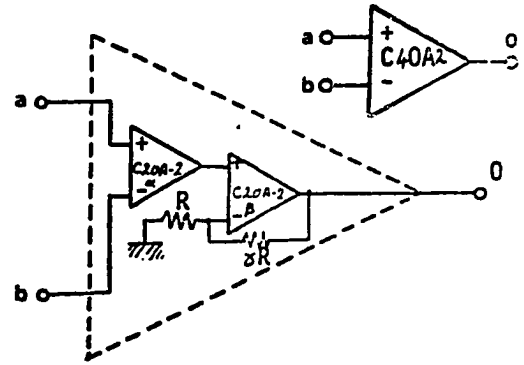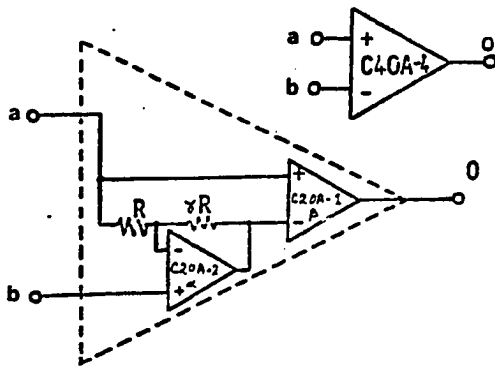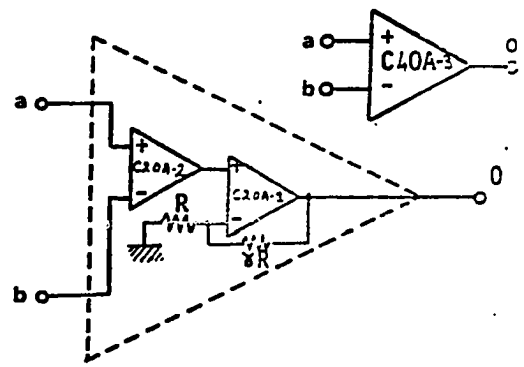
C40A-8

C40A-7

C40A-18

C40A-17

C40A-20

C40A-19

```
C                   *            C40A - 24          *
      F=G*(1.+(1./A+B)*S*Y+B*(C+1.)/C*S*S*Y*Y+B*S**3*Y**3)/
     %(1.+((B-1.)+G/A/C)*S*Y+(B*G/C/A+G/C)*S*S*Y*Y+
     %(G*B/C+G*B/A)*S**3*Y**3+B*G*S**4*Y**4)
      F=-(G-1.)*(1.+(B-1.)*S*Y)/
C                   *            C40A - 25          *
      F=G*(1.+(((A-1.)+(C-1.)*A)/C+B)*S*Y+B*(((A-1.)+(C-1.)*A)/C+1.)
     %*S*S*Y*Y+(A-1.)*B*S**3*Y**3)/
     %(1.+(A+B-1.)*S*Y+((B-1.)*A+A*G/C)*S*S*Y*Y+A*B*G/C*S**3*Y**3+
     %A*B*G*S**4*Y**4)
      F=-(G-1.)*(1.+(A+B-1.)*S*Y+(B-1.)*A*S*S*Y*Y)/
C                   *            C40A - 29          *
      F=G*(1.+(B+C-1.)/B*S*Y+(C-1.)*S*S*Y*Y)/
     %(1.+C/B*S*Y+(C+C*G/A/B)*S*S*Y*Y+(C*G/A+C*G/B)*S**3*Y**3+
     %C*G*S**4*Y**4)
      F=-(G-1.)*(1.+C/B*S*Y+C*S*S*Y*Y)/
C                   *            C40A - 30          *
      F=G*(1.+A*S*Y+(A-1.)*S*S*Y*Y)/
     %(1.+((A-1.)+G/B/C)*S*Y+(A*G/B/C+G/C)*S*S*Y*Y+(A*G/C+A*G/B)*S**3
     %*Y**3+A*G*S**4*Y**4)
      F=-(G-1.)*(1.+(A-1.)*S*Y)/
C                   *            C40A - 31          *
      F=G*(1.+(1./B+(C-1.)*A/C+(A-1.)/C)*S*Y+(1.+(A-1.)/B)*S*S*Y*Y+
     %(A-1.)*S**3*Y**3)/
     %(1.+A*S*Y+A*G/C*S*S*Y*Y+A*G/B*S**3*Y**3+A*G*S**4*Y**4)
      F=-(G-1.)*(1.+A*S*Y)/
C                   *            C40A - 33          *
      F=G*(1.+B*S*Y+B*S*S*Y*Y)/
     %(1.+((B-1.)+G/A/C)*S*Y+(G/C+G*B/A/C)*S*S*Y*Y+
     %(B*G/C+B*G/A)*S**3*Y**3+B*G*S**4*Y**4)
      F=-(G-1.)*(1.+(B-1.)*S*Y)/
C                   *            C40A - 34          *
      F=G*(1.+B*S*Y+(B-1.)*S*S*Y*Y)/
     %(1.+(B+1.)*S*Y+(B+B*G/C)*S*S*Y*Y+B*G/A*S**3*Y**3+B*G*S**4*Y**4)
      F=-(G-1.)*(1.+(B+1.)*S*Y+B*S*S*Y*Y)/
C                   *            C40A - 35          *
      F=G/
     %(1.+G/C*S*Y+G/B*S*S*Y*Y+G/A*S**3*Y**3+G*S**4*Y**4)
      F=-(G-1.)/
C                   *             -              *
```

```
      F =    TRANSFER FUNCTION
        =    N / D
      Y =    1 / GRWP
      G =    FINITE GAIN
      A =    ( ALPHA + 1 )
      B =    ( BETA  + 1 )
      C =    ( GAMMA + 1 )
      W =    1 / INEGRATOR TIME CONSTANT
```

C40A-22

C40A-23

C40A-24

C4CA-25

C40A-29

C40A-30

C40A-31

C40A-33

C30A-34

C40A-35

```
*************************
*                       *
*     APPENDIX D-1      *
*                       *
*************************
```

```
****************************************************************
*                                                              *
*    EXAMPLE PROGRAM FOR SIMULATING THE AMPLITUDE AND          *
*    PHASE RESPONSE OF THE C40A-1 FINITE GAIN AMPLIFIFR        *
*                                                              *
****************************************************************
```

```
//WYL17CD   JOB (EE2917CD,1168),'SHERIF',TIME=2
/*JOBPARM I=5,L=5
/*ROUTE PRINT RMT29
// EXEC FORTGCLG
//FORT.SYSIN DD *
C                     *****************************
C                     *                           *
C                     *                           *
C                     *                           *
C                     *        C40A - 1           *
C                     *                           *
C                     *                           *
C                     *           +               *
C                     *                           *
C                     *                           *
C                     *                           *
C                     *****************************
      AA=1.3
      DO 1 L = 1,50
      BB=1.3
      DO 2 M = 1,50
      CC=1.3
      DO 3 N = 1,50
```

```
      CALL CURVE(AA,BB,CC)
    3 CC = CC + .3
    2 BB = BB + .3
    1 AA = AA + .3
      STOP
      END
      SUBROUTINE CURVE(A,B,C)
      DIMENSION AY(101),AX(101),NPT(1),ICHAR(1),AZ(101)
      COMPLEX FF
      DATA NPT/1*101/,ICHAR/'****'/
      OMEGA = 160.
      CALL FUN(FF,OMEGA,A,B,C)
      F1 = 20.*ALOG10(CABS(FF))
      IF(F1.LT.39.5) RETURN
      IF(F1.GT.40.5) RETURN
      OMEGA = 200.
      CALL FUN(FF,OMEGA,A,B,C)
      F1 = 20.*ALOG10(CABS(FF))
      IF(F1.LT.39.5)RETURN
      IF(F1.GT.40.5)RETURN
      OMEGA = 240.
      CALL FUN(FF,OMEGA,A,B,C)
      F1 = 20.*ALOG10(CABS(FF))
      IF(F1.LT.39.5)RETURN
      IF(F1.GT.40.5)RETURN
      OMEGA = 300.
      CALL FUN(FF,OMEGA,A,B,C)
      F1 = 20.*ALOG10(CABS(FF))
      IF(F1.LT.39.5)RETURN
      IF(F1.GT.40.5)RETURN
      OMEGA = 360.
      DO 10 M = 1,10
      CALL FUN(FF,OMEGA,A,B,C)
      OMEGA = OMEGA + 40.
      FN = 20.*ALOG10(CABS(FF))
      IF(FN.GT.40.5)RETURN
   10 CONTINUE
      A1=A-1.
      B1=B-1.
      C1=C-1.
```

```
      DO 20 K = 1,101
      OMEGA = OMEGA + 5.0
      AX(K) = OMEGA
      CALL FUN(FF,OMEGA,A,B,C)
      AZ(K) = 20.0*ALOG10(CABS(FF))
      AR = REAL(FF)
      AI = AIMAG(FF)
      AY(K) = ATAN2(AI,AR)
   20 CONTINUE
      CALL FPPLOT(AX,AZ,NPT,ICHAR,1,101)
      WRITE(6,60)A1,B1,C1
      WRITE(6,66)
      CALL FPPLOT(AX,AY,NPT,ICHAR,1,101)
      WRITE(6,60)A1,B1,C1
      WRITE(6,66)
   60 FORMAT('  ALPHA   = ',F10.2,/,'  BETA    = ',F10.2,/,'  GAMA
     1=  ',F10.2,///////)
   66 FORMAT('1')
      RETURN
      END
      SUBROUTINE FUN(F,OMEGA,A,B,C)
      COMPLEX S,F
      G = 101.
      Y=.001
      S =CMPLX(0.0,OMEGA)
C
      F=G*(1.+(1./B+1./C)*S*Y+(B+1.)/B*S*S*Y*Y+S**3*Y**3)/
     1(1.+(1.+G/A/C)*S*Y+(G/C+G/A/B)*S*S*Y*Y+(G/A+G/B)*S**3*Y**3+
     1G*S**4*Y**4)
      RETURN
      END
/*
//
/*
```

```
      F  =    TRANSFER FUNCTION
         =    N / D
      Y  =    1 / GBWP
      G  =    FINITE GAIN
      A  =    ( ALPHA + 1 )
      B  =    ( BETA  + 1 )
      C  =    ( GAMMA + 1 )
      W  =    1 / INEGRATOR TIME CONSTANT
```

```
**************************
*                        *
*      APPENDIX D-2       *
*                        *
**************************
```

```
*********************************************************************
*                                                                   *
*  EXAMPLE  ECAP  PROGRAM  TO  SIMULATE  THE  COMPOSITE  *
*       GIC  USING  C20A-4 & C20A-3  IN  BP  FILTER        *
*                    APPLICATIONS                                    *
*                                                                   *
*********************************************************************
```

```
//WYL17CDD JOB (17CD,****),'SHERIF',TIME=(2,00),REGION=512K
/*ROUTE PRINT RMT29
/*JOBPARM L=2
//S1 EXEC RECAP
//ECAP.INPUT DD *
       AC ANALYSIS
B1     N(1,0),R=1E8
B2     N(2,0),R=1F8
B3     N(3,0),R=1E-2
B4     N(4,0),R=1E-2
B5     N(3,5),R=1E3
B6     N(4,5),R=1E3
B7     N(5,0),R=1F3
B8     N(5,0),R=1E8
B9     N(6,0),R=1E-2
B10    N(6,7),R=1E3
B11    N(7,0),C=16E-6
B12    N(7,0),R=1E8
B13    N(8,0),R=1E-2
B14    N(9,0),R=1E8
B15    N(10,0),R=1E8
B16    N(11,0),R=1E-2
B17    N(12,0),R=1E-2
B18    N(11,13),R=1E3
B19    N(12,13),R=1E3
B20    N(13,0),R=1E3
B21    N(13,0),R=1E8
B22    N(14,0),R=1E-2
B23    N(14,15),R=1E3
B24    N(15,0),C=16E-6
```

```
B25    N(15,0),R=1E8
B26    N(16,0),R=1E-2
B27    N(17,0),R=1E8
B28    N(18,0),R=1E8
B29    N(19,0),R=1E-2
B30    N(20,0),R=1E-2
B31    N(19,21),R=1E3
B32    N(20,21),R=1E3
B33    N(21,0),R=1E3
B34    N(21,0),R=1E8
B35    N(22,0),R=1E-2
B36    N(22,23),R=1E3
B37    N(23,0),C=16E-6
B38    N(23,0),R=1E8
B39    N(24,0),R=1E-2
B40    N(25,0),R=1E8
B41    N(26,0),R=1E8
B42    N(27,0),R=1E-2
B43    N(28,0),R=1E-2
B44    N(27,29),R=1E3
B45    N(28,29),R=1E3
B46    N(29,0),R=1E3
B47    N(29,0),R=1E8
B48    N(30,0),R=1E-2
B49    N(30,31),R=1E3
B50    N(31,0),C=16E-6
B51    N(31,0),R=1E8
B52    N(32,0),R=1E-2
B53    N(2,10),R=1.75E3
B54    N(10,8),R=3.78E4
B55    N(9,1),R=1E-5
B56    N(26,25),R=3.82E3
B57    N(24,26),R=4.775E4
B58    N(25,17),R=1E-5
B59    N(1,17),R=1E-5
B60    N(0,33),R=1E-2,E=1
B61    N(32,1),R=4.6E3
B62    N(32,2),R=4.6E3
B63    N(16,17),C=.688E-9
B64    N(16,18),R=4.6E3
B65    N(33,2),R=1E20
B66    N(0,2),R=4.6E3
B67    N(33,18),R=9.2E4
B68    N(0,18),C=.688E-9
T1     B(1,3),BETA=1E15
T2     B(2,4),BETA=-1E15
T3     B(8,9),BETA=3E10
T4     B(12,13),BETA=1E10
T5     B(14,16),BETA=1E15
T6     B(15,17),BETA=-1E15
```

```
T7      B(21,22),BETA=3E10
T8      B(25,26),BETA=1E10
T9      B(27,29),BETA=1E15
T10     B(28,30),BETA=-1E15
T11     B(34,35),BETA=3E10
T12     B(38,39),BETA=1E10
T13     B(40,42),BETA=1E15
T14     B(41,43),BETA=-1E15
T15     B(47,48),BETA=3E10
T16     B(51,52),BETA=1E10
        FREQUENCY=47E3
        PRINT,VOLTAGES,CURRENTS
        MODIFY
        FREQUENCY=47.3E3(1.005476044)60E3
C*      STORE(FREQ,NV(32,MAG))
        EXECUTE
        END
//S2 EXEC FORGO
//FT01F001 DD DSN=&&ECAPDATA,DISP=(OLD,DELETE)
//SOURCE DD *
        DIMENSION AY(23),AX(23),NPT(1),ICHAR(1),AZ(23)
        DATA NPT/1*23/,ICHAR/'****'/
        DO 88 L =1,23
        READ(1,900,END=110) AX(L),AZ(L)
        AY(L)=20.0*ALOG10(AZ(L))
        WRITE(6,900)AX(L),AZ(L)
     88 CONTINUE
    110 J=L-1
        DO 15 K = 1,23
        IF(AY(K).LT.AY(K+1))GO TO 15
        WRITE(6,500)AX(K),AY(K)
        GO TO 50
     15 CONTINUE
     50 F =1.
    500 FORMAT(10X,'CENTER FREQUENCY = ',F10.4,5X,'GAIN AT CENTER = ',
       *F6.2)
    900 FORMAT(2E20.6)
        CALL FPPLOT(AX,AY,NPT,ICHAR,1,23)
        END
//INPUT DD *
/*
//
/*
```
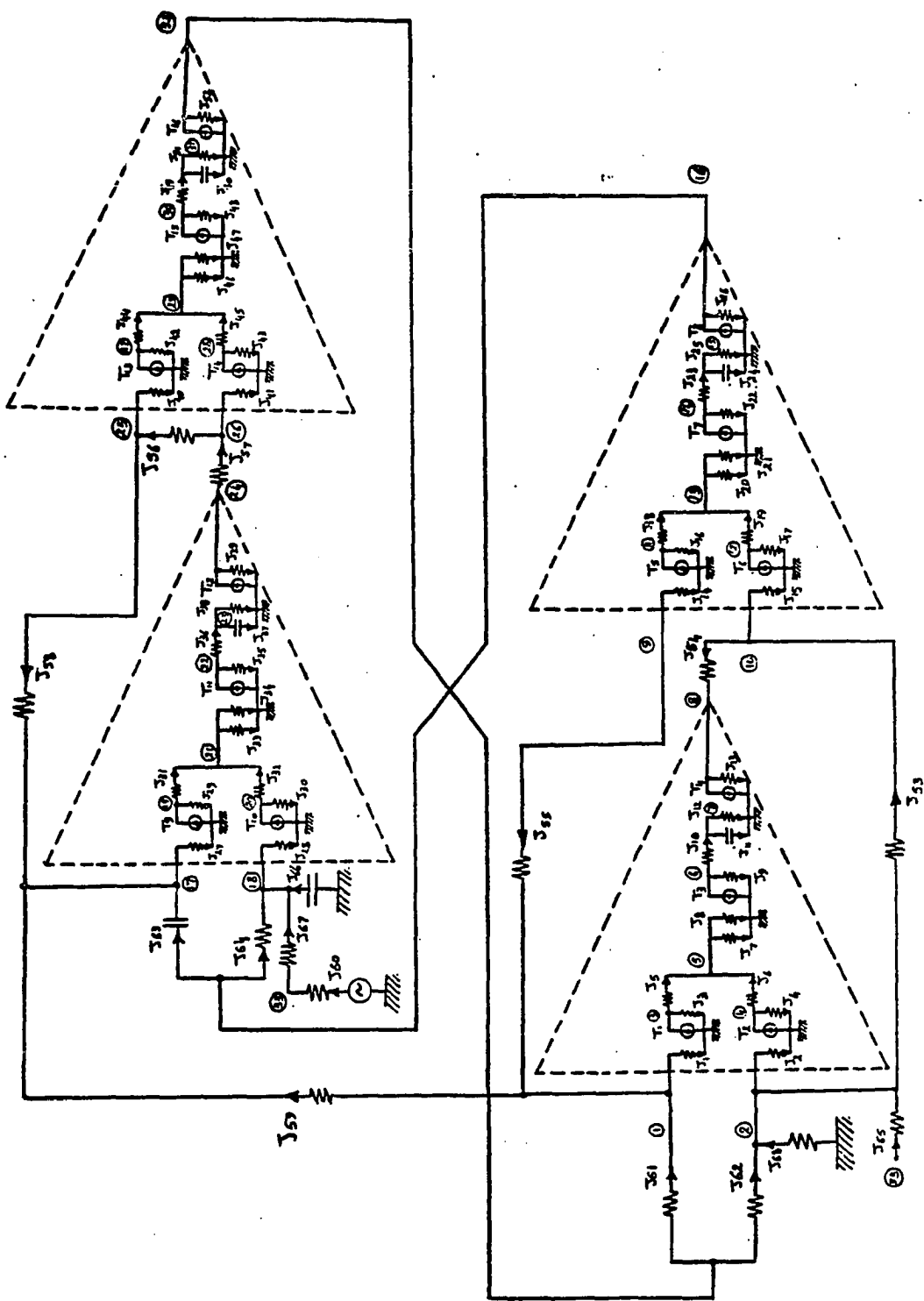
Fig. D.2. ECAP Diagram for the Composite GIC

VITA

Sherif Michael-Nessim, was born in Alexandria, Egypt, on September 6, 1951. He received his Bachelor's Degree in Electrical Engineering (Electronics & Communications) in July 1974, from the Faculty of Engineering Cairo University, Egypt.

After graduating from the Academy of Military Engineers in July 1975, he served as a first Lieutenant in Engineering Corps, specialized in water wells drilling. He was responsible, as a field engineer, for conducting different electronic tests on water wells, and supervising the drilling operations.

In August 1977, he received a research assistantship from West Virginia University, where he received his Master's Degree in Industrial Engineering in May 1980. He worked with the National Transportation Research Center as a research engineer, to implement and field test the new digital communication system for Morgantown Personal Rapid Transit System (MPRT).
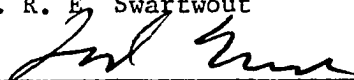
He worked as a teaching and research fellow in the Department of Electrical Engineering, West Virginia University, where he received his Ph.D. in August 1983.

He is a member of the following societies, ETA KAPPA NU, ALPHA PI MU, IIE, and IEEE. He is registerd as a Professional Engineer, with the State of West Virginia.
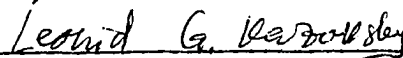
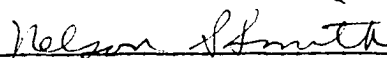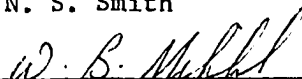APPROVAL OF EXAMINING COMMITTEE

_____
Dr. R. E. Swartwout

_____
Dr. L. T. Moore

_____
Dr. W. H. Iskander

_____
Dr. L. G. Kazovsky

_____
Dr. N. S. Smith

_____
Dr. W. B. Mikhael, Chairman

_____8 · 11 · 83_____
Date